

HUMAN HEALTH

ENVIRONMENTAL HEALTH

BEVERAGES



BEVERAGES

Table of Contents

Geographical Differences of Trace Elements in Wines – Analysis with NexION 300/350 ICP-MS and Visualization with TIBCO Spotfire® Software	3
Wine Analysis Using the LAMBDA Series Spectrophotometers	9
The Analysis of Copper, Iron, and Manganese in Wine with FAST Flame Atomic Absorption	16
Clarus® SQ 8 GC/MS with TurboMatrix Headspace Trap System Application Pack for Monitoring Volatile Organic Compounds in Beer Production	20
The Determination of Low Levels of Nitrosamines in Beer Using the Clarus 680 GC/MS and a D-Swafer System	22
Elemental Analysis of Beer by Flame Atomic Absorption Spectrometry with the PinAAcle 900 AAS	31
Beer Analysis Using the Optima ICP	34
Determination of α -acids in Hops Using Third Party Software	37
Characterization of Hop Aroma Using GC/MS, Headspace Trap and Olfactory Port	40
Aroma Study of Potable Spirits	48
Analysis of the Mycotoxin Patulin in Apple Juice Using the Flexar FX-15 UHPLC-UV	52
Determination of Arsenic Speciation in Apple Juice by HPLC/ICP-MS Using the NexION 300/350	56
Rapid Screening of Adulteration in Pomegranate Juice with Apple Juice Using DSA/TOF with Minimal Sample Preparation	60
Rapid Analysis of Apple Juice Adulteration with Pear Juice Using LC/TOF	64
Rapid Screening of Adulteration in Pomegranate Juice with Grape Juice Using DSA/TOF with No Sample Preparation	67
Pomegranate Juice Adulteration	70
The Qualitative Characterization of Fruit Juice Flavor using a TurboMatrix HS Trap and a Clarus SQ 8 GC/MS	74
A Method for the Quantification of Ethanol Content in Consumable Fruit Juices by Headspace Injection	77
Rapid Quantitative Analysis of Carbendazim in Orange Juice using UHPLC Coupled to the AxION 2 TOF Mass Spectrometer	81
Verification of Coffee Roast Using Fourier Transform Near-Infrared Spectroscopy	85
Dynamic Mechanical Analysis of Coffee	89
Coffee Characterization Using Clarus SQ 8 GC/MS, TurboMatrix HS Trap and GC SNFR Olfactory Port	91
TG-GC/MS Technology – Enabling the Analysis of Complex Matrices in Coffee Beans	99
Analysis of Pb, Cd and As in Tea Leaves Using Graphite Furnace Atomic Absorption Spectrophotometry	102
Total Quant Analysis of Teas and Wines by ICP-MS	107



APPLICATION BRIEF

ICP - Mass Spectrometry Analytics

Authors:

Catherine Stacey

Roberto Forlani

Angelo Piron

PerkinElmer, Inc.
Shelton, CT

Geographical Differences of Trace Elements in Wines – Analysis with NexION 300X/350X ICP-MS and Visualization with TIBCO Spotfire Software

Introduction

Traceability of the wine origin is important for brand protection. Elemental profiles of wines have been shown to be specific for their geographic origin^{1,2}, since the levels of trace metals in wines are related to the soil in the grapevine cultivation area.

In this study, a total of 75 Italian red wines from different regions and grape types were analyzed by ICP-MS to determine whether elemental profiles correlate to the region of origin. Results were imported into TIBCO Spotfire® software for statistical calculations and to display geospatial distribution.

Methods

All wines in this study were red wines produced in different regions of Italy and from various grape types, the majority bottled in 2011 or 2010, with a few older wines. Regions were Lombardy (Lombardia), Abruzzo, Tuscany (Toscana), Trentino-Alto Adige, Apulia (Puglia), Sicily (Sicilia) and Sardinia (Sardegna).

All analyses were performed on a PerkinElmer NexION® 300X ICP-MS in both Standard and Collision modes.

Table 1. Instrumental Conditions

Parameter	Condition
Instrument	NexION 300X ICP-MS
Nebulizer	Glass concentric
Spray chamber	Glass cyclonic
Sample uptake rate	0.25 mL/min
RF power	1500 W
Internal standard	Ge, Rh, Re at 10 ppb
Dwell time	50 ms
Collision mode	He = 4 mL/min

All samples were filtered and diluted four times with 2% (v/v) HNO₃. Internal standards were used to compensate for possible matrix effects during sample introduction. An internal standard mix (Ge, Rh, and Re) was added on-line by merging flows of the sample and internal standard mix.

Results for all samples were compiled into a single table in Microsoft® Excel, with columns of elements, and the ICP-MS values (in cps) for each sample in rows. For most of the samples, information on the region and city of origin, the type of grape, and year of production were available, and added as additional category columns to the table. The table was opened in TIBCO Spotfire software and the data used for various calculations and visualizations. Standard S Plus statistical algorithms such as Principal Component Analysis (PCA) were used. The category columns enable different grouping and sorting options for raw data and the resulting statistical outputs, and for color coding of graphs.

Results

The levels of 39 elements were measured for each sample; these vary widely, from phosphorus at high mg/L levels to rare earth elements at sub µg/L levels. PCA was used to investigate the relationship between the geographic origin of wines and their elemental profiles.

PCA is a data analysis method used to reduce the dimensionality of multivariate data and to derive meaningful patterns from the complex information.

PCA transforms or projects the variables for each sample into a lower dimensional space, while retaining the maximal amount of information about the variables. Resulting principal components for each sample are a combination of the original variables after the transformation. The largest difference in the combined variables between the samples is described by Principle Component 1 (PC1), the next largest by component 2 and so on.

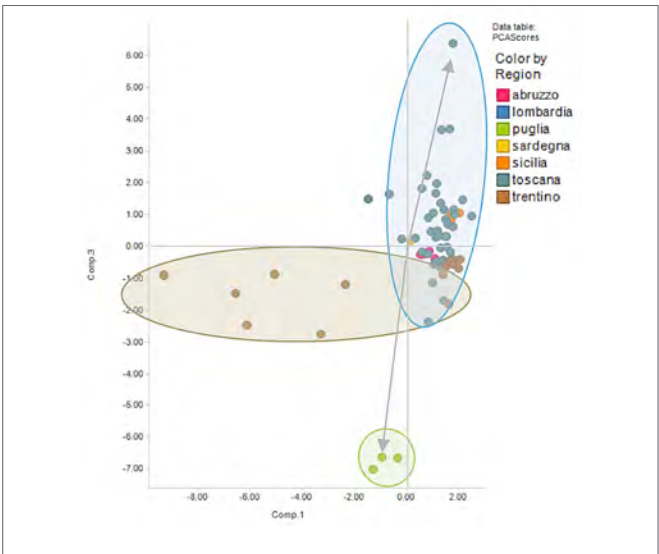


Figure 1. Scores Plot for PC1 vs. PC3 showing separation of the Puglia (Apulia) wines in green from the Toscana (Tuscany) wines in blue and the Trentino wines in brown.

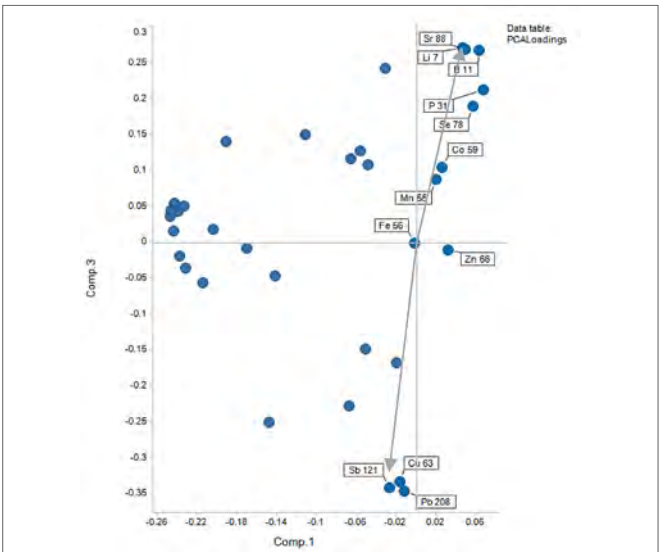


Figure 2. Loadings Plot of PC1 vs. PC3 showing that the strongest contributors to the separation of the Puglia (Apulia) wines are the higher levels of Sb, Cu and Pb, with some Toscana (Tuscany) wines having higher levels of Sr, Li and B.

A Scores Plot summarizes the relationship between the samples, a plot of PC1 vs. PC2, or PC1 vs. PC3 will show the samples grouped according to the larger differences between them; this information is displayed in TIBCO Spotfire software scatter plots. A Loadings Plot of the same components shows the weighting for each variable as a distance from the origin. The plot is a means of interpreting the patterns seen in the Scores Plot.

For these wine analyses, the levels of the 39 different elements from the ICP-MS results are the variables. PCA calculations used the functions within the TIBCO Spotfire Statistics Services, including autoscaling of values in each element column, thus giving the same variance ranges across the samples, independent of concentration and ICP-MS instrument response.

The Scores Plot from the initial autoscaled PCA results show a strong separation of the three Puglia wines from all other wines using PC1 vs. PC3 (Figure 1). The corresponding Loadings Plot (Figure 2) indicates that this separation was most strongly

correlated to the higher levels of Cu, Sb and Pb in these wines. Other wines, particularly those from Tuscany, are partly grouped by having higher levels of Sr, Li and B. Trentino wines correlate to increased levels of a number of elements, which will be described for the PC1 vs. PC2 interpretation that follows.

A bar chart of the levels of Cu and Pb for each sample, sorted by region, confirms the higher levels for the Puglia samples (Figure 3). It is not known whether these relatively high levels are due to the soil type, grape type, or cultivation and production methods for these wines. For example, high levels of Cu may be due to the use of copper compounds as mildewcides and fungicides. Increased levels may also relate to the use of brass equipment during production and bottling.

The various wines from the Trentino region were also partly grouped in a Scores Plot of PC1 vs. PC2; the loadings plot (Figure 4) suggests that these wines have higher levels of a number of rare earth elements. These elements have been reported previously^{3, 4}, as having variable levels in wines due to the use of bentonite, an absorbent clay, to precipitate proteins from the wine. Thus, these elements are not considered to be reliable indicators of geographic origin.

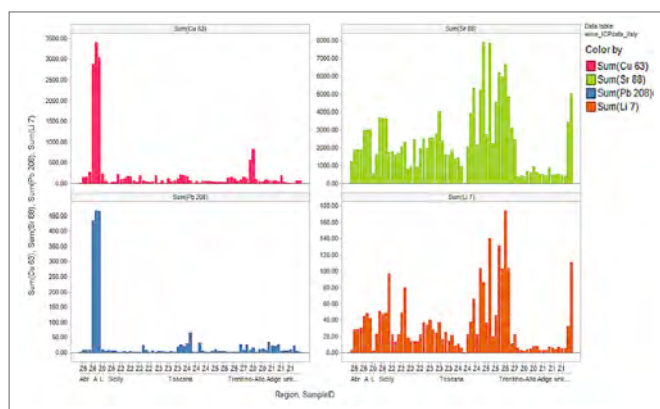


Figure 3. Bar chart of the concentration of Cu (red), Pb (blue), Sr (green), and Li (orange) for each sample, grouped by region, shows that the wines from Puglia (Apulia) have higher levels of Cu and Pb, while several of the wines from Toscana (Tuscany) have higher levels of Sr and Li.

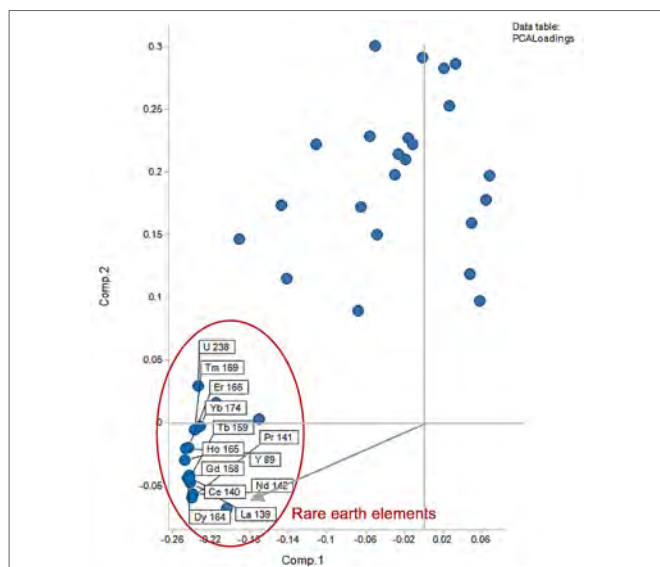


Figure 4. Loadings Plot of PC1 vs. PC2 showing that the increased levels of many rare earth elements differentiate the Trentino wines.

A new PCA analysis of the data was made, after excluding the data columns for the rare earth elements. The new Scores Plot of PC1 vs. PC2 (Figure 5) gave a clearer differentiation of the groupings for the Tuscany and Trentino regions.

The differentiators in the loadings plot (Figure 6) are clustered into groups of elements, which may be classified by geochemistry. This grouping has been reported for other wines⁵, and may relate to the local rainfall and climate of the grapevines. The chalcophilic elements (Cu, Zn, Sb, As, Sn) have a lower affinity for oxygen and prefer to bind to sulfur as insoluble sulfides. These elements are at higher levels in Tuscany wines, as are siderophilic elements such as Ni and Co which track with Fe. Lithophilic elements (Li, Ba, Cs, Sr etc.) are highly soluble and associate with the soil; these are at lower levels in Trentino wines.

TIBCO Spotfire software visualizations allow the user to quickly group information in the element data table in different ways.

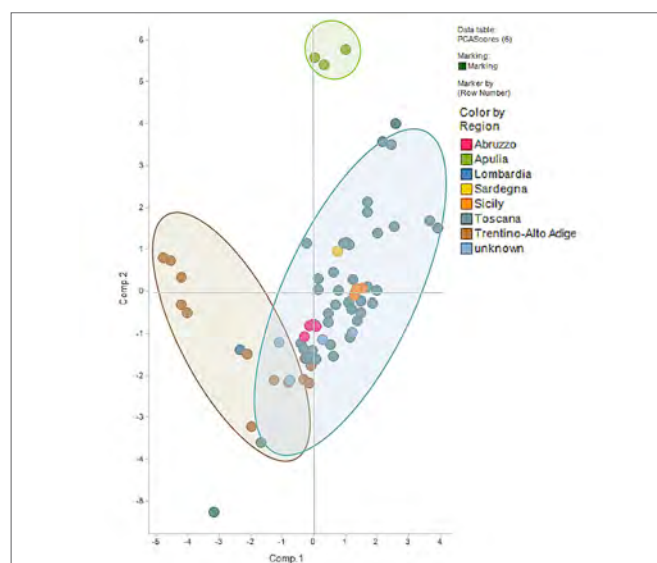


Figure 5. Scores Plot for PC1 vs. PC2 using only the non-rare-earth elements, showing separation of the groups of the Puglia (green), Trentino (brown), and Toscana (blue) wines.

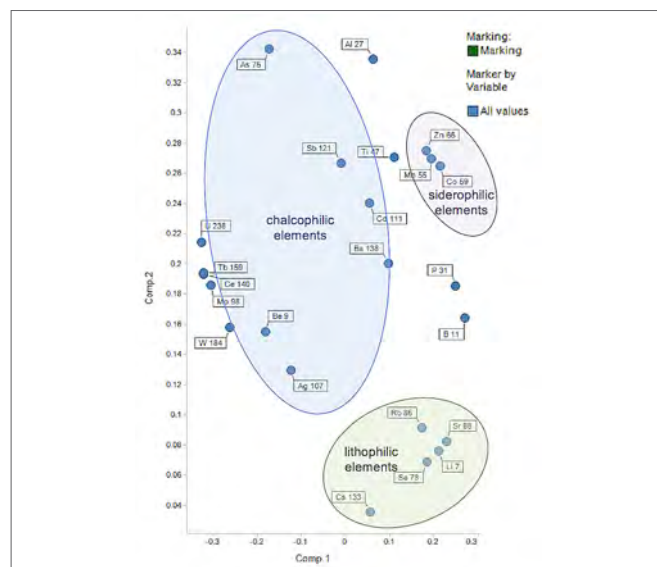


Figure 6. Loadings Plot showing a partial grouping of elements that differentiate the wines into the categories of the Goldschmidt geochemical classification of elements.

For example, a bar chart showing concentrations of Li for each sample (Figure 7), is ordered first by region, and then color-coded by city. This view of the data highlights the difference in Li levels by region. The higher levels in many wines from Florence in Tuscany are clearly visible.

Custom expressions are easily created to show the levels for a combined group of elements. A category for various chalcophilic elements (the sum of concentration for Zn, Sb, As, and Sn but not Cu) gives a clear view of the differences in concentration of this group of elements for all the samples (Figure 8).

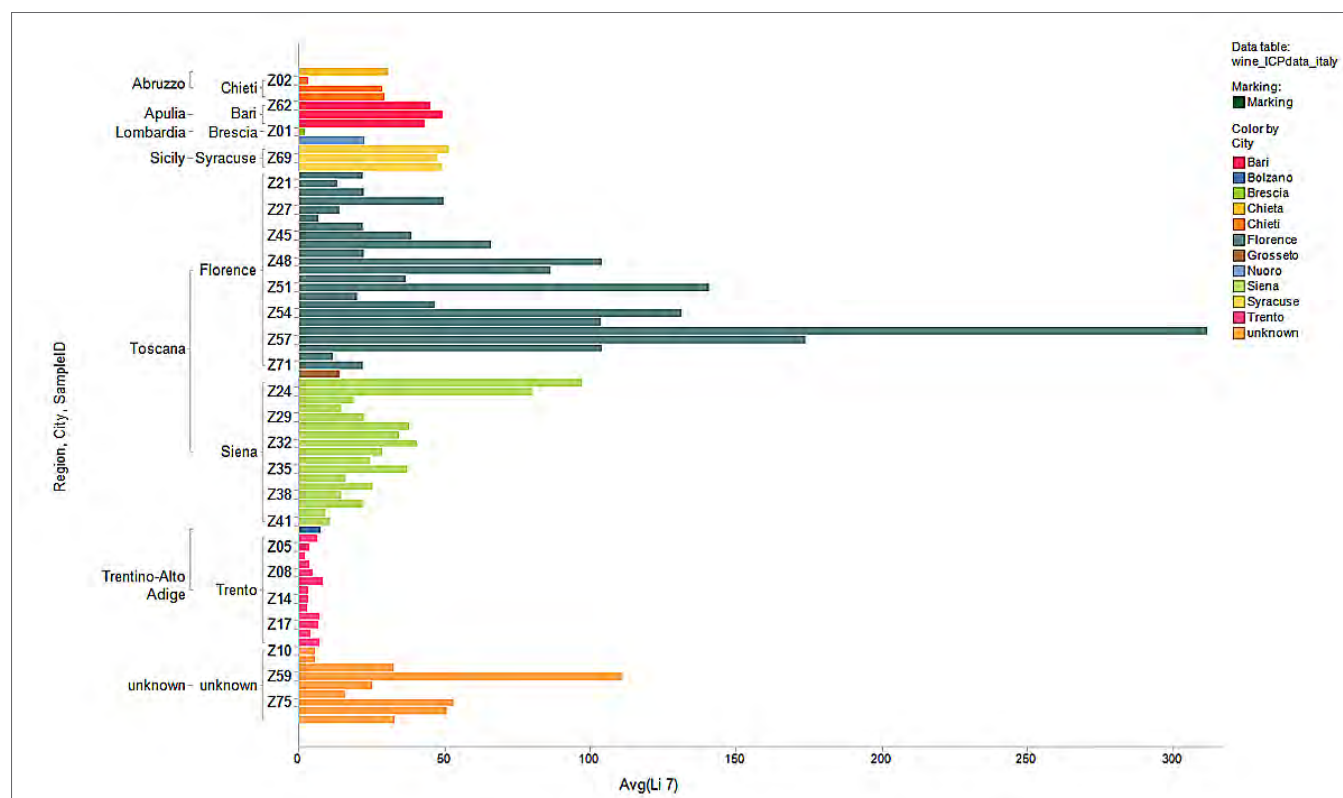


Figure 7. Bar chart showing the Li level for each sample, with samples ordered by region, then grape type and colored by city. Highest levels are for the wines from Florence in Tuscany, shown in blue.

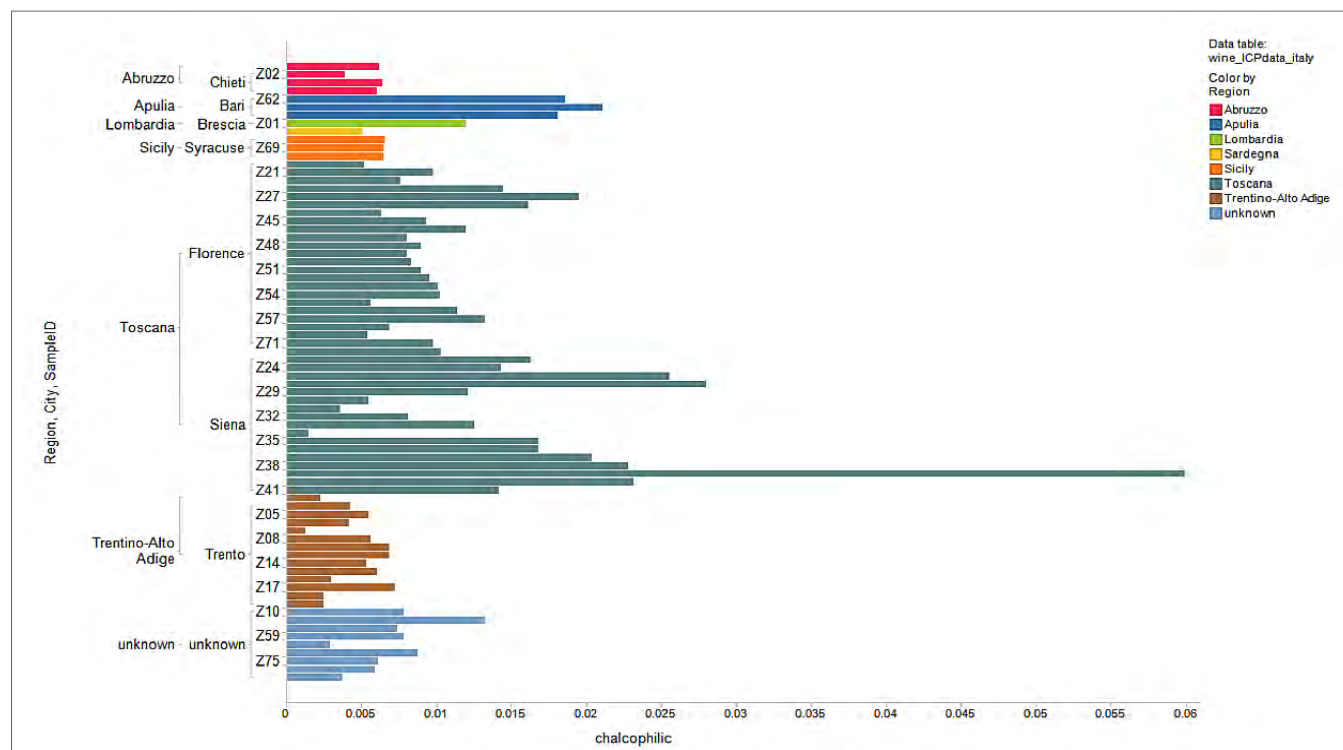


Figure 8. Bar chart for samples ordered by region then city, with bars colored by region, showing that levels for the custom chalcophilic category (sum of Zn, Sb, As, and Sn levels) are higher for the Toscana (Tuscany) wines (blue) than for the Trentino wines (brown).

Previously reported elemental analysis of Italian wines⁶ suggested that Sr and Rb levels were correlated to the soils of origin in provinces of Abruzzo in central Italy. With these results, levels of Rb were quite constant for all samples, although Sr levels did vary. The levels of Sr were highest in some of the wines from Florence in Tuscany and Syracuse in Sicily (Figure 9).

A map chart (Figure 10) shows the geospatial distribution of a selected element or customized group of elements. The region

names for a shape file of Italy are linked in TIBCO Spotfire software to the region column in the data table, and regions in the map chart are color-coded by intensity for an element. Here, chalcophilic and lithophilic element groups are contrasted with high intensity levels in red and low levels in blue. Wines from the Florence area of Tuscany are relatively low in chalcophilic elements compared with other regions, but higher in lithophilic elements. Wines from Sicily are relatively high in lithophilic elements, but lower in chalcophilic elements.

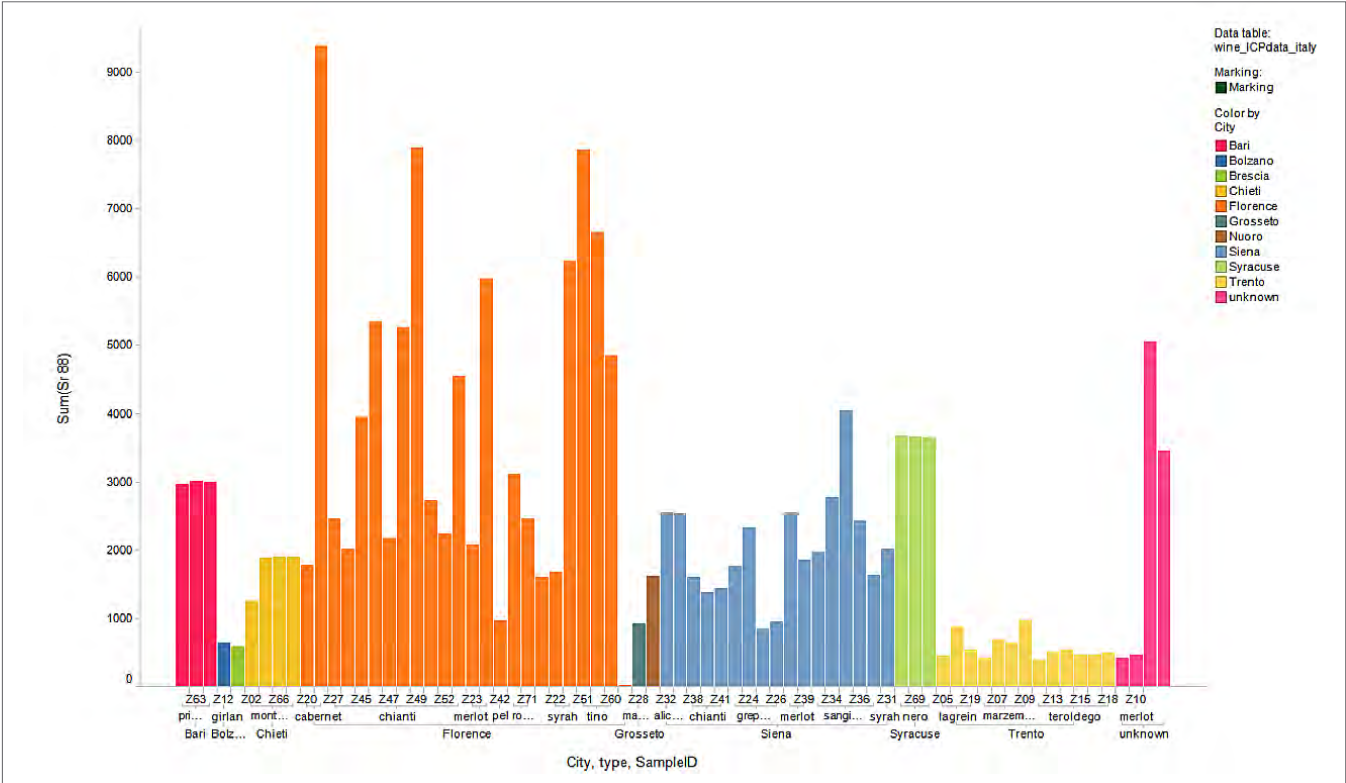


Figure 9. Bar chart showing levels of Sr for each sample, with columns colored by city, and ordered by city and grape type.

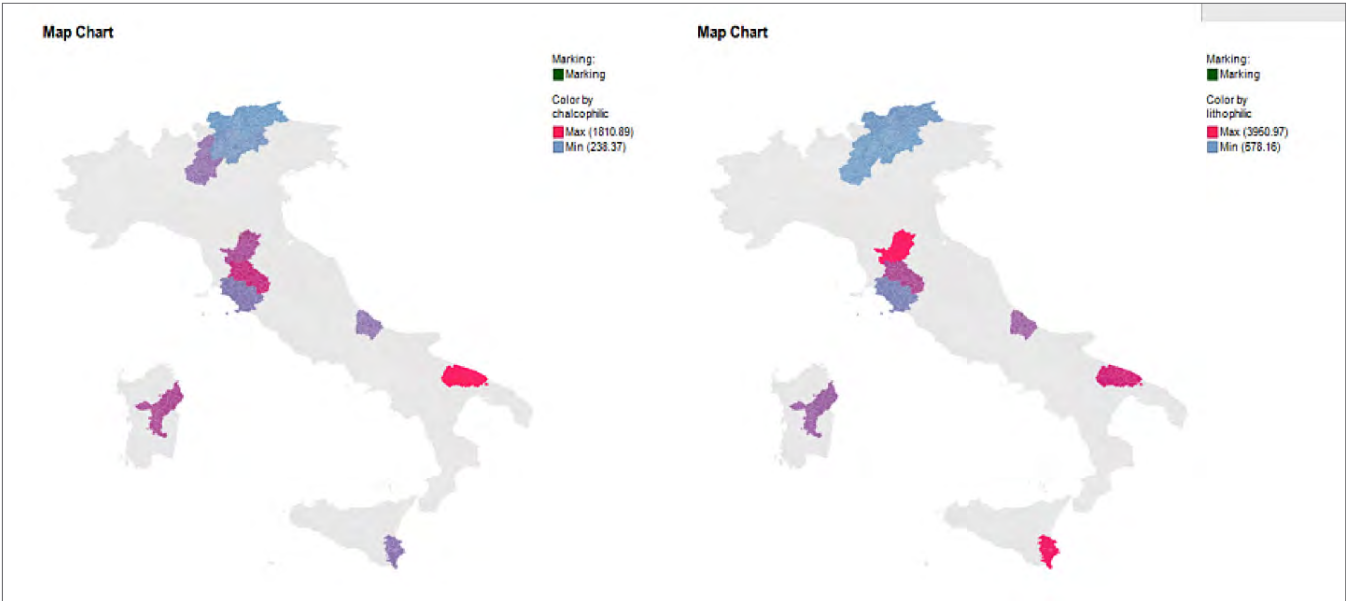


Figure 10. Map charts showing the distribution by region of the chalcophilic elements (Zn, Sb and As) on the left and lithophilic (Li, Ba, Cs, Sr etc.) elements on the right, with red for the highest intensity and blue as the lowest.

Conclusion

The ICP-MS analysis of a large number of wines from Italy provided results which were used for statistical analysis and geospatial mapping with TIBCO Spotfire software. Results indicated significant differences in elemental levels in many of the wines, some of which were linked to specific geographical regions. Further research will be needed to investigate whether these differences relate to soil and rainfall, or are correlated to viniculture production differences.

References

1. Cichelli, A. ICP-MS analysis for the characterization of the origins of wine. *Agro Food Industries* 2013, 24 (1).
2. Vicentini, A.; Giaccio, M. Determination of the geographical origin of wines by means of the mineral content and the stable isotope ratios: a review. *J Commodity Sci Technol. Quality* 2008, 47, 267-284.
3. Nicolini, G.; Larcher, R.; Pangrazzi, P.; Bomtempo, L. Changes in the contents of micro- and trace-elements in wine due to winemaking treatments. *Vitis* 2004, 41 (5), 41-45.
4. Aceto, M. e. a. A traceability study on the Moscato wine chain. *Food Chemistry* 138 2013, 1914-1922.
5. Greenough, J.; Mallory-Greenough, L.; Fryer, B. Regional Trace Element Fingerprinting of Canadian Wines. *Geoscience Canada* 2005.
6. Galgano, F.; Favati, F.; Caruso, M.; Scarpa, T.; Palma, A. Analysis of trace elements in southern Italian wines and their classification according to provenance. *Food Science and Technology* 2008, 41.



UV/Visible Spectroscopy

Author:

Steve Upstone

PerkinElmer, Inc.

Seer Green

Bucks HP9 2FX, UK

Wine Analysis Using the LAMBDA Series Spectrophotometers

Introduction

Wine has been made for the past 8,000 years using traditional methods. In recent years, there has been an worldwide increase in production – much of it coming from “New-World” wine producers such as the USA (California, in particular), Australia, New Zealand, South Africa, and some South American countries – notably Argentina and Chile. Even unlikely candidates as wine producers, such as the UK and Canada, are producing quality wines in relatively small quantities. This broadening of geographic locations has also led to an increase in the technology used in both the manufacturing and testing of the product to ensure consistency of flavor and product safety. Modern analytical techniques, such as Gas and Liquid Chromatography (GC and HPLC), are used by big producers. Another technique is UV/Visible spectroscopy.

One indicator of wine quality is its color. In previous times, this would have been done by eye but this is semi-quantitative at best. It is useful to be able to assign numbers to wine color using instrumentation. Although color is mainly a quality consideration, it does also help with safety issues as a change in color may indicate a fault in the brewing process or indicate bacterial or other contamination.

Wine Color Intensity and Hue

One of the simplest approaches is to measure the absorbance at three wavelengths in the visible region. Normally, these are at 420 nm, 520 nm, and 620 nm. These can be summed (the Wine Color Intensity) or a ratio of A_{420} / A_{520} can be measured (Wine Hue). The calculations are based on the absorption of wine in a 1cm (10 mm) pathlength cuvette. In the case of red wines, it is necessary to use shorter pathlengths (e.g. 1 mm) in order to obtain spectra within the range of the instrument. The readings can then be recalculated for a 1 cm cuvette.

This simple approach has been adopted as it allows measurement in relatively simple instrumentation without wavelength scanning ability.

CIE Color Based Analysis

A more accurate approach is to utilize the entire visible region from 380 nm to 780 nm, and apply standard color methodology as developed by CIE (Commission Internationale D'Eclairage, based in Vienna). This is an international body responsible for the whole area of representing colors numerically. Its first specification was issued in 1931 and has been developed steadily over the years. The color calculation is a weighted transmittance value that takes into account the illumination conditions and the spectral responses of the eye to the three primary colors of light – red, green, and blue. It also takes into account the two types of receptor in the retina – rods (for monochromatic vision in low-light conditions) and cones (color receptors which work in relatively well illuminated conditions).

Wine analysis is normally performed using the 1964 calculation. This uses a 10° observer angle (this takes into account the contribution of both rods and cones whereas the earlier 1931/ 2 degree standard was biased towards cones only) and Illuminant D65 (daylight with a color temperature of 6500 K). This calculation produces three values for the amount of each of the three primary colors – red, green, and blue. These are the tristimulus values and are X, Y, and Z for red, green, and blue, respectively. The calculation involves adjusting the absorbance scan to the equivalent of a 1 cm pathlength and then converting it to transmittance (%T). CIE publish weighting tables for the illuminant and for red, green, and blue responses in the eye. The calculation is as follows:

$$X_{10} = K \int_{380}^{780} S(\lambda) \cdot \bar{x}(\lambda) \cdot R(\lambda) d\lambda \quad (1)$$

$$Y_{10} = K \int_{380}^{780} S(\lambda) \cdot \bar{y}(\lambda) \cdot R(\lambda) d\lambda \quad (2)$$

$$Z_{10} = K \int_{380}^{780} S(\lambda) \cdot \bar{z}(\lambda) \cdot R(\lambda) d\lambda \quad (3)$$

$$K = \frac{100}{\int_{380}^{780} S(\lambda) \cdot \bar{y}_{10}(\lambda) \cdot R(\lambda) d\lambda} \quad (4)$$

Where $S(\lambda)$ = relative spectral power distribution of the illuminant (D65) as supplied by CIE

x_{10} , y_{10} and z_{10} = the color matching functions for a 10 degree observer (as supplied by CIE 1964)

$R(\lambda)$ = Spectral reflectance of sample

These values can then be normalized so that $x + y + z = 1$. This means that the value of z is no longer necessary as it is implied and so a color can be described using the x and y values.

$$x = \frac{X}{X+Y+Z} \quad (5) \quad y = \frac{Y}{X+Y+Z} \quad (6) \quad z = \frac{Z}{X+Y+Z} \quad (7)$$

When quoting a color using this system, it is usual to include the un-normalised Y value. The x and y data can be plotted against each other to produce a graph – the CIE color space diagram.

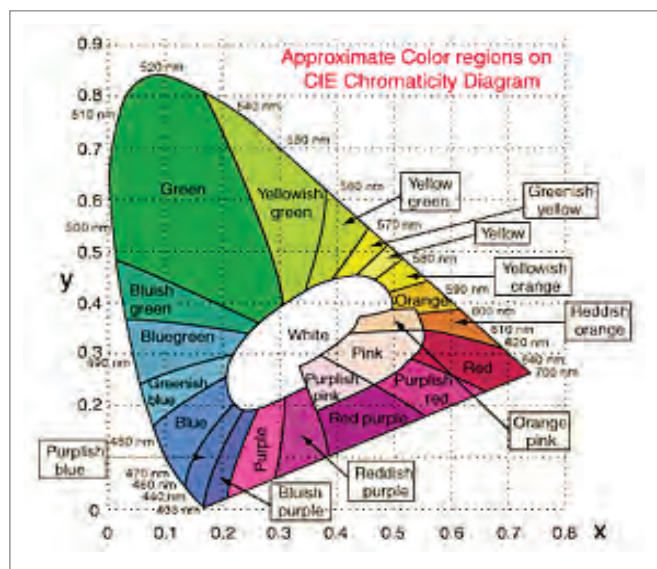


Figure 1. CIE Color Space Diagram

This diagram can represent any possible color (the “impossible” ones being outside of the colored area). There is also an area in the center which is called the white point.

One further refinement of the color measuring system was made by CIE in 1976. This is the $L^* a^* b^*$ system. This system is basically a way of representing color in three dimensional space using Cartesian coordinates. The transform to $L^* a^* b^*$ is as follows. (X_n , Y_n , and Z_n are the white point values of X , Y , and Z and for a 10° observer are 94.811, 100, and 107.304, respectively).

$$L^* = 116 \cdot \left(\frac{Y}{Y_n} \right)^{1/3} - 16 \quad (8)$$

$$a^* = 500 \cdot \left[\left(\frac{X}{X_n} \right)^{1/3} - \left(\frac{Y}{Y_n} \right)^{1/3} \right] \quad (9)$$

$$b^* = 200 \cdot \left[\left(\frac{Y}{Y_n} \right)^{1/3} - \left(\frac{Z}{Z_n} \right)^{1/3} \right] \quad (10)$$

There is a special case to the equation if either X/X_n , Y/Y_n , or Z/Z_n is less than 0.008856. In this case, the calculation becomes:

$$7.787 \cdot \left(\frac{X}{X_n} \right) + \frac{16}{116} \text{ replaces } \left(\frac{X}{X_n} \right)^{1/3} \quad (11)$$

$$7.787 \cdot \left(\frac{Y}{Y_n} \right) + \frac{16}{116} \text{ replaces } \left(\frac{Y}{Y_n} \right)^{1/3} \quad (12)$$

$$7.787 \cdot \left(\frac{Z}{Z_n} \right) + \frac{16}{116} \text{ replaces } \left(\frac{Z}{Z_n} \right)^{1/3} \quad (13)$$

The L^* a^* b^* values can then be represented in three-dimensional space as

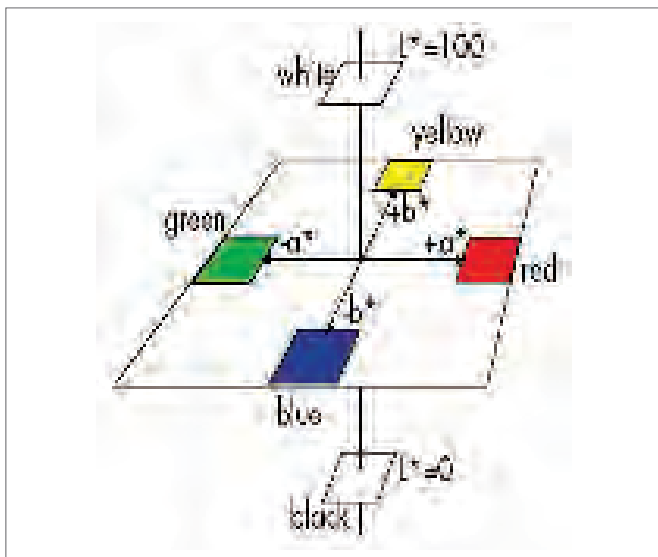


Figure 2. L^* a^* b^* Color Space

The final part of the calculation is to calculate the Chroma (C^*ab) and Hue Angle (h^*ab). These are a conversion of L^* a^* b^* values from Cartesian to polar coordinates. This is also termed $L^*C^*h^*$ color space.

The L^* term is the same as for $L^*a^*b^*$ color space.

The Chroma value is the perpendicular distance from the Lightness axis.

The Hue Angle is the angular component.

The wine industry also uses these values to produce some additional parameters based on the $L^*a^*b^*$ and C^*ab values. These are:

$$S^* = \frac{C^*ab}{L^*} \quad (14)$$

$$Q^* = (0.15 \cdot L^*) \cdot \log(Y_n) + (0.6 \cdot L^*) + 40 \quad (15)$$

Experimental

Wine samples were measured a Lambda 25, 35, or 45 using a standard quartz cuvette. The pathlength depends on the type of wine being measured. For full bodied red wines a 1 mm cuvette should be used. For white wines, a 10 mm pathlength is fine. The instrument was autozeroed using a distilled water blank using the same pathlength cuvette as the test sample. For short pathlength cells, the use of a suitable spacer is recommended.

The measurement was carried out using the Wine Analysis method which is supplied as an example method with UV WinLab version 6 software.

Table 1. Part numbers of cuvettes and spacers.

Part Number	Description
B0631025	1 mm pathlength quartz cuvette with PTFE stopper (pk/2)
B0631008	5 mm pathlength quartz cuvette with PTFE lid (pk/2)
B0631009	10 mm pathlength quartz cuvette with PTFE lid (pk/2)
N9302471	Spacer for 1 mm pathlength cuvette (pk/2)
N9302743	Spacer for 5 mm pathlength cuvette (pk/2)

UV WinLab v6 software is compatible with the LAMBDA 20, 40, 25, 35, 45, 650, 750, 800, 850, 900, and 950 instruments. The program is designed to work with the medium performance instruments (LAMBDA models with double-digit numbers – eg. LAMBDA 25), but data can be imported into the method from all the listed models.

Results

A variety of different wines was analyzed using a LAMBDA 25 with UV WinLab version 6.0 and the results are shown in the table.

In terms of wine tasting and appreciation, wine can be classified under the following headings. These were taken from a Spanish publication, the classification is subjective and will vary slightly from country to country.

Soft straw yellow: Very young wines with a light body and alcohol content. This color can also indicate a defective wine that has been over-filtered or that uses too many clarifying agents.

Straw yellow with green tones: A very fresh white wine with greenish reflections because of the presence of chlorophyll. The wine tends to retain the green pigment of the grapes.

Straw yellow: A term for white wines that are at peak maturity.

Golden yellow: Indicates that a white wine is aging and oxidizing.

Yellow amber: Typical of wines made from partially dried grapes or fortified grapes. When straw yellow wines develop this color they are losing their quality due to oxidation.

Pink: Wines with a reddish color and soft, lighter reflections.

Pale pink: Wines with a soft red color, almost transparent.

Cherry red: Wines with no more than 100 milligrams per liter of anthocyanins (plant pigments that produce a blue to red color) and that are made with longer skin contact.

Purple red: A red wine with purple reflections towards the edge of the glass.

Ruby red: Describes a healthy red wine in the early stages of maturity.

Garnet: Burgundy color typical of mature red wines with a remarkable structure.

Mahogany: Wines with a warm orange color at the rim of the glass during their prime maturation period.

Table 2. Wine analysis using LAMBDA 25.

Wine Type	Type	Color Intensity	Color Hue	X	Y	Z	x	y	L*	a*	b*	C*ab	h* _{ab}	S*	Q*
Spanish Tempranillo	Full Red														
Australian Shiraz	Full Red														
Chilean Merlot	Full Red														
French Cabernet Sauvignon															
Californian White Zinfandel															
French Beaujolais	Light Red														
French Rose D'Anjou															
Portugese Vinho Verde															
Australian Oaked Chardonnay															
New Zealand Sauvignon Blanc															
South African Unoaked Chenin Blanc	Straw Yellow with green tones	0.1045	4.0241	91.12	96.42	95.94	0.3214	0.3401	98.60	-0.53	4.91	4.94	96.14	0.05	118.74

L* a* b* values can be used to produce a color difference from a known standard (or ideal value) by calculating the ΔE value. This is calculated as follows:

$$\Delta E = \left((L_1^* - L_2^*)^2 + (a_1^* - a_2^*)^2 + (b_1^* - b_2^*)^2 \right)^{1/2}$$

This value assumes color space is uniform (which it is not) but is still widely used in the wine industry and is useful for the small color differences as would be expected in this type of analysis.

It is possible to use L* a* b* color data to analyze individual pigments for identification purposes. Some pigments, such as malvidin 3-glucoside, exhibit a large color change up to acidification whereas others, such as vinylcatechol pyranocyanidin are virtually unchanged.

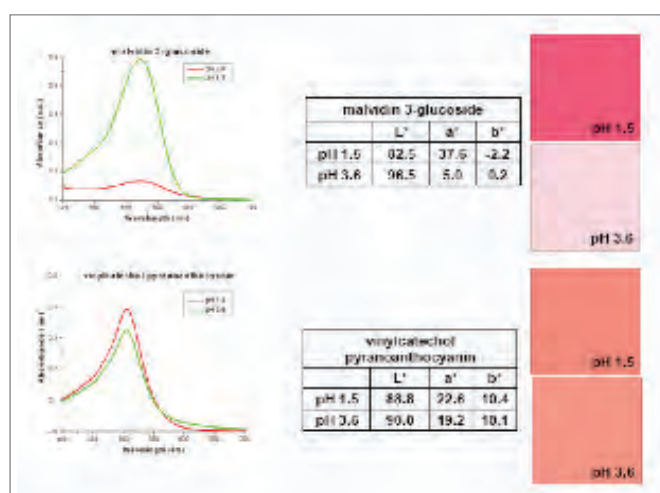


Figure 3. L* a* b* color data to analyze individual pigments.

Other Wine Assays Using UV/Visible Spectrophotometers

Absorbance at 280 nm

This is a very non-specific assay for phenolics which all absorb around 280 nm due to their aromatic nature. Its simplicity is countered by the fact that it will measure other aromatic compounds (eg nucleic acids and aromatic peptides/proteins) and will not differentiate between the different phenolic types. This assay requires a spectrophotometer that is capable of measuring in the UV region (ie below 320 nm)

Folin-Ciocalteu Assay for Phenolics

This assay is used to measure phenols and is based on the fact that phenols ionize completely under alkaline conditions and can, therefore, be readily oxidized by the Folin-Ciocalteu reagent. This oxidation causes a color change from yellow to blue, which is easy to measure in a UV/Visible spectrophotometer at 765 nm. The Folin-Ciocalteu reagent is very reactive and can oxidize unintended components in the wine such as fructose, ascorbic acid, bisulfite, and amino acids. This can be prevented by adding acetaldehyde (to bind the bisulfite) or, for a sweet wine, applying a correction factor.

Enzymatic Methods for Phenolics

A recent method involving horseradish peroxidase (HRP) has been introduced as an alternative to the Folin-Ciocalteu Assay. It works by converting phenolics into quinine-imine products. The assay is fast (less than five minutes). The method is still in development and has not been shown to work well with all types of phenolics.

Iron Chloride Assay for Polyhydroxylated Phenolics

Iron Chloride will bind to certain phenolics that contain more than one hydroxyl group, so all phenolics in wine can be measured except anthocyanins and other monohydroxylated phenolics.

Tannin Assays

There are three main assays for the measurement of tannins in wine. These are the Glories Gelatin Index, the Llaudy Method, and the UC Davis Assay. These three methods are all based on the precipitation of tannin by proteins and vary in their complexity. The Glories Assay (which uses gelatin as a protein) suffers from the fact that the precipitation step is very long. The Llaudy method uses ovalbumin and is quicker and more reproducible than the Glories method but still requires a total of twelve measurements to be made for each wine sample. The UC Davis Assay uses Bovine Serum Albumin (BSA) for the precipitation. These are then reacted with Iron (III) Chloride and measured at 510 nm.

Enzymatic Measurement of Sulfite, Ethanol

As an alternative to chromatography, it is possible to measure several analytes in wine, such as sulfites and ethanol, by using kits like those sold by r-Biopharm (a division of Hoffmann La Roche). In the case of ethanol, the ethanol is oxidized to acetaldehyde in the presence of nicotinamide adenine dinucleotide (NAD+) in the presence of alcohol dehydrogenase. The assay is designed to work at 20 °C. In the case of sulfite, this is a two stage reaction. The first stage involves oxidation of the sulfite with sulfite oxidase (SO₂-OD). The product of this reaction is hydrogen peroxide which is then reacted with NAD+ in the presence of NADH peroxidase (NADH-POD).

Other Useful Analytical Techniques for Wine Analysis

For the busy laboratory where sample throughput is an important factor, there are other techniques that can be considered including gas and liquid chromatography. Head Space gas chromatography is particularly useful as it allows for rapid analysis for volatile components such as alcohol in wine. For metal analysis (such as copper), atomic absorption (AA) or Inductively Coupled Plasma (ICP) instruments should be considered.

Conclusion

The LAMBDA 25, 35, or 45 provides an accurate simple means to acquire high-quality spectra of wine and to calculate the required parameters automatically without the need to export to a spreadsheet or external program. The dual-beam optics and low-stray light ensure excellent performance with highly colored wine samples and the flexible reporting allows for customized reports to suit both internal and external clients.

Appendix

We have documented the UV WinLab method calculation processing chain should you wish to modify it or check the calculations. The method, as supplied, is ready to run so no modification or adjustment should be necessary.

Table 3. UV WinLab method calculation processing chain.

No	Process	Description	Equation
1	Equation	Adjust Absorbance Spectrum to 1cm pathlength	$All * 10 / \text{Pathlength}$
2	Equation	Absorbance at 420 nm	$Yval[All, 420]$
3	Equation	Absorbance at 520 nm	$Yval[All, 520]$
4	Equation	Absorbance at 620 nm	$Yval[All, 620]$
5	Equation	Color Intensity (CI)	$A420 + A520 + A620$
6	Equation	Color Hue	$A420 / A520$
7	Convert X	Convert absorbance to transmittance	No equation
8	Equation	Interpolate 380 to 780, Data Interval=5	No equation
9	Equation	K part 1 (not shown in results table)	$"Illuminant_D65.asc" * "Y_1964.asc"$
10	Equation	Final K calculation (not shown)	$100 / ([\text{Mean}[K \text{ part } 1]] * 160)$
11	Equation	X calculation part 1 (not shown)	$\text{Sample} * "X_1964.asc" * "Illuminant_D65.asc"$
12	Equation	Final X calculation	$[[[\text{Mean}[X \text{ part } 1]] * 160] * K] / 100$
13	Equation	Y Calculation part 1 (not shown)	$\text{Sample} * "Y_1964.asc" * "Illuminant_D65.asc"$
14	Equation	Final Y Calculation	$[[[\text{Mean}[Y \text{ part } 1]] * 160] * K] / 100$
15	Equation	Z Calculation part 1 (not shown)	$\text{Sample} * "Z_1964.asc" * "Illuminant_D65.asc"$
16	Equation	Final Z Calculation	$[[[\text{Mean}[Z \text{ part } 1]] * 160] * K] / 100$
17	Equation	x Calculation	$X \text{ part } 2 / [X \text{ part } 2 + Y \text{ part } 2 + Z \text{ part } 2]$
18	Equation	y Calculation	$Y \text{ part } 2 / [X \text{ part } 2 + Y \text{ part } 2 + Z \text{ part } 2]$
19	Equation	Y/Yn Calculation for 10 degree Obs	$Y \text{ part } 2 / 100$
20	Equation	X/Xn Calculation for 10 degree Obs	$X \text{ part } 2 / 94.811$
21	Equation	Z/Zn Calculation for 10 degree Obs	$Z \text{ part } 2 / 107.304$
22	Equation	L* Calculation	$116 * [([Yn]^{1/3}) - 16]$
23	Equation	a* Calculation	$500 * [([Xn]^{1/3}) - ([Yn]^{1/3})]$
24	Equation	b* Calculation	$200 * [([Yn]^{1/3}) - ([Zn]^{1/3})]$
25	Equation	Chroma (C*ab) Calculation	$\text{Sqrt}([[\text{Sqr}[a^*] + [\text{Sqr}[b^*]]])$
26	Equation	Standard Hue Angle Calculation using Pi variable (Pi())	$ATan[b^*/a^*] * 180 / \text{Pi}()$
27	Equation	Conditional Hue Angle Calculation using IF statements	$\text{if } [a^*] > 0 \text{ and } [a^*] > 0, hstar, \text{if } [a^*] < 0, [180 + hstar], \text{if } [b^*] < 0 \text{ and } [a^*] > 0, [hstar + 270], hstar]]$
28	Equation	S* Calculation	$Cstar / lstar$

References

Birse, M , Pollnitz, A, Herderich, M CIELab Colour Values: Enhanced Wine Colour Measurement for Use by the Wine Industry and in Research Applications, Poster by the Australian Wine Institute, Adelaide, Cooperative Research Centre for Viticulture, School of Agriculture and Wine, University of Adelaide.

Singleton VL, Orthofer R, Lamuela-Raventos RM. Analysis of total phenols and other oxidation substrates and antioxidants by means of Folin-Ciocalteu reagent. Meth Enzymol 1999; 99: 152-178.

Harbertson, J.F., Picciotto, E. A., and Adams, D.O. Measurement of Polymeric Pigments in Grape Berry Extract and Wines Using a Protein Precipitation Assay Combined with Bisulfite Bleaching , Am. J. Enol. Vitic. 54:4:301-306 (2003) r-Biopharm Kit.

Atomic Absorption

Authors:

Nick Spivey

Petrina Thompson

PerkinElmer, Inc.
Shelton, CT

Andrew Kavan

Elemental Scientific Inc.



The Analysis of Copper, Iron, and Manganese in Wine with FAST Flame Atomic Absorption

Introduction

With the growing popularity of wine consumption in China, regulations on the safety and quality of wine are being implemented. Recent wine imports into China are required to meet mandated elemental limits and are subject to local testing

upon arrival. If a wine does not meet the specifications listed in Table 1, it can be subject to destruction or return to its point of origin.

These elements are naturally occurring in wine grapes and, as such, are normally present in the wine produced from them. Concentrations of these elements can vary from region to region and from variety to variety due to the presence of nutrients in the soil the grapes are grown in, the uptake of these nutrients by the vine itself, and the process by which the wine is made. Because of this great variability, there is no way to ensure that a given wine meets the import specifications without undertaking analytical testing. Due to the possibility of the wine being rejected upon arrival into China and the financial impact this

represents, wine producers and exporters are interested in a simple and accurate method for determining the concentrations of elements of interest in their wine.

Table 1. Elemental limits on wines imported into China.

Element	Limit (mg/L)
Copper (Cu)	1
Iron (Fe)	8
Manganese (Mn)	2

Experimental

Nine different wines were acquired (Table 2) for the analysis of copper (Cu), iron (Fe), and manganese (Mn) using the conditions outlined in Table 3. All analyses were performed on a PerkinElmer PinAAcle™ 900T atomic absorption spectrometer operating in flame mode. A high-efficiency nebulizer was used with the standard spray chamber and a 10 cm burner head. External calibrations were created using a single intermediate standard made in 2% HNO₃/deionized water which was then diluted in-line using the capabilities of the PerkinElmer FAST Flame 2 sample automation accessory. The highest standard exceeded the concentrations of the upper regulatory limit for each element to ensure a broad range of detection capability. The wine samples were run directly without preparation other than spiking and were introduced with the use of the FAST Flame 2 accessory.

The FAST Flame 2 accessory is a combination of high-speed autosampler, peristaltic pumps and switching valve. It provides quick sample turnaround with fast rinse-out, short signal stabilization times and no sample-to-sample memory effect. The FAST Flame 2 sample automation accessory rapidly fills a sample loop via vacuum and then switches to inject the sample

loop while the autosampler moves to the next sample. This removes the wait time associated with self-aspiration or peristaltic pumping and the long rinse-in and rinse-out times associated with autosampler movement and flushing, resulting in sample-to-sample times as short as 15 seconds.

The ability of the FAST Flame 2 accessory to mechanically pump the sample during injection allows for ideal optimization of nebulizer and flame conditions, eliminates variability due to changes in sample viscosity, dissolved solids and tubing length, and also provides long-term sample flow stability. The in-line dilution capability allows the analyst to create a single intermediate standard, and then the FAST Flame 2 accessory automatically generates all calibration standards in-line, as required. In addition, the instrument can be set to identify QC over-range samples and then utilize the in-line dilution capability to automatically re-run a sample that falls outside the calibration range at an increased dilution factor to bring the signal within the calibration and provide accurate measurement along with a passed QC check.

Each wine sample was spiked at levels both below and above the regulatory limit to assess accuracy. The highest spike in each case was purposefully out of range of the calibration, and the instrument software identified and then auto-diluted the samples using the in-line capabilities of the FAST Flame 2 accessory. This demonstrates the ability of the PinAAcle 900 AA spectrometer coupled with FAST Flame 2 accessory to accurately and quickly assess samples at a wide range of concentrations without user intervention.

Results and Discussion

The calibration curves were created using the in-line dilution capabilities of the FAST Flame 2 accessory. Calibration results are shown in Table 4. The excellent correlation for the calibration standards demonstrates the value of the automatic in-line sample and standard dilution available on the FAST Flame 2 accessory. The independent calibration verification recoveries ensure that the calibration is valid and that the creation of standards via the dilution system is very accurate.

Table 2. Wines analyzed.

Type	Country of Origin	Identifier
Cabernet	Argentina	AR Cab
Cabernet	Australia	AU Cab
Cabernet	USA	USA Cab A
Cabernet	USA	USA Cab B
Chardonnay	Argentina	AR Chard
Chardonnay	Australia	AU Chard
Chardonnay	USA	USA Chard A
Chardonnay	USA	USA Chard B
Red Zinfandel	USA	USA Zin

Table 3. PinAAcle 900T instrument and analytical conditions.

Parameter	Copper (Cu)	Iron (Fe)	Manganese (Mn)
Wavelength (nm)	324.75	248.33	279.48
Slit (nm)	0.7	0.2	0.2
Air Flow (L/min)	2.5	2.5	2.5
Acetylene Flow (L/min)	10	10	10
Integration Time (sec)	3	3	3
Replicates	3	3	3
Sample Flow Rate (mL/min)	6	6	6
Intermediate Standard	20	40	20
Auto-Diluted Calibration Standards (mg/L)	0.5, 2, 5	1, 4, 10	0.5, 2, 5
Calibration Curve Type	Non-Linear Through Zero	Non-Linear Through Zero	Non-Linear Through Zero

Table 4. Calibration results.

Element	Correlation Coefficient	ICV Concentration (mg/L)	ICV (% Recovery)
Copper (Cu)	0.99999	2	101
Iron (Fe)	0.99999	4	99.4
Manganese (Mn)	0.99983	2	102

Tables 5-7 show the results for the analyses for copper, iron, and manganese, respectively. The results indicate that the wines are under the regulatory limits with the exception of the Australian chardonnay which is over the limit for manganese. From the limited samples analyzed, it appears that the 2 mg/L specification for manganese could be a critical parameter for qualification of a wine for importation into China. Spike recoveries for all elements are within 10% of the spiked values, even when spiked at or below half the regulated values and when diluted via the in-line dilution capability of the FAST Flame 2 sample automation accessory, demonstrating the excellent accuracy needed to ensure successful analysis.

The addition of the FAST Flame 2 accessory reduced the creation of standards from one intermediate and three final standards to a single intermediate standard with a commensurate reduction in human error during standard creation. The FAST Flame 2 accessory was also able to react to the over-range spikes and auto-dilute the samples accurately and consistently without interaction from an analyst, saving time and eliminating additional sample handling and re-prep.

These results demonstrate the robustness and accuracy of the analysis and the speed and increased productivity available from the PinAAcle 900 AA spectrometer and the FAST Flame 2 accessory.

Table 5. Copper in wine (regulated limit = 1 mg/L).

Wine	Measured Conc. (mg/L)	Measured Spikes			Spike Recoveries %		
		0.5 mg/L	1.0 mg/L	10.0 mg/L *	0.5 mg/L	1.0 mg/L	10.0 mg/L *
AR Cab	0.046	0.558	1.08	10.4	103	104	104
AU Cab	0.603	1.11	1.61	10.8	100	101	102
USA Cab A	0.088	0.579	1.11	10.3	98.3	102	102
USA Cab B	0.088	0.611	1.12	10.8	105	103	107
AR Chard	0.013	0.527	1.03	10.5	103	101	105
AU Chard	0.478	0.969	1.38	10.3	98.2	90.3	98.6
USA Chard A	0.120	0.637	1.15	10.7	104	103	106
USA Chard B	0.099	0.609	1.13	10.8	102	103	1076
USA Zin	0.256	0.746	1.20	10.1	98.0	94.2	98.6
* = 5X Online Dilution							

Table 6. Iron in wine (regulated limit = 8 mg/L).

Wine	Measured Conc. (mg/L)	Measured Spikes			Spike Recoveries %		
		1.0 mg/L	5.0 mg/L	20.0 mg/L *	1.0 mg/L	5.0 mg/L	20.0 mg/L *
AR Cab	1.80	2.72	6.78	21.4	92.1	99.5	97.9
AU Cab	2.18	3.20	7.35	22.8	103	104	103
USA Cab A	2.32	3.24	7.69	21.9	92.7	1085	98.1
USA Cab B	2.31	3.25	7.42	22.1	93.9	102	98.8
AR Chard	1.65	2.61	6.69	21.0	95.5	101	96.7
AU Chard	2.92	3.91	7.86	23.6	99.2	98.8	103
USA Chard A	1.68	2.67	6.62	21.3	98.7	98.8	98.1
USA Chard B	1.16	2.15	6.17	21.0	99.5	100	99.3
USA Zin	2.80	3.77	7.70	23.7	97.6	98.1	104
* = 5X Online Dilution							

Table 7. Manganese in wine (regulated limit = 2 mg/L).

Wine	Measured Conc. (mg/L)	Measured Spikes			Spike Recoveries %		
		1.0 mg/L	4.0 mg/L	10.0 mg/L *	1.0 mg/L	4.0 mg/L	10.0 mg/L *
AR Cab	1.36	2.31	5.20	11.0	95.0	95.9	96.0
AU Cab	1.93	2.90	6.07	12.3	97.1	104	104
USA Cab A	1.51	2.45	5.41	11.0	94.3	97.6	94.7
USA Cab B	1.50	2.45	5.45	10.9	94.5	98.8	93.9
AR Chard	1.01	1.98	5.03	10.5	97.2	101	94.4
AU Chard	2.09	3.07	6.29	12.4	97.2	105	103
USA Chard A	1.07	2.04	5.05	10.6	97.2	99.6	95.6
USA Chard B	0.968	1.94	4.96	10.8	97.1	99.8	97.8
USA Zin	1.67	2.66	5.85	11.9	98.6	105	102
* = 5X Online Dilution							

Conclusion

This work has demonstrated the ability of the PinAAcle 900 AA spectrometer to accurately measure Cu, Fe, and Mn in a variety of wine samples at levels which meet the regulations imposed by China for imported wine. Using the FAST Flame 2 sample automation accessory minimizes user errors when performing dilutions and making calibration standards, increasing sample throughput. For labs with low sample throughput, these same analyses can also be performed without the FAST Flame 2 sample automation accessory¹.

References

1. Neubauer K., Lim S., "The Analysis of Copper, Iron, and Manganese in Wine with the PinAAcle 500", PerkinElmer Application Note.

Consumables

Component	Part Number
Red/Red PVC Pump Tubing	N8145158
Black/Black PVC Pump Tubing	N8145153 (unflared) N8145202 (flared)
Autosampler Tubes	B0193233 (15 mL) B0193234 (50 mL)
Cu Hollow Cathode Lamp	N3050121
Fe Hollow Cathode Lamp	N3050126
Mn Hollow Cathode Lamp	N3050145
Pure-Grade Cu Standard (1000 mg/L)	N9300183 (125 mL) N9300114 (500 mL)
Pure-Grade Fe Standard (1000 mg/L)	N9303771 (125 mL) N9300126 (500 mL)
Pure-Grade Mn Standard (1000 mg/L)	N9303783 (125 mL) N9300132 (500 mL)

Gas Chromatography/
Mass Spectrometry

Clarus® SQ 8 GC/MS with TurboMatrix Headspace Trap System Application Pack for Monitoring Volatile Organic Compounds in Beer Production



Beer is a popular beverage produced by the fermentation of hopped malt extracted from barley and other grains. Although simple in concept, beer is a highly complex mixture of many compounds including sugars, proteins, alcohols, esters, acids, ketones and terpenes. Flavor is an important quality of any beer and the chemical content of the beer is responsible for that flavor. Aroma is also an extremely important part of the beer's trademark, so there is a strong interest by brewers in the volatile organic compounds (VOCs) in beer.

Some VOCs have a positive effect on aroma (attributes) and some have a negative effect (defects). The ability to characterize these in beer products before, during and after fermentation is an important tool in process control, quality assurance and product development. This application pack contains all the consumables needed to perform your analysis.

Monitoring Volatile Organic Compounds in Beer Production Application Pack**Part No. N9300908**

Pack includes one of each of the following items (some items may ship separately):

Description	Part No.
Application note: Monitoring Volatile Organic Compounds in Beer Production Using the Clarus SQ 8 GC/MS and TurboMatrix™ Headspace Trap Systems	
Elite-5 Column Length: 60 m, Inner Diameter: 0.25 mm, Film Thickness: 1.00 µm, Temperature Limits: -60 to 325/350 °C	N9316080
2 mm Split Mode Quartz Liner for Programmable Split/Splitless Injector	N6121004
Thermogreen Low Bleed Injector Port Septa – 6/Pkg.	N6101748
Graphite/Vespel Ferrules, 1/16 in x 0.4 mm – 10/Pkg.	09920104
20 mL PTFE/Silicone Convenience Kit: contains 20 mm PTFE/Silicone assembly (100/pack), 22 mL crimp clear vials (100/pack) with write on patch and 20 mm caps (100/pack)	N9303992
TurboMatrix Air Monitoring Headspace Trap	M0413628
Ferrules for PTFE Cold Trap – 10/Pkg.	L4275110
Marathon Filament for GC/MS	N6470012
Ergonomic Manual 20 mm Hand Crimper	N6621037
<i>All contents can be ordered individually.</i>	

Every day, you can count on PerkinElmer to provide you with solutions that deliver reliable performance, control operating costs and maximize operational time. Our complete portfolio of consumables, part, supplies, training and service helps you meet both routine and demanding measurement challenges. We invest heavily in testing and validating our products to ensure you receive guaranteed compatibility and performance – on-time, for every instrument in your laboratory.

For complete listing of consumables and supplies, please visit www.perkinelmer.com/gcsupplies

PerkinElmer, Inc.
940 Winter Street
Waltham, MA 02451 USA
P: (800) 762-4000 or
(+1) 203-925-4602
www.perkinelmer.com



For a complete listing of our global offices, visit www.perkinelmer.com/ContactUs

Copyright ©2011, PerkinElmer, Inc. All rights reserved. PerkinElmer® is a registered trademark of PerkinElmer, Inc. All other trademarks are the property of their respective owners.

009790_01



Gas Chromatography – Mass Spectrometry

Author

Andy Tipler

PerkinElmer
Shelton, CT USA

The Determination of Low Levels of Nitrosamines in Beer Using the Clarus 680 GC/MS and a D-Swafer System

Introduction

Nitrosamines are a class of compounds that are often found in food and other organic products. They are highly carcinogenic and many countries apply controls on the acceptable levels of these compounds in food. Nitrosamines are formed as food is heated through the reaction of amines with nitrites, which are sometimes added as a preservative.

Malt and its derivative products are of particular concern and beer represents (along with fried bacon and tobacco) the major source of ingested nitrosamines in humans. Historically, malt was roasted over open fires and the nitrogen oxide gases in the smoke would react with amines in the malt to form nitrosamines. Modern malt production uses indirect fire roasting and the levels of nitrosamines have consequently dropped significantly – by a factor of over 50x from malt produced 20 years ago.

Nitrosamines generated during malt production will pass into beer. Examples of maximum acceptable levels of nitrosamines in beer are 5 µg/kg in the United States, 0.5 µg/kg in Italy, Switzerland and Germany and 2-15 µg/kg in Russia.

The main compound that is monitored in malt and beer is nitrosodimethylamine (NDMA). This compound and its homolog, nitrosodiethylamine (NDEA) are the compounds targeted in this application note.

To determine NDMA and NDEA at low concentrations in beer typically involves a liquid-liquid extraction followed by a multi-step extensive sample clean-up regime and determination by gas chromatography, including a highly specific and selective detector, such as a thermal energy analyzer (TEA) detector.

In this application note, we present a more efficient and rapid method of analysis. It uses a fast and simple single-step liquid-liquid extraction technique followed by direct injection of the extract into a GC/MS system for separation and quantification.

A Swafer™ heartcutting system is used to selectively transfer timed cuts of the effluent, that contain the analytes, from one GC column into the inlet of a second column with a different stationary phase. This technique eliminates the solvent and bulk of other compounds extracted from the sample matrix from the chromatography in the second column, which provides an extra level of analytical selectivity and reduces the need for the sample clean-up procedures.

A quadrupole MS detector system was used in electron ionization mode to monitor the chromatography on the second column. This approach means that more sample residue is likely to accumulate over time in the injector liner, but liner replacement is a much easier option than a multi-stage sample clean-up regime. To achieve the detection limits sought, data collection used single ion recording (SIR). This provided another degree of selectivity to overcome potential matrix interferences.

A second detector (flame ionization) was used to monitor the chromatography on the precolumn and establish the heartcut and the backflush timings.

Experimental

Instrumentation

Figure 1 gives a schematic diagram of the analytical system, which is from the Swafer Utilities Software that was used to develop this method. Table 1 lists the full operating conditions for the final method.

Table 1. Analytical Conditions for the Determination of Nitrosamines in Beer.

Gas Chromatograph	PerkinElmer Clarus 680
Oven Temperature	35 °C for 1 min., then 10 °C/min. to 185 °C (16-minute run)
Injector	Programmable Split/Splitless (PSS)
Injector Temperature	35 °C for 1 min., then 200 °C/min. to 250 °C and hold until the end of the run
Carrier Gas	Helium
Injector Pressure	Initially 27 psig then 2 psig at 12.81 min. Maintained at 2 psig during oven cooldown.
Injector Split Flow Rate	Initially Off, then 25 mL/min. at 3 min.
Detector	a) Flame Ionization (FID) b) Mass Spectrometer (MS)
FID Temperature	250 °C
FID Combustion Gases	Air: 450 mL/min., Hydrogen: 45 mL/min.
FID Range	x1
FID Attenuation	x4
MS Transfer Line Temperature	200 °C
MS Filament Temperature	200 °C
MS Data Collection	a) SIR m/z 74 from 12.00 – 13.50 min. (for NDMA) b) SIR m/z 102 from 15.00 – 16.00 min. (for NDEA) Dwell Time 0.5 sec Interchannel Delay 0.02 sec
Switching/Backflush System	D-Swafer configured in D4 mode
Precolumn	30 m x 0.250 mm x 0.25 µm PerkinElmer Elite™ 1
Analytical Column	30 m x 0.250 mm x 0.25 µm PerkinElmer Elite Wax (connected to MS)
Restrictor Tubing	51 cm x 0.100 µm deactivated fused silica (connected to FID)
(Midpoint) Pressure at D-Swafer	18 psig throughout
Timed Events	PSS Pressure set to 27 psig at -1.50 min. (to raise pressure after oven cooldown) PSS Split Flow set to 0 mL/min. at -1.00 min. (for splitless mode) PSS Split Flow set to 25 mL/min. at 3.00 min. (to vent liner) Switching Valve On at 9.27 min. (to cut NDMA) Switching Valve Off at 9.48 min. Switching Valve On at 12.60 min. (to cut NDEA) Switching Valve Off at 12.80 min. PSS Pressure set to 2 psig at 12.81 min. (to backflush)
Sample Injection	Normal injection of 3.0 µL of sample dichloro-methane extract using an autosampler

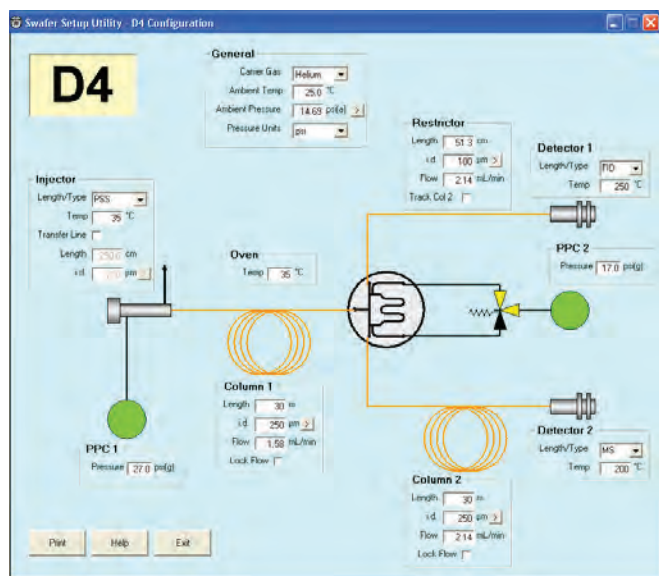


Figure 1. Swafer Utilities Software used for the determination of nitrosamines in beer.

Sample Preparation

Approximately 25 mL of the beer sample was poured into a 50 mL beaker and placed in a cool ultrasonic bath for two minutes to de-gas the sample.

10.0 \pm 0.5 g of de-gassed beer were weighed to a precision of 0.01 g into a 15-mL polypropylene centrifuge tube.

1-mL of 1.0 M sodium hydroxide solution prepared in de-ionized water and 3.0 \pm 0.1 g of crystalline sodium chloride were added to the sample and shaken to dissolve the salt.

1-mL of dichloromethane was added using a Grade-A bulb pipette and carefully shaken with a gentle rocking motion with the treated beer sample for 10 minutes. Vigorous shaking was avoided to minimize the formation of emulsions.

The tube was centrifuged at high speed for 20 minutes. In instances where emulsions had formed, the contents of the tube were rocked backwards and forwards a few times and then re-centrifuged (this was usually effective at breaking up the emulsion). An example of a successful extraction is given in Figure 2.



Figure 2. Example of successful beer extraction.

Using a dropper pipette, a sufficient volume of the lower organic layer was transferred directly into an autosampler vial for GC analysis. Note that it was not necessary to transfer the whole extract. Care was taken to ensure that none of the aqueous phase was transferred to the vial along with the extract. The vial was sealed with a suitable cap and refrigerated until analysis.

Method Development

Figure 3 shows a TIC of a concentrated standard mixture containing a series of nitrosamines including NDMA and NDEA. In this chromatogram, the D-Swafer has been set to direct the effluent from the precolumn into the analytical column, which is connected to the mass spectrometer. In practice we will need to see nitrosamines at a concentration below the 1 ppb level in the samples (equivalent to 10 ppb in the extracts). This is more than 1000x less than the concentration shown here.

Another point that should be mentioned is the role of the PSS injector in this analysis. The sample extracts are in dichloromethane. This is a highly volatile solvent that boils at 40 °C (at atmospheric pressure). It is not a good solvent to use for splitless injection as it is difficult to refocus at the column inlet. The injection of large volumes will easily cause injector blow-out and cause peak distortion and loss of injected sample. In this method the PSS is set to a low temperature (35 °C) during injection and then heated to vaporize the rest of the injected sample. This provides a much more controlled vaporization process and the 3 μ L injection volume provides symmetrical and well separated peaks as shown in Figure 3. One concern in using the PSS at low temperatures like this is the time needed to cool the injector back to this temperature before the next run. The Clarus® 680 PSS uses an optimized heatsink and a high-speed dedicated cooling fan to achieve this cooling in less than four minutes.

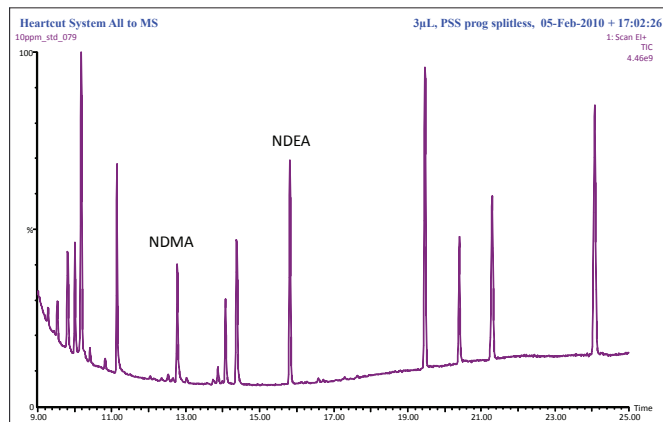


Figure 3. Total ion chromatogram (m/z 35 to 150) from a 3 μ L injection of a 10 ppm standard mixture of nitrosamines with the precolumn effluent directed to the second column and the MS detector.

The concern regarding detection limits is illustrated in Figure 4. This shows a TIC obtained from a beer extract run under the same conditions as used for Figure 3. The chromatogram is plotted with an expanded time scale but with a similar response scale. Expected elution times of the two nitrosamines are indicated. We need to see peaks at less than 1000x the size of those shown in Figure 3 without significant interference from co-eluting peaks from the sample matrix. This is clearly a challenge using this type of method as much better sensitivity and much better selectivity are needed.

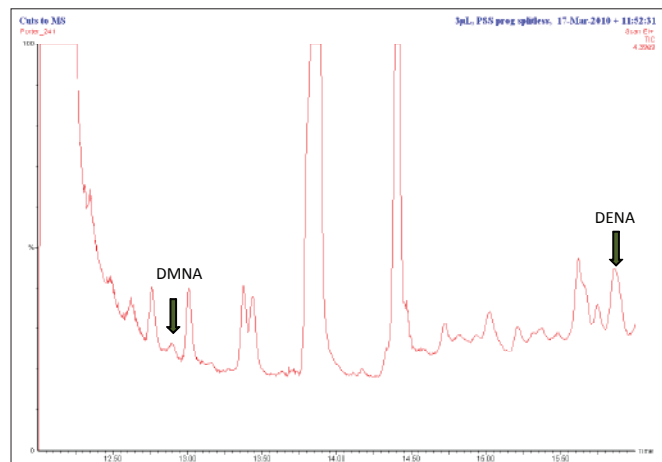


Figure 4. Total ion chromatogram of an extract taken from an American porter ale sample with the precolumn effluent directed to the second column and the MS detector.

Better sensitivity and selectivity are easily obtained on a quadrupole mass spectrometer by operating it in the SIR mode.

Figure 5 and Figure 6 give the structures and mass spectra of the two nitrosamines being monitored. These figures were taken from the NIST® Mass Spectral Search Program v. 2.0 supplied with the Clarus 680 MS system. In each case there is a strong molecular ion at m/z 74 and m/z 102 for NDMA and NDEA respectively. These ions were used in a SIR MS method to collect and process the data.

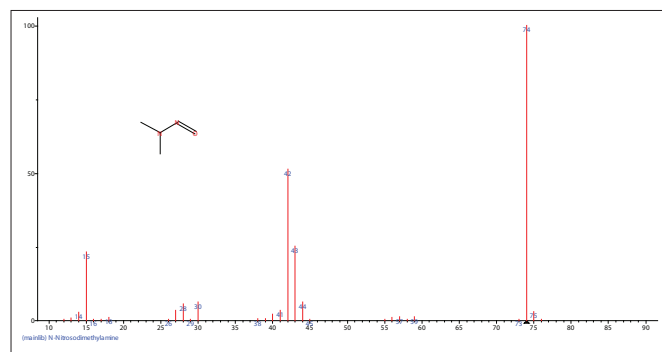


Figure 5. Structure and mass spectrum of nitrosodimethylamine.

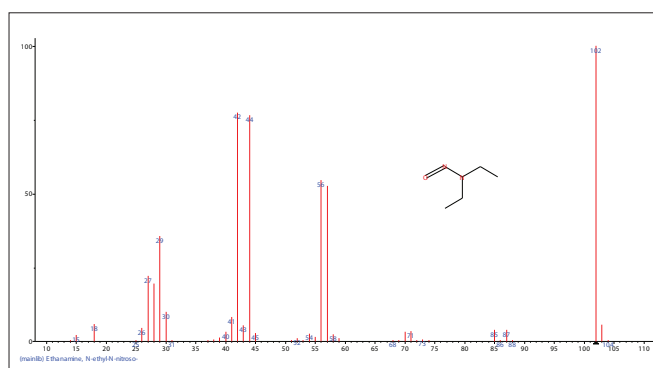


Figure 6. Structure and mass spectrum of nitrosodiethylamine.

Figure 7 shows chromatography of a much more dilute standard mixture of nitrosamines under the same conditions as used for Figure 3 and Figure 4. These peaks would represent nitrosamine concentrations of 1 ppb in the samples, and clearly indicate the potential to detect nitrosamines at levels below 1 ppb in the samples.

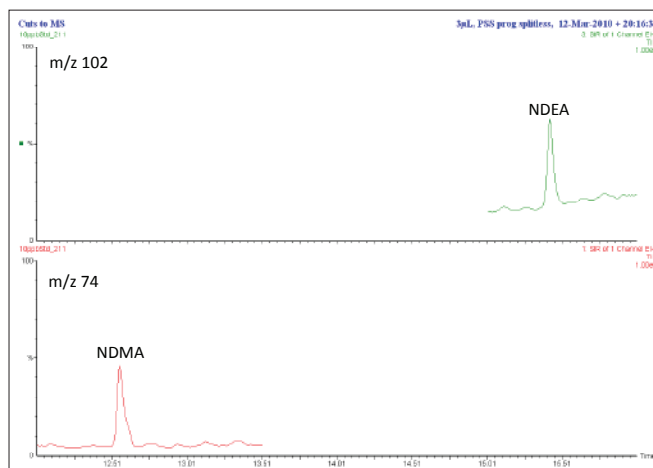


Figure 7. SIR chromatographic traces at m/z 74 and 102 showing expected elution times of NDMA and NDEA respectively from an injection of a 10 ppb stand mixture of nitrosamines (equivalent to 1 ppb in samples).

However, when a beer extract is chromatographed as shown in Figure 8 under the same conditions as used for Figure 7, there are significant interferant peaks in the chromatography that would obscure the nitrosamine peaks at the required levels. This chromatogram has the same scaling as Figure 7. Some further improvements to the selectivity are required.

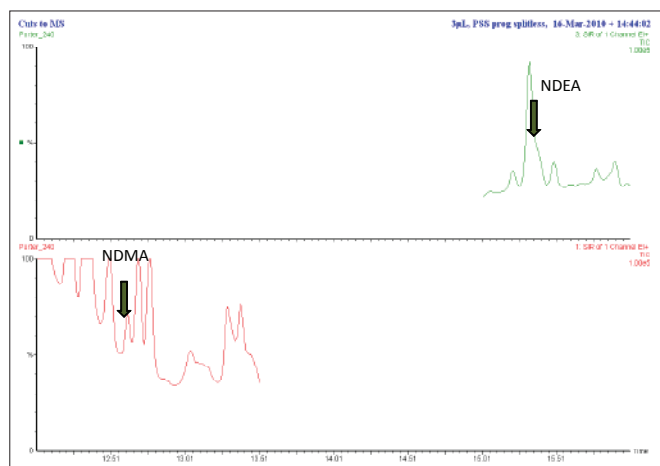


Figure 8. SIR traces at m/z 74 and 102 showing expected elution times of NDMA and NDEA respectively.

The use of the D-Swafer in the D4 heartcutting configuration provides an additional high degree of selectivity by transferring narrow cuts around the elution times of the nitrosamines from the precolumn on to the analytical column. This way, the solvent and the bulk of the extracted sample matrix are eliminated completely from the chromatography being monitored. Because the analytical column stationary phase is very polar, peaks that would co-elute with the nitrosamines on the non-polar precolumn and cut with them to the analytical column, would become separated by the different stationary phase. Figure 9 shows chromatography of the concentrated nitrosamine standard mixture indicating the regions around the eluting nitrosamines that are to be heartcut to the analytical column.

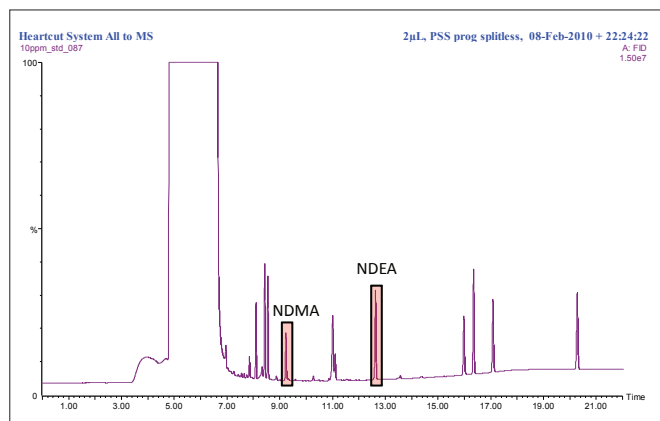


Figure 9. Precolumn chromatogram of 10 ppm nitrosamine standard mixture. This chromatogram was produced with the precolumn effluent switched to the D-Swafer outlet restrictor and the FID. The regions to be heartcut are highlighted.

Figure 10 shows a chromatogram from the same beer extract shown in Figure 4 and Figure 8, which was run under the same conditions used for Figure 9 but with the heartcutting switching applied. The heartcut regions are indicated by the drop in signal from the FID. After the NDEA peak has been heartcut, the pressure at the GC injector is reduced to a low value to initiate backflushing of the pre-column. This is indicated by the absence of chromatography beyond the last heartcut. Backflushing helps keep heavy sample material out of the Swafer and the detector, eliminates the need for extended temperature programming to elute heavy sample material from the system and reduces the analysis time.

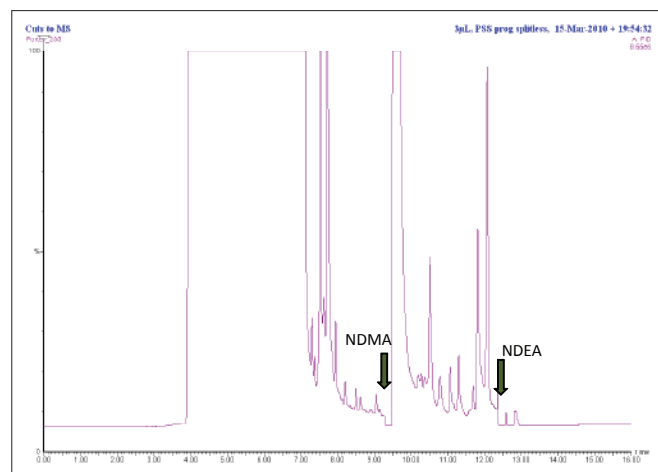


Figure 10. FID precolumn chromatogram of an American porter ale extract showing regions that have been heartcut to the analytical column.

Figure 11 shows the corresponding SIR chromatography of the heartcuts directed to the analytical column illustrated in Figure 10. Now the traces are very clean and the nitrosamine peaks, which are 0.39 ppb and 0.11 ppb for NDMA and NDEA respectively are seen and quantified with confidence. Compare these chromatograms against those in Figure 8 to see the improvements in selectivity brought about by the D-Swafer heartcutting technique.

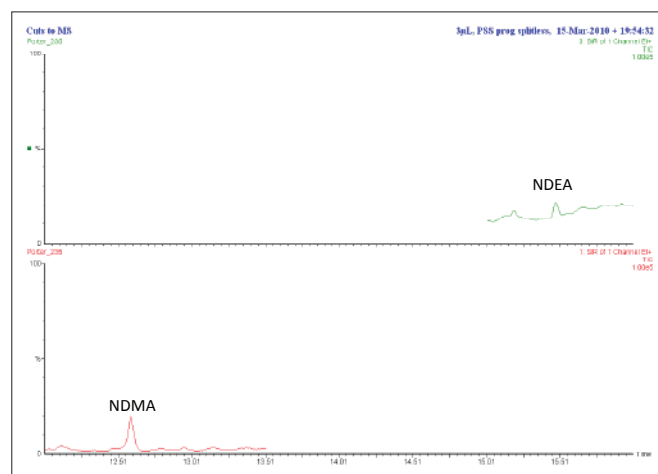


Figure 11. Analytical column SIR chromatography of an American porter ale extract.

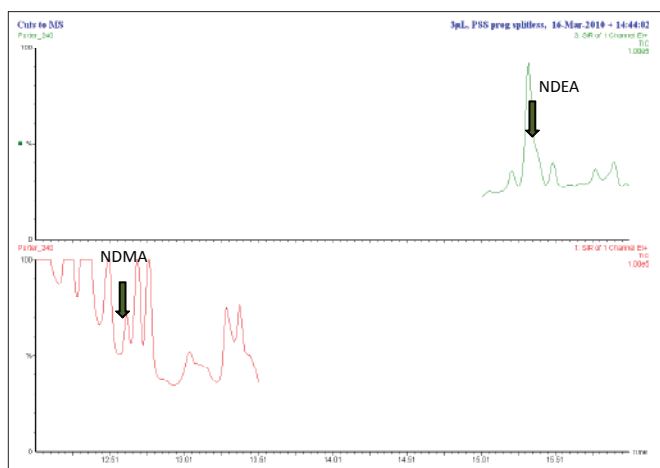


Figure 8. SIR traces at m/z 74 and 102 showing expected elution times of NDMA and NDEA respectively.

The use of the D-Swafer in the D4 heartcutting configuration provides an additional high degree of selectivity by transferring narrow cuts around the elution times of the nitrosamines from the precolumn on to the analytical column. This way, the solvent and the bulk of the extracted sample matrix are eliminated completely from the chromatography being monitored. Because the analytical column stationary phase is very polar, peaks that would co-elute with the nitrosamines on the non-polar precolumn and cut with them to the analytical column, would become separated by the different stationary phase. Figure 9 shows chromatography of the concentrated nitrosamine standard mixture indicating the regions around the eluting nitrosamines that are to be heartcut to the analytical column.

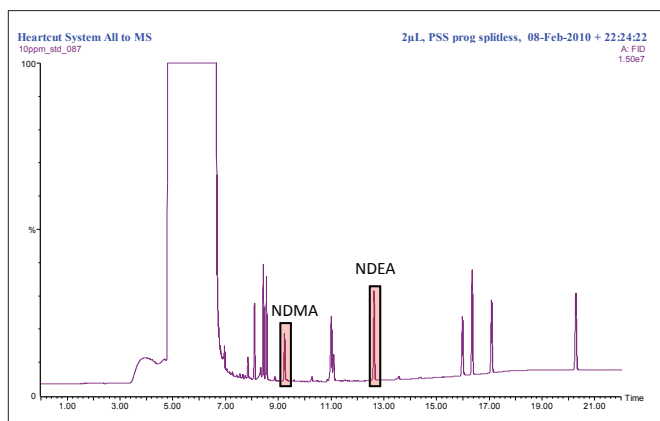


Figure 9. Precolumn chromatogram of 10 ppm nitrosamine standard mixture. This chromatogram was produced with the precolumn effluent switched to the D-Swafer outlet restrictor and the FID. The regions to be heartcut are highlighted.

Figure 10 shows a chromatogram from the same beer extract shown in Figure 4 and Figure 8, which was run under the same conditions used for Figure 9 but with the heartcutting switching applied. The heartcut regions are indicated by the drop in signal from the FID. After the NDEA peak has been heartcut, the pressure at the GC injector is reduced to a low value to initiate backflushing of the pre-column. This is indicated by the absence of chromatography beyond the last heartcut. Backflushing helps keep heavy sample material out of the Swafer and the detector, eliminates the need for extended temperature programming to elute heavy sample material from the system and reduces the analysis time.

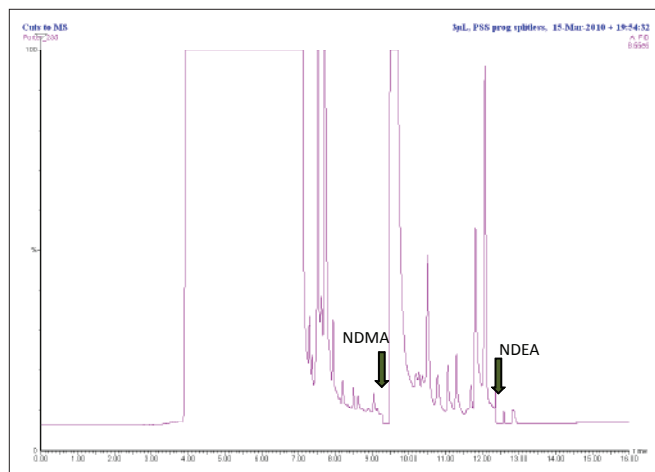


Figure 10. FID precolumn chromatogram of an American porter ale extract showing regions that have been heartcut to the analytical column.

Figure 11 shows the corresponding SIR chromatography of the heartcuts directed to the analytical column illustrated in Figure 10. Now the traces are very clean and the nitrosamine peaks, which are 0.39 ppb and 0.11 ppb for NDMA and NDEA respectively are seen and quantified with confidence. Compare these chromatograms against those in Figure 8 to see the improvements in selectivity brought about by the D-Swafer heartcutting technique.

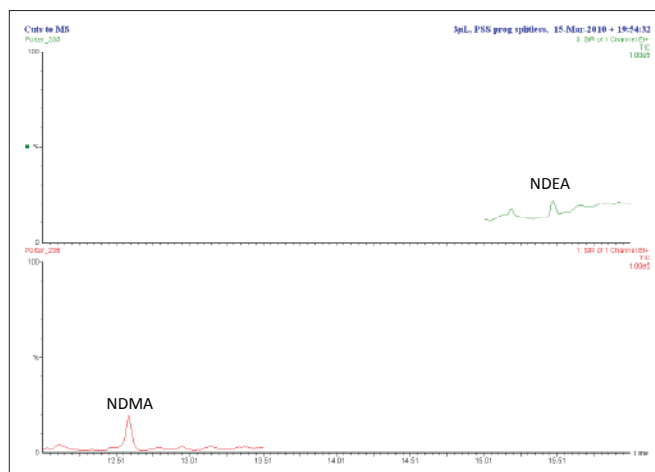


Figure 11. Analytical column SIR chromatography of an American porter ale extract.

Performance

Using these conditions, the performance of the system was checked using standard mixtures of known concentrations. Figure 12 and Figure 13 show the calibrations for NDMA and NDEA respectively over a range of effective sample concentrations from 0.05 ppb or less to 2.0 ppb. Excellent linearity for this method is demonstrated for both analytes.

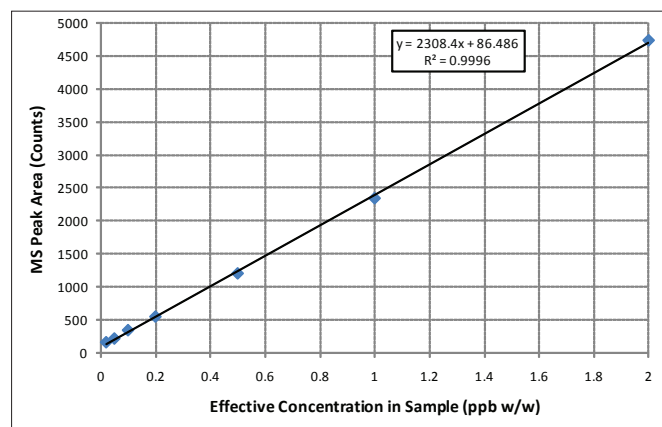


Figure 12. Calibration data for NDMA.

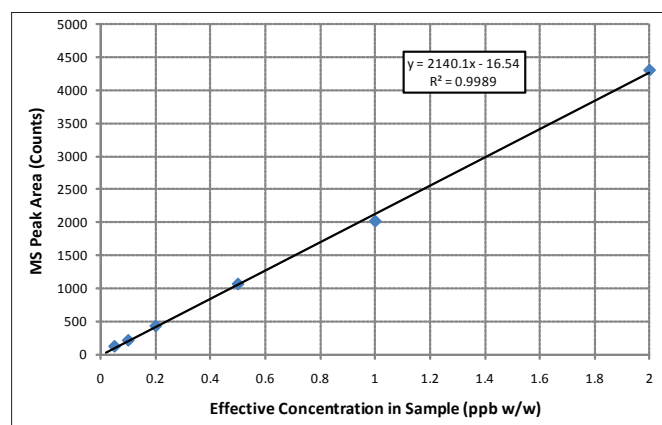


Figure 13. Calibration data for NDEA.

Results from Beer Samples

A variety of commercial beers were purchased from a local store and samples of home brewed beer (all grain recipes) were extracted and chromatographed using this method. The results are given in Table 2. All results are well within the USA FDA guideline of 5.0 ppb (CPG 510.600).

Table 2. Results obtained from various beer samples.

Sample	NDMA (ppb)	NDEA (ppb)
Oktoberfest (Germany)	<0.02	<0.05
IPA (USA)	0.09	<0.05
English Bitter (Home Brew)	0.08	<0.05
Pilsner Lager (Home Brew)	<0.02	<0.05
Imperial Stout (USA)	0.25	<0.05
Coffee Porter (USA)	0.39	0.11
IPA-B (USA)	0.08	<0.05
Pale Ale (Home Brew)	0.16	<0.05
Paler Ale (USA)	0.14	<0.05

Making the Method More Robust

The use of an internal standard would improve the robustness of the method by reducing errors that result from partitioning the solvent into the sample or evaporation of the solvent during sample handling.

A deuterated form of NDMA was obtained and added at the 50 ppb level (equivalent to 5 ppb in the sample) to the dichloromethane extraction solvent. This NDMA-D6 compound had a primary (molecular) ion of m/z 80 in its mass spectrum so the SIR method was adjusted to also monitor the signal at this mass.

This deuterated compound is a perfect internal standard as it is chemically equivalent to the NDMA being determined and is subjected to the same sources of error.

Figure 14 shows chromatography of a standard mixture that included the internal standard.

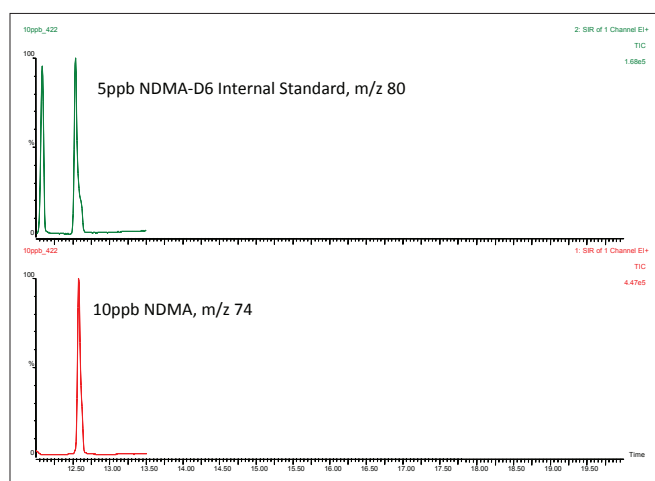


Figure 14. Chromatography of a standard mixture showing peaks for both NDMA and NDMA-D6 internal standard. Concentrations reflect those in the sample.

Figure 15 shows a calibration profile for the response ratio versus the concentration ratio for NDMA versus NDMA-D6. Excellent linearity is demonstrated at levels down to 0.1 ppb.

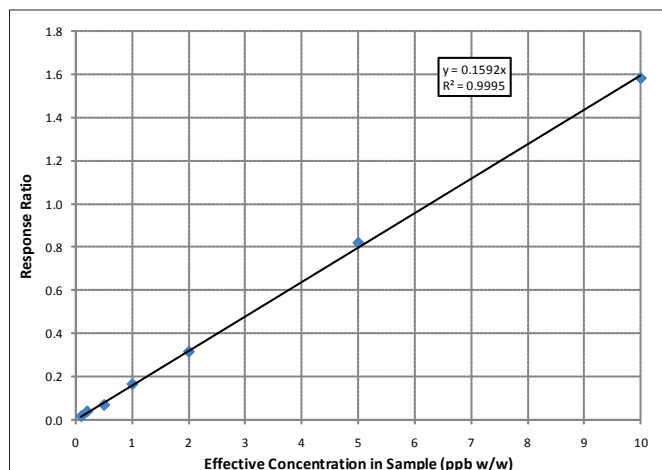


Figure 15. Calibration data for NDMA based on ratio to internal standard response.

Table 3 shows the instrumental precision obtained for multiple injections of the same standard mixture of NDMA and NDMA-D6. A relative standard deviation of 2.5% for the quantitative precision is excellent for this type of analysis – low level analytes in a very dirty sample matrix.

Table 3. Precision data obtained for NDMA using NDMA-D6 internal standard.	
n	10
Mean Result (ppb)	2.27
RSD %	2.46

Another set of beer samples was selected for analysis. These were strong beers (apart from the American cream ale) with final alcohol concentrations of 7 to 10 ABV% so significant amounts of malt were used in their production. This is a severe test for the method as interferences from the sample matrix will be higher.

Figure 16 shows chromatography of an extract taken from one of the strong beer samples and Table 4 summarizes the results for all the samples tested.

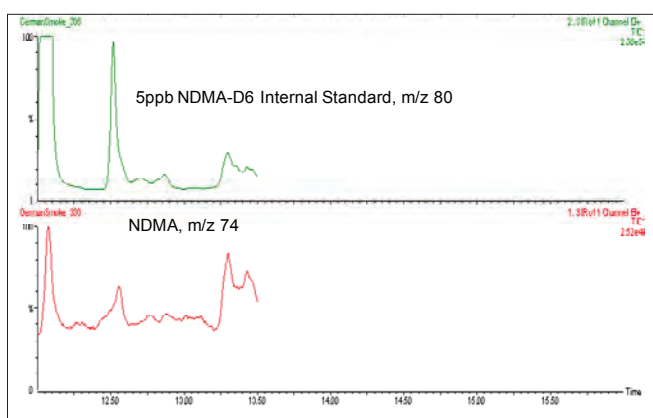


Figure 16. Chromatography of extract taken from Czech dark lager sample using DMA-D6 internal standard.

Table 4. Results from various beer samples.

Beer Sample	NDMA (ppb)
Polish Porter	0.43
German Rauchbier	0.32
Russian Porter	0.80
Italian Birra Blonde	0.22
USA Cream Ale	<0.2
Czech Dark Lager	0.76

Extending the Method to Other Nitrosamines

Although the initial work focused on two nitrosamines, this method may be easily adapted to monitor other nitrosamines.

Figure 17 through Figure 19 shows how the method was extended to include nitrosopyrrolidine (NPYR) by simply adding another heartcut and extending the run time.

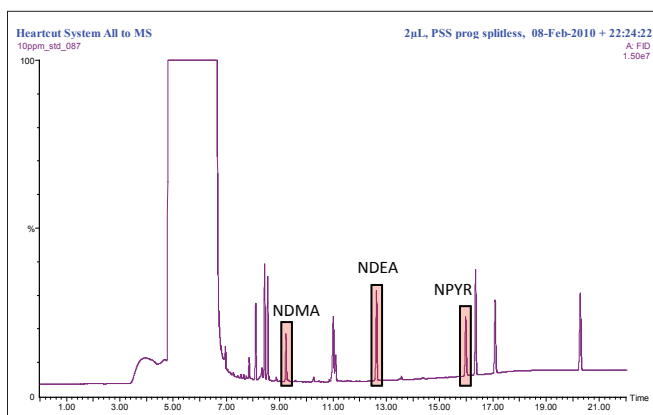


Figure 17. Precolumn FID chromatogram of 10 ppm standard mixture showing elution of NPYR and suggested additional heartcut times.

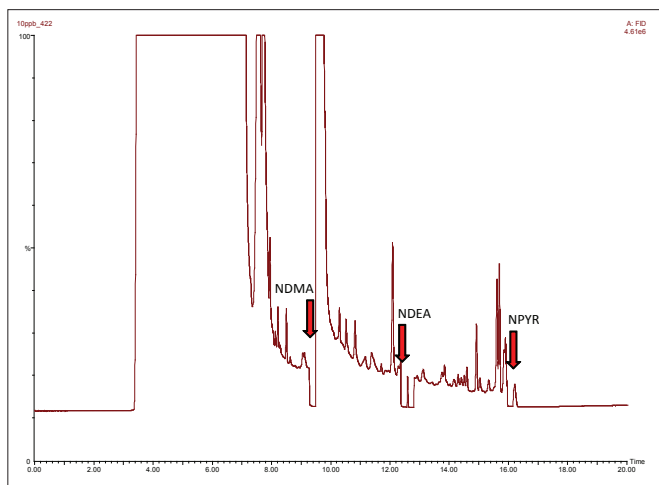


Figure 18. Precolumn FID chromatogram of beer extract showing cuts transferred to analytical column. Temperature program was extended to 225 °C and chromatographic run time was extended to 20 minutes.

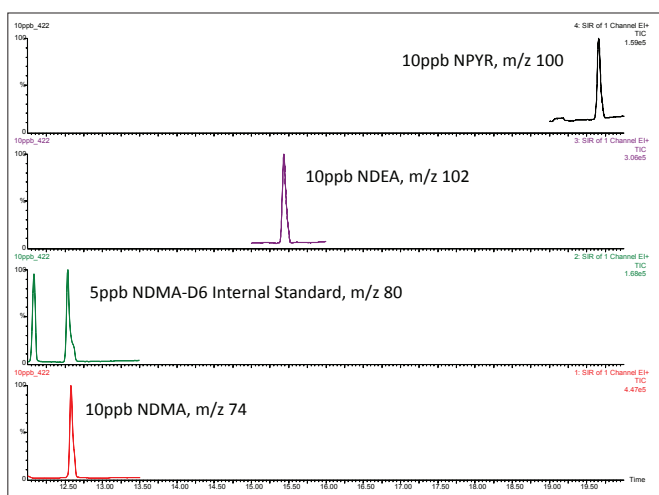


Figure 19. Analytical column SIR chromatography of spiked beer sample showing three analytes and the internal standard.

Conclusion

The need for methods to determine the levels of nitrosamines in beer has been a requirement for many years. Over time, a succession of different methods were developed yet need extensive sample clean-up, concentration procedures and exotic detection systems. The method presented in this application note uses a very simple and straightforward single-step extraction procedure with a minimum of solvent (1 mL). Sample extracts are much 'dirtier' than those produced in other methods but the combination of the heartcutting technique with SIR data collection on a mass spectrometer delivers the necessary selectivity without compromising the detection limits.

The combination of the heartcut technique and the fast cooling oven and PSS injector of the Clarus 680 enables the total chromatographic cycle time to be reduced to less than 20 minutes.

Examples have been shown in which nitrosamines in beer are seen at levels of 0.1 ppb or even lower.

Although this method is targeted towards beer analysis, it can be applied to the analysis of nitrosamines in other sample types.

Atomic Absorption

Author:

Riccardo Magarini

PerkinElmer, Inc.

Milano, Italy



Elemental Analysis of Beer by Flame Atomic Absorption Spectrometry with the PinAAcle 900 AAS

Introduction

Beer is a widely consumed beverage with both organic and inorganic components. The concentrations of the inorganic components may vary depending on raw materials and brewing processes. Knowledge of

the type and concentration of inorganic components in beer is of considerable interest from various perspectives, as they may affect taste, appearance, product stability, and health of the consumer¹. The determination of elements in beer by flame atomic absorption spectrometry (FAAS) is a well-known procedure². For example, the American Society of Brewing Chemists (ASBC) in St. Paul, Minnesota, USA, is proposing the regular determination of calcium (Ca), copper (Cu), iron (Fe), and sodium (Na) in beer by FAAS³.

FAAS has the benefit of providing precise and accurate measurements at a lower cost per element than more advanced elemental techniques, and also requires less operator training than many other trace elemental techniques. The PinAAcle™ 900 FAAS provides an intuitive, highly efficient system capable of simplifying analyses while maintaining peak performance and unmatched productivity.

Experimental

Instrumentation

All measurements were performed on a PerkinElmer PinAAcle 900T atomic absorption spectrometer equipped with high sensitivity nebulizer (HSN) and ceramic impact bead. An air-C₂H₂ flame with a 10 cm 3-slot solid titanium burner head was used for the determination of copper (Cu), iron (Fe), zinc (Zn), and manganese (Mn). Aluminum (Al) was determined with N₂O-C₂H₂ flame on a 5 cm solid titanium burner head. A nebulizer spacer was used for calcium (Ca) and sodium (Na) to reduce sensitivity, and for Al to improve N₂O flame stability and minimize interferences. Lumina™ cableless hollow cathode lamps were used for all elements.

Sample Preparation

Several brands of beer were purchased in a local supermarket in Singapore. When available, the same brand was purchased in two different packaging materials: a glass bottle and a metal can. A total of five bottled and six canned beers were analyzed. Sample aliquots for analyses were obtained by pouring the beers in 50 mL polyethylene autosampler tubes with caps. Samples were degassed of CO₂ by ultra-sonication at full power for 30 minutes and then acidified to 2 % (v/v) with HNO₃ (70 % w/v, Clean Room Chemical, Air Products and Chemicals Inc, Allentown, Pennsylvania, USA).

All elements were measured against external calibration curves with linear-through-zero regression, except Na, which used a non-linear through zero regression. Standards were prepared by serial dilutions of 1000 mg/L PerkinElmer Pure single-element standards in 2 % HNO₃ (v/v).

Elements usually present at trace levels (Al, Cu, Fe, Mn, and Zn) were determined directly in the undiluted beers. The calibration solutions for these elements were prepared in 5 % (v/v) ethanol (99.5 % GR grade, Kanto Chemical Co. Inc., Japan) for matrix matching. For Al determination, 0.2 % lanthanum (La) (w/v) was

added to all samples and standards as an ionization buffer (La₂O₃ 99.5 % LAB grade, Merck, Germany).

For the determination of Ca and Na, the samples were diluted 30 fold with ≥ 18 MΩ ultrapure water (MilliQ system, Millipore, Billerica, Massachusetts, USA). Calibration standards were prepared in 1 % HNO₃ (v/v). No ethanol was added, due to the dilution factor. La 0.2 % (w/v) was added as a releasing agent (to avoid phosphate suppression on Al) and as an ionization suppressant for Na and Ca (releasing agents are cations that react preferentially with an interferent). Table 1 shows the instrumental conditions used for this work.

Results and Discussion

Each beer sample was given a number to identify the brand and container type. Samples labeled “G” were from glass bottles, while samples labeled “M” were from metal cans. Results, reported in Table 2, show that Ca and Na are present at high concentrations (mg/L), while other elements are present at µg/L levels, as expected. The data showed good quality for all beers tested, with respect to their elemental contents, based on the current ASBC guidelines. These results indicate that the container material (glass or can) does not significantly contribute to the element content of the beer, with the exception of Mn, which is always a little higher in the bottled beers.

Due to the low level of Al in the beer samples tested, it could not be detected by FAAS in most samples. Instead, a more sensitive technique, such as graphite furnace atomic absorption spectrometry (GFAAS), should be used for Al determination. The PinAAcle 900T (and 900H) can easily be switched between flame and graphite furnace modes, offering the capability to determine the low concentration elements by GFAAS using a single system. For analysis using flame-only atomic absorption, the PinAAcle 900F is also available.

Table 1. Instrument settings for the analysis of beer.

Element	Wavelength (nm)	Slit (nm)	Lamp Current (mA)	Units	Calibration Standards	Air (L/min)	Nitrous Oxide (L/min)	Acetylene (L/min)
Al	309.27	0.7	25	mg/L	2, 5	---	10.0	7.98
Ca	422.67	0.7	10	mg/L	0.5, 0.8, 2.5	8.68	---	2.48
Cu	324.75	0.7	15	µg/L	40, 100, 200	10.0	---	3.16
Fe	248.33	0.2	30	µg/L	100, 250, 500	10.0	---	3.16
Mn	279.48	0.2	20	µg/L	50, 125, 250	10.0	---	3.16
Na	589.00	0.2	8	mg/L	0.5, 0.8, 2.5	8.68	---	2.48
Zn	213.86	0.7	15	µg/L	50, 125, 250	10.0	---	3.16

Table 2. Results for the analysis of multiple beer samples using flame atomic absorption.

Sample	1M	2G	3M	3G	4M	4G	5M	5G	6G	7M	7G
Al (mg/L)	0.14	ND	ND	ND	ND	ND	ND	ND	ND	0.19	ND
Ca (mg/L)	79	104	72	93	139	143	107	143	96	77	76
Cu (µg/L)	35	31	63	62	37	33	45	44	46	36	35
Fe (µg/L)	43	42	45	31	22	30	52	68	54	25	25
Mn (µg/L)	62	144	107	136	87	118	123	153	190	64	72
Na (mg/L)	40	47	35	46	86	82	72	69	207	196	187
Zn (µg/L)	2.4	0.7	6.1	3.6	1.2	0.3	2.5	29	1.2	4.4	5.3

ND = not detected

Quality Control

For beer analysis, there are no certified reference materials (CRMs) available with certified elemental content. For this reason, quality control (QC) procedures were implemented by running selected samples in duplicate and after performing a spike to demonstrate the method's capability for precision and recovery. Due to the spread in concentration levels, spike additions were performed at mid-range of calibration curves, to provide a detectable signal increase (Table 3). Due to limited sample, not all elements were analyzed in all samples.

Analytical results of some samples run in duplicate were utilized to demonstrate analytical precision. Sample duplicates were carried through the full sample preparation process. The obtained results, reported in Table 4, show a good level of repeatability, even when using disposable plastic-ware, which was used in this application, instead of the typical calibrated glassware.

Conclusions

The present work reports the usage of the PinAAcle 900T AAS in flame mode for the determination of several elements relevant to the beer industry. The procedure is simple, fast, and accurate, requires no sample digestion, and can be applied to the quality control of beer manufacturing products when using a customer-validated application. The reported results prove that the PinAAcle 900 FAAS has the capability to determine elements in beer with high accuracy and precision.

Table 3. Spike recovery tests.

Element	Spike Level	% Recovery					
		3M	3G	4M	4G	6G	7G
Ca	1 mg/L		90	105			103
Cu	100 µg/L	93			97	95	
Fe	250 µg/L	98			98	101	
Mn	125 µg/L		100	95			94
Na	1 mg/L		103	110			103
Zn	125 µg/L		99	96			93

Table 4. Duplicate tests.

Sample	3M		3G		4M		4G		6G		7G	
Replicate	1	2	1	2	1	2	1	2	1	2	1	2
Ca (mg/L)			93	93	139	134					76	75
Cu (µg/L)	63	59					33	32	46	43		
Fe (µg/L)	45	42					30	31	54	40		
Mn (µg/L)			136	135	87	89					72	69
Na (mg/L)			46	46	86	85					187	189
Zn (µg/L)			3.6	3.2	1.2	1.2					5.3	4.0

References

1. S. Caroli "The Determination of Chemical Elements in Food: Applications for Atomic and Mass Spectrometry", Wiley 2007.
2. PerkinElmer Flame-AAS Cook Book 03030152 rev. 2009.
3. American Society of Brewing Chemists (ASBC), <http://www.asbcnet.org>, International Check Sample Service, May 2010.

Consumables Used

Component	Part Number
Al Hollow Cathode Lamp	N3050103
Ca Hollow Cathode Lamp	N3050114
Cu Hollow Cathode Lamp	N3050121
Fe Hollow Cathode Lamp	N3050126
Mn Hollow Cathode Lamp	N3050145
Na Hollow Cathode Lamp	N3050148
Zn Hollow Cathode Lamp	N3050191
10 cm 3-slot Titanium Burner Head	N0400103
5 cm 1-slot Titanium Burner Head	N0400101
Al – 1000 mg/L Standard	N9300184 (125 mL) N9300100 (500 mL)
Ca – 1000 mg/L Standard	N9303763 (125 mL) N9300108 (500 mL)
Cu – 1000 mg/L Standard	N9300183 (125 mL) N9300114 (500 mL)
Fe – 1000 mg/L Standard	N9303771 (125 mL) N9300126 (500 mL)
Mn – 1000 mg/L Standard	N9303783 (125 mL) N9300132 (500 mL)
Na – 1000 mg/L Standard	N9303785 (125 mL) N9300152 (500 mL)
Zn – 1000 mg/L Standard	N9300178 (125 mL) N9300168 (500 mL)
Autosampler Tubes	B0193233 (15 mL) B0193234 (50 mL)



Beer Analysis Using the Optima ICP

Introduction

Beer is one of the oldest beverages with references dating all the way back to 6000 B.C. The analysis of elements is an important parameter for determining the quality of beer. The analysis of beer is complicated by the presence of alcohol, dissolved solids and carbonation. Some elements affect the taste of beer, including Fe and Cu. These are usually found in very low concentrations, so the instrument's detection limits are important. Because of the low levels found, it is desirable to avoid dilution of the samples. Some elements are found at much higher concentrations, such as K, which can be several hundred mg/L. Inductively coupled plasma optical emission spectroscopy's (ICP-OES) multi-element capabilities, large dynamic range, and low detection limits (using axial viewing), make it ideal for the determination of metals in beer. The extensive linear range of ICP allows the analysis of both the low level elements as well as the major elements, without further dilution.

The direct analysis of beer by ICP can be challenging. The alcohol content requires matrix matching the standards to the samples containing ethanol. Also, the sample introduction system must be optimized for the volatile, organic ethanol component of the matrix. Due to high levels of dissolved solids, the nebulizer and injector must be capable of handling the samples without clogging. The carbonation in the beer samples must be removed to prevent out-gassing during the nebulization process and to eliminate poor reproducibility.

Authors:

Randy Hergenreder
Cynthia P. Bosnak
PerkinElmer, Inc.
Shelton, CT

The American Society of Brewing Chemists, Inc.¹ has undertaken a round robin study to develop a method for the determination of beer using ICP. Most of the parameters used in the latest study were also used in this analysis. Four beer samples were analyzed using PerkinElmer Optima™ ICP optical emission spectrometers. The samples represented different brands and types and they were split between the two labs.

Experimental

Instrumentation

Either the PerkinElmer Optima 5300DV or the PerkinElmer Optima 2100DV ICP model can be used for this analysis. The Optima 5300DV ICP system is a simultaneous ICP system with an echelle polychromator and a Segmented-Array Chargecoupled Detector (SCD). Simultaneous measurement of the background and analyte emission allows for accurate correction of transient background fluctuations. The Optima 2100DV ICP has a high speed, high resolution, double monochromator with a CCD array detector. Dynamic Wavelength Stabilization ensures wavelength accuracy and reliability.

A baffled cyclonic spray chamber with a Burgener Mira Mist® nebulizer and the 1.2 mm quartz injector were used for this analysis to minimize the volatility affect of the ethanol and the presence of high dissolved solids. The hardware and instrument parameters are detailed in Tables 1 and 2, respectively.

Table 1. Hardware

Nebulizer	Burgener Mira Mist® N077-5330
Spray Chamber	Baffled, Glass Cyclonic N077-6053
Injector	1.2 mm i.d. Quartz N077-5226
Injector Support Adapter	1.2 mm i.d. N077-6091
Torch	Quartz, Single Slot Paddle Torch N077-0338

Table 2. Instrument Parameters

RF Power	1400 W
Plasma gas	17 LPM
Aux gas	1.0 LPM
Nebulizer gas	0.5 LPM
Pump	2.0 ml/min
Torch cassette position	-3.0 mm
Replicates	3
Integration Time	5 min. 20 max.
Radial viewing distance	15 mm

Due to the different viscosities and alcohol content of the various beers, internal standards were used. Yttrium and gallium were used as internal standards for both radial and axial viewing. All solutions were spiked with Ga and Y so that the final concentration in solution was 100 mg/L Ga and 20 mg/L Y. The elements, wavelengths, viewing mode, and internal standards used are listed in Table 3.

Table 3. Instrument Parameters

Element	Wavelength nm	Viewing Mode	Internal Standard
K	766.490	Radial	Ga Radial
Na	589.592	Radial	Ga Radial
Mg	279.077	Radial	Y Radial
Ca	317.933	Radial	Y Radial
Fe	238.204	Axial	Y Axial
Cu	324.752	Axial	Ga Axial
Zn	213.857	Axial	Ga Axial
Y	371.031	Radial & Axial	—
Ga	417.206	Radial & Axial	—

Sample Preparation

A portion of each of the beers was taken and allowed to stand for several minutes with mild shaking to release the majority of the carbonation. They were then degassed in an ultrasonic bath for 15 minutes. An aliquot of beer was taken and spiked with the internal standard. The samples were also acidified with trace metal grade nitric acid to 7% (7 ml concentrated HNO₃/100 mL). The standards and blank were made to contain 5% ethanol and 7% HNO₃ to matrix match the beer sample matrix.

Results

As can be seen in Table 4, the concentration values for K can reach very high levels in the beer, while Fe and Cu are present at very low concentrations. Due to the large linear dynamic range of ICP, it is possible to calibrate for K up to as high as 1000 mg/L. This allows the analysis of very high levels of K without the need for further dilution and the need for a second analysis of each sample after dilution. (Figure 1)

Table 4. Concentration, mg/L

Element	Beer A	Beer B	Beer C	Beer D
K	590	203	273	212
Na	42.6	15.8	58.9	13.6
Mg	106	48.5	60.1	52.1
Ca	47.1	29.6	34.0	49.7
Fe	0.053	0.032	0.025	0.044
Cu	0.044	0.002	0.014	0.013
Zn	<0.002	0.152	<0.002	<0.002

The analysis was performed using several wavelengths to check for potential spectral interferences. The agreement between the wavelengths was better than 4% RSD for the major elements and typically less than 10% RSD for elements above 0.05 mg/L. Four separate aliquots of the samples were analyzed and the % RSD was less than 5% for the major elements. Some variations were higher because of potential contamination, especially for Cu and Zn which were near detection limits for some samples.

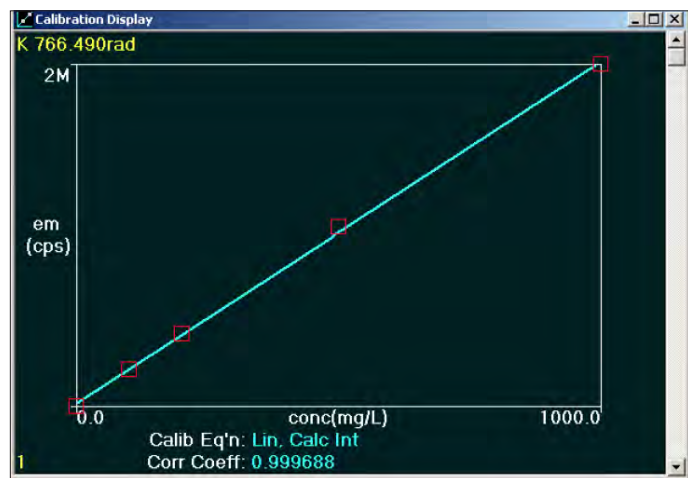


Figure 1. Potassium Calibration Curve.

As a sample, beer presents significant challenges for accurate and precise analysis. ICP can meet the challenge with the use of Dual View optics, optimized sample introduction systems and careful preparation of samples and standards. The samples had no spectral interferences at the chosen wavelengths. Internal standards are necessary for accurate analysis. Using this procedure the analysis of beer can be straight forward.

References

1. American Society of Brewing Chemist, Inc. Report of sub committee, Elemental Analysis of Beer and Wort by Inductively Coupled Plasma – Atomic Emission Spectroscopy. D. Sedin Chairman, Journal 62:190, 2004.

UHPLC

Authors

Njies Pedjie
Jon Benedon

PerkinElmer, Inc.
Shelton, CT USA

Determination of α -acids in Hops Using Third Party Software

Introduction

Hops are a major ingredient used in beer brewing. They preserve beer and provide it with its recognizable bitter taste and aroma. Hops come from a cone like plant called *Humulus lupulus*, which houses a lupulin gland containing

resins and oils. The resins contain a number of α -acids that impart the bitter taste to most beers; the oils in large part give beers their aroma.

In beer breweries around the world, one essential part of quality control is ensuring that the type and amount of α -acids are the same from batch to batch, and that their transformation into the bitter iso- α -acids during the brewing process consistently gives individual brands their recognizable taste (Fig. 1).

This application note presents a straightforward method to determine the type and amount of α -acids in pellets from three hops varieties.

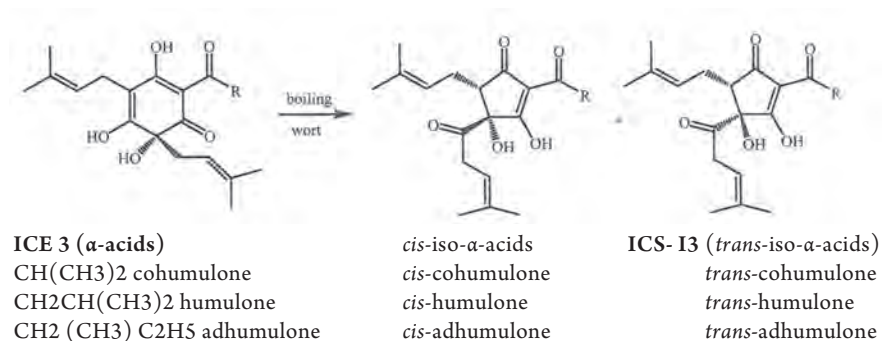


Figure 1. Isomerization of hop α -acids to iso- α -acids during brewing.

Experimental

A stock solution of 7.0 mg/mL of ICE 3(α -acids), and another of 1.4 mg/mL of ICS-I3 (isomerized α -acids) were prepared by transferring the appropriate net weights into a 10 mL vol. flask. Methanol was added to volume followed by 10 min. of sonication. From the stock solutions, a 413 μ g/mL working standard was prepared by dilution with sample solvent. Repeatability was evaluated with six injections of the working standard.

About 0.2 g of each of the hop pellets (American Cascade, American Summit, and New Zealand Nelson) were transferred into individual 10 mL volumetric flasks. The flasks were half filled with the sample solvent and left to soak for four hours while vortexing every hour. The preparation was sonicated for 15 min in cold water, and flasks were brought to volume with the sample solvent and centrifuged for 10 min at 7000 RPM. Each supernatant was transferred into a 25 mL vol. flask and set aside. 10 mL of sample solvent was added on each remaining precipitate followed by a vigorous vortexing for about two minutes. This latter preparation was also centrifuged for 10 min at 7000 RPM. The supernatant was collected and transferred into the corresponding 25 mL vol. flask previously set aside. The volumetric flask was brought to volume with sample solvent and samples were filtered through a 0.2 μ m nylon filter prior to testing.

Chromatographic conditions

Platform:	Flexar™ FX-15UHPLC
Autosampler Setting:	20 μ L loop and 250 μ L Sample Syringe Volume Variable Loop injection mode Injection: 4 μ L; Flush solvent: 1:1 methanol/water
Flow:	1.0 mL/min
UV detector:	270 nm
Column:	Brownlee™ SPP C18, 150 x 3.0 mm, 2.7 μ m at 40 ° C cat# N9308411
Isocratic :	35% Mobile Phase A: 0.1% phosphoric acid, 0.2 mmol/L EDTA 2NA 65 % Mobile Phase B: acetonitrile
Sample solvent:	8:2 methanol / 0.1% Trifluoroacetic acid (TFA) in water (HPLC grade solvent and ACS grade reagent)
Software:	Agilent® EZChrom Elite™ Version 3.32
Sampling Rate:	5 pts/s

Results and Discussion

A PerkinElmer Flexar FX-15 fitted with a UV/VIS Detector was the platform used for this analysis. The separation was achieved using a Brownlee™ SPP C18, 150 x 3.0 mm, 2.7 μ m column. The run time was eight min, the optimal flow rate

was 1.0 mL/min with a modest back pressure of approximately 3500 PSI (241 bars). Method performance was excellent: repeatability % RSD values ranged from 0.4% to 0.8%, resolution between peaks ranged from 1.8 to 7.7, and peaks' tailing were less than 2.0. Assay results were 73%, 73% and 77% for the American Cascade, the American Summit and New Zealand Nelson, respectively. The α -acid in hops were lower than the label claims. Method performance results are shown in Table 1, Hops assay results are shown in Table 2. Representative chromatograms of the standard, American Cascade and American Summit solutions are shown in Figures 2, 3, 4.

Conclusion

In this analysis, the six α -acids were well resolved. The method was precise with %RSDs \leq 0.8%. Assay results of hops pellets showed levels of α -acids 23% and 27% lower than the labels' claims. The column used was a Brownlee superficially porous particle column specifically designed to reduce the sample diffusion path and thereby deliver faster separation, sharp peaks, and modest back pressure. This analysis was done with the PerkinElmer FX -15 system reliably under the control of Agilent's® EZChrom Elite™ chromatography data system.

Table 1. Method Performance of RSD Standards.

α - acids	Repeatability % RSD (n=6)	Resolution	Tailing
t-isocohumulone	0.5	N/A	1.7
t-isohumulone	0.6	5.1	1.8
t-isoadhumulone	0.4	1.8	0.0
cohumulone	0.4	4.2	1.1
humulone	0.7	7.7	1.2
adhumulone	0.8	2.3	1.1
Average	0.55	----	----

Table 2. % Weight/Weight Analysis Results.

Species of Hops	% Results	% Label Claim	% of Claim
American Cascade	4.0	5.5	73
American Summit	12.2	16.8	73
New Zealand Nelson	9.2	12.0	77
Average	----	----	74%

References

Enhance Quantitative Extraction and HPLC Determination of Hop and Beer Bitter Acids
B. Jaskula, K. Goiris., G. De Rouck, G. Aert, L. De Cooman: J. of The Institute of Brewing, 2007, Vol.113 (4), 381-390.

Note: this application note is subject to change without prior notice.

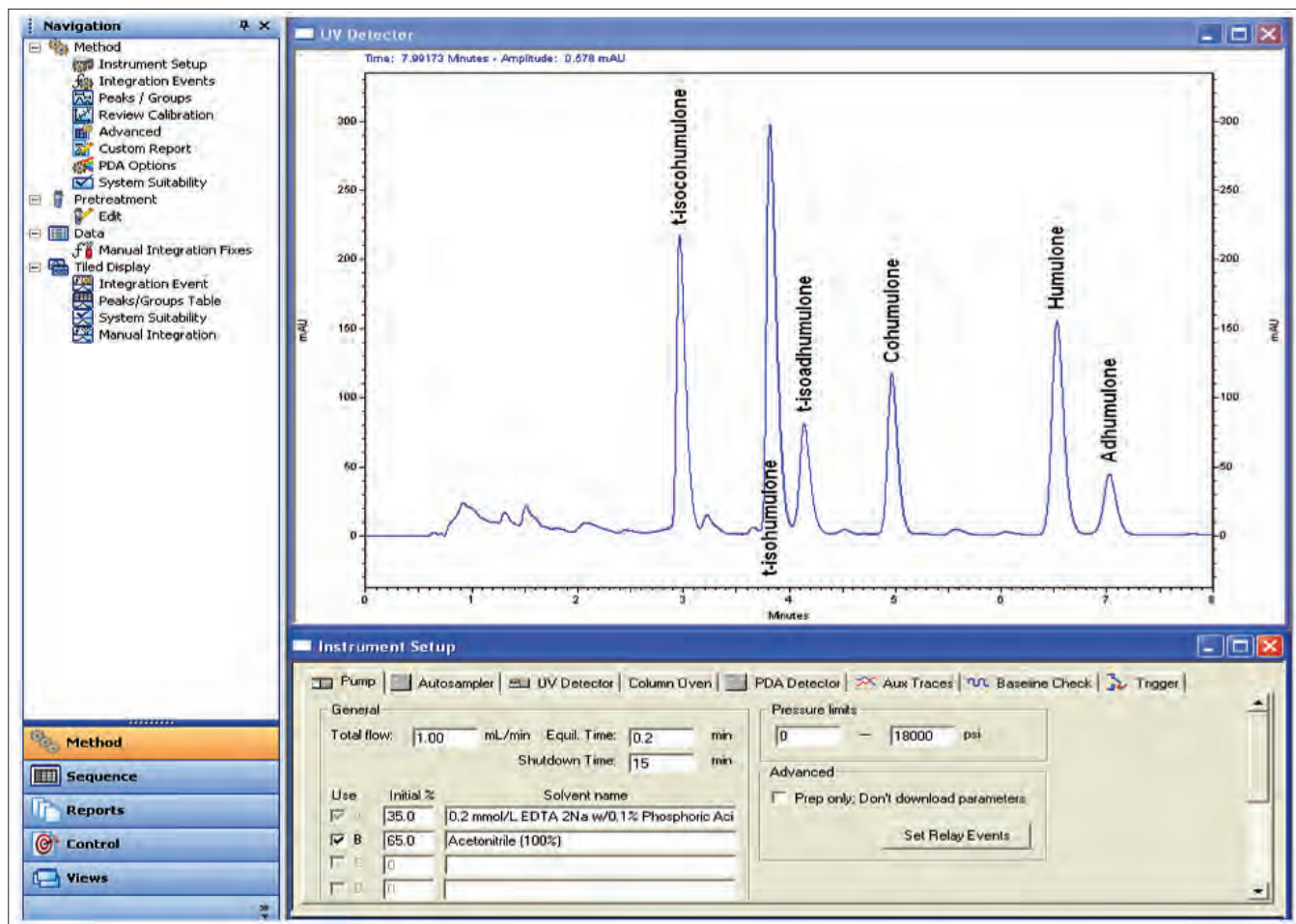


Figure 2. Chromatogram of a Standard With ICE 3 and ICS-I3.

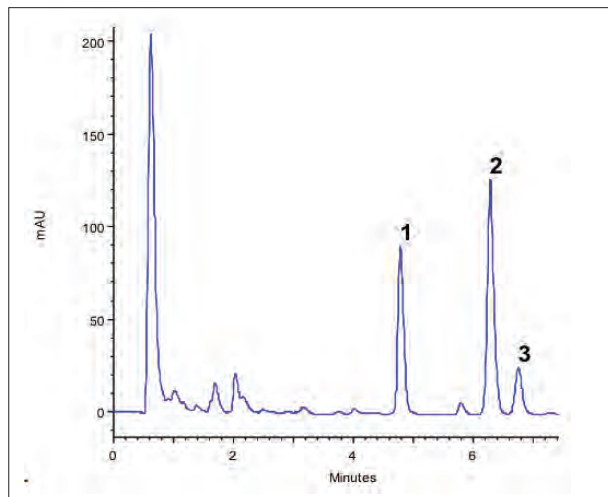


Figure 3. Chromatogram of the American Cascade Hops.
1. Cohumulone, 2. Humulone 3. Adhumulone

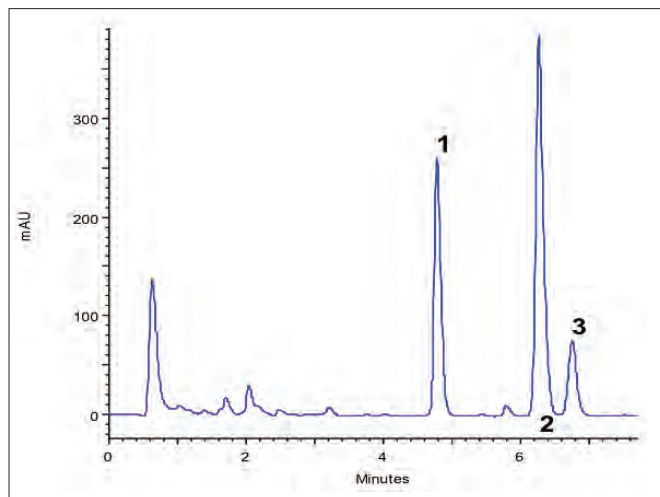


Figure 4. Chromatogram of the American Summit Hops.



APPLICATION NOTE

Gas Chromatography/ Mass Spectrometry

Author:

Andrew Tipler

PerkinElmer, Inc.
Shelton, CT

Characterization of Hop Aroma Using GC/MS, Headspace Trap and Olfactory Port

Introduction

Hops are a critical ingredient in beer. They provide an important balance to the malt in the taste of many beers. They also aid the

brewing process in precipitating out proteins, etc. during the boil. Hops also have preservative properties that help keep beer fresh and free from bacteriological attack.

Hops contribute to the taste of beer in three ways:

- Bittering – hops contain compounds such as humulones that are very insoluble in water but isomerize on boiling to form isohumulones, which are partially soluble and impart the bitter flavor to beer.
- Flavoring – compounds such as terpenes and esters provide the fruity, citrus, earthy, resinous flavors to many beers.
- Aroma compounds – these are the volatile organic compounds that migrate into the vapor above the head of beer and give the beer its characteristic smell. This can be flowery, citrusy, fruity, etc. They form a very important part of the overall flavor of beer.

There are many types of hops that deliver a very wide range of flavors. Hops need to be stored carefully and be used when fresh since the flavor will degrade as they age. Consequently there is a need to characterize the quality of hops so that the brewer can develop and deliver the required product.

Aroma characterization of hops is complex; there are many compounds in hops that contribute to flavor. Table 1 lists the composition of typical hops and Table 2 lists some of the key aroma compounds. The traditional way to evaluate hop quality is to use an experienced brewer to assess the hops organoleptically by crushing a few of the hops in their fingers and smelling the released aroma. This is effective but not objective and lacks the quantitative information needed to make correct decisions on how to utilize the hops.

Table 1. Composition of typical hops.

Component	%
Vegetative material (cellulose, lignin, etc.)	40
Proteins	15
Total resins (bittering compounds)	15
Water	10
Ash	8
Lipids, wax, pectin	5
Tannins	4
Monosaccharides	2
Essential oils (flavor/aroma compounds)	0.5 to 2

Table 2. Key hop aroma compounds.

Component	Comment
Myrcene	Pungent flavor; normally oxidized during the boil into other flavor compounds such as linalool and geraniol and their oxides
Humulene	Delicate and refined flavor characteristic of noble hops; broken down by boiling into oxidative flavors
Caryophyllene and farnesene	Herbal spicy character -- not well characterized

This application note describes a system that is able to provide both an objective chemical analysis of hop aroma using gas chromatography/mass spectrometry and, at the same time, provide the means for the user to monitor the olfactory character of each component as it elutes from the chromatographic column. Such an approach allows the user to gain a fuller characterization of a particular hop sample.

Analytical System

The analytical system comprises five main components:

HS Trap

Static headspace (HS) sampling is very suited for extracting aroma compounds out of hops. A weighed amount of hops (pellets or leaves) is placed in a glass vial and sealed as shown in Figure 1. This vial is then heated in an oven at a set fixed temperature and for a set fixed time period. A portion of the vapor is then extracted from the vial by the headspace sampling system and introduced into the GC column for separation and analysis.

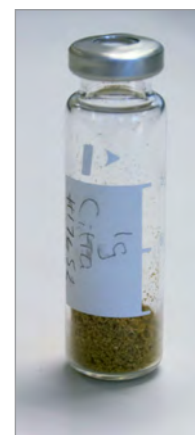


Figure 1. Hops inside a headspace vial awaiting analysis.

While extremely convenient, static headspace sampling only delivers a very small fraction of the headspace vapor into the GC column and so it is really best suited to high concentrations of compounds. In the analysis of complex samples, it is often found that low levels of some components are critical to the overall aroma of that sample. To increase the amount of sample value introduced into the GC column, a headspace trap system was used.

Using this technology, most or even the entire headspace vapor is passed through an adsorbent trap to collect and focus the VOCs. The trap is then rapidly heated and the desorbed components are transferred to the GC column. In this way, the amount of sample vapor entering the GC column can be increased by a factor of up to 100x. This technique is ideally suited for hop aroma analysis.

Figures 2 to 4 are simplified representations of the HS trap operation – there are other valves and plumbing needed to ensure that sample vapor goes where it should and not anywhere else. Essentially, the principle is very similar to classical static headspace but at the end of the vial equilibration step, after the vapor is pressurized, it is fully vented through an adsorbent trap. This process may be repeated to effectively vent the entire headspace vapor through the adsorbent trap. Once the trap is loaded, it is rapidly heated and the desorbed VOCs are transferred to the GC column.

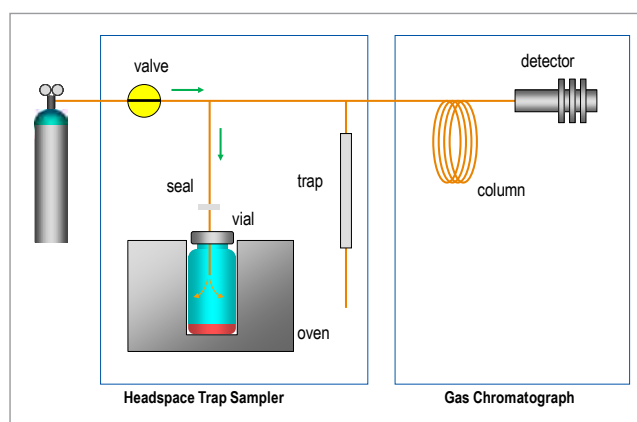


Figure 2. Schematic diagram of the HS trap system showing the equilibrated vial being pressurized with carrier gas.

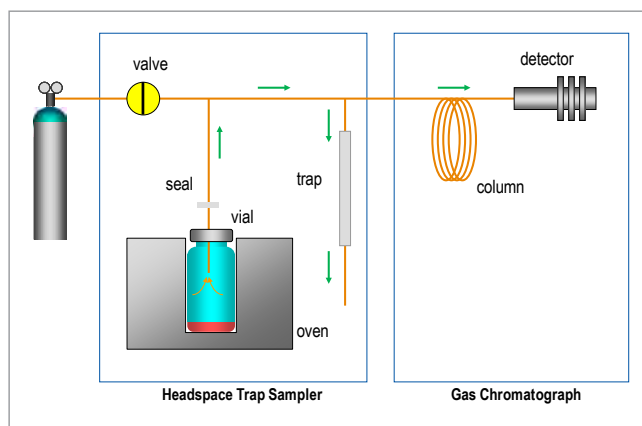


Figure 3. Schematic diagram of the HS trap system showing the pressurized headspace being released from the vial into the adsorbent trap.

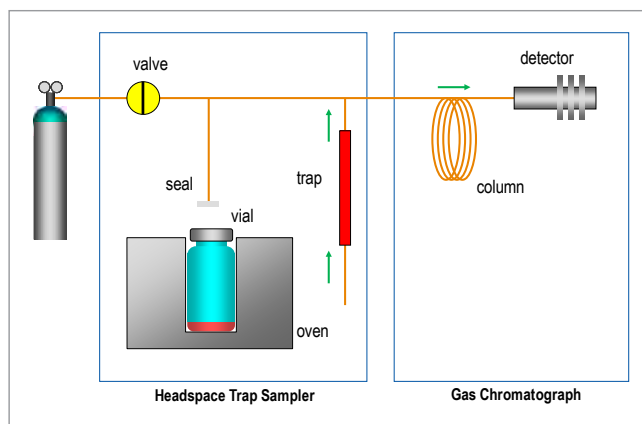


Figure 4. Schematic diagram of the HS trap system showing the VOCs collected in the adsorbent trap being thermally desorbed and introduced into the GC column.

Clarus 680 GC

The workhorse Clarus® 680 GC is an ideal complement to the rest of the system. The chromatography is undemanding so simple methods may be used. For olfactory monitoring, it is important to have sufficient time between adjacent peaks for the user to discern them from each other. It is also beneficial to load the column with as much sample as possible without overload to provide the best opportunity for the user's nose to detect them. For this reason, a long column with a thick stationary phase is used. Because many of the components in



Figure 5. The Clarus 680 SQ 8 GC/MS system.

hops are highly polar (acids, esters, ketones, etc.) a very polar Carbowax®-type stationary phase is used for the separation.

S-Swafer System

Because the column effluent needs to supply both the MS and the olfactory port, some form of splitting device is required. This should not affect the integrity of the chromatography in any way and so should be highly inert and have low-volume internal geometry. The use of a make-up gas in the splitter provides additional control and stability of the split flow rates.

S-Swafer™ is an excellent active splitting device and well suited to this purpose. Figure 6 shows the S-Swafer configured to split the column effluent between the MS detector and the SNFR olfactory port. The split ratio between the detector and the olfactory port is defined by the choice of restrictor tubes connected between the Swafer outlets and the MS and SNFR.

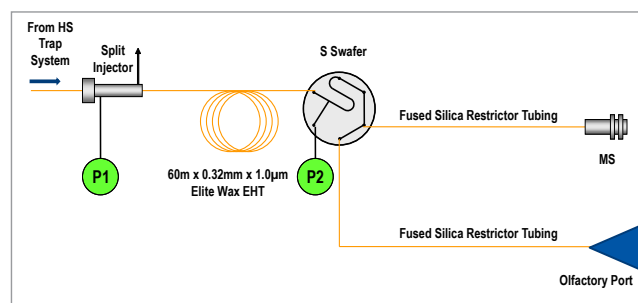


Figure 6. S-Swafer configured for use with the Clarus SQ 8 GC/MS and the SNFR.

The Swafer utility software, which is included with the Swafer system, may be used to calculate this split ratio. Figure 7 shows how this calculator was used to establish the operating conditions for the S-Swafer for this application.

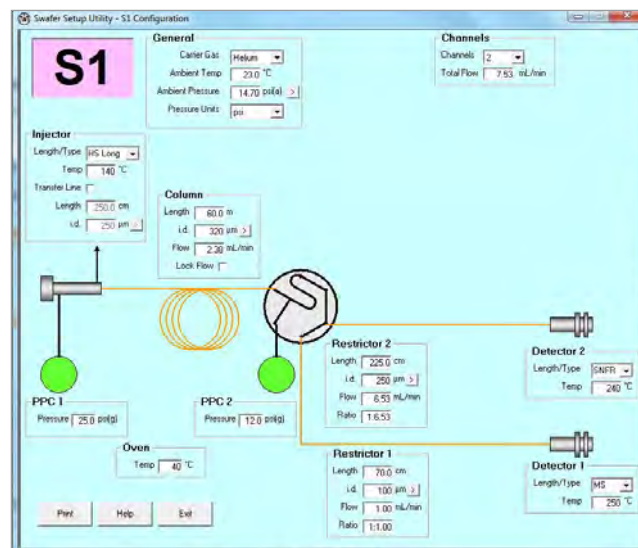


Figure 7. The Swafer utility software showing the settings used for this hop aroma characterization work.

Clarus SQ 8 Mass Spectrometer

A mass spectrometer is an important part of an aroma characterization system. It's important not only to detect and describe the aromas of the various components eluting from the GC column but to also to identify what those components are and possibly what their levels in the hops are.

The Clarus SQ 8 quadrupole mass spectrometer is ideally suited for this purpose and will quickly identify and quantify components using classical spectra in the supplied NIST library. This software is also able to interact with the olfactory information as described later in this document.

GC SNFR Accessory

Figure 8 shows a picture of the SNFR accessory. This is connected to the GC via a flexible heated transfer line. The split column effluent travels to the glass nose-piece through deactivated fused silica tubing.

While monitoring the aroma compounds eluting from the GC column, the user is able to capture vocal narration via a built-in microphone and aroma intensity by adjustment of a joystick.



Figure 8. The SNFR olfactory port accessory.

Analytical Conditions

Table 3. HS Trap conditions.

Headspace system	PerkinElmer® TurboMatrix™ 110 HS Trap
Vial equilibration	80 °C for 15 minutes
Needle	120 °C
Transfer line	140 °C, column connected directly to HS trap
Carrier gas	Helium at 25 psig
Dry purge	5 min
Trap	Air toxics, 30 °C to 300 °C, hold for 5 min
Extraction cycles	1 with 40 psig extraction pressure

Table 4. GC conditions.

Gas Chromatograph/ Mass Spectrometer	PerkinElmer Clarus 680 SQ 8
Column	60 m x 0.32 mm x 1.0µm Elite-5MS connected directly to the HS trap
Oven	40 °C for 2 min, then 4 °C/min to 240 °C for 8 min
Carrier gas	13 psig at Swafer
Injector	PSS at 300 °C, carrier gas off

Table 5. MS conditions.

Scan range	m/z 35 to 350
Scan time	0.8 s
Interscan delay	0.1 s
Source temp	250 °C
Inlet line temp	250 °C

Table 6. Olfactory port conditions.

Olfactory port	PerkinElmer SNFR
Transfer line	225 cm x 0.250 mm at 240 °C
Humidified air	500 mL/min with jar set to 37 °C

Table 7. Swafer conditions.

Swafer	PerkinElmer S-Swafer in the S1 configuration
Settings	Developed using the Swafer utility software – see Figure 7

Table 8. Sample details.

Sample preparation	Hops (leaves or pellets) were ground with a rotary coffee grinder and 1 g was weighed into a sample vial and sealed
Vial	Standard 22-mL vial with aluminum crimped cap with PTFE lined silicone septum

Typical Chromatography

Figure 9 shows total ion chromatograms (TIC) of four typical hops from different countries. Part of the German Hallertau is highlighted and is expanded in Figure 10. The power of the MS enables a particular peak to be identified from its mass spectrum (as shown in Figure 11) by searching the NIST spectral library supplied with the Clarus SQ 8 system. The results of this search are given in Figure 12. Results of this search very strongly indicate that the peak eluting at 36.72 minutes is 3,7-dimethyl-1,6-octadien-3-ol, otherwise known as linalool. Linalool is a very important aroma compound and will provide a delicate flowery aroma to the beer. The amount of linalool (or any other compound once identified) may be quantified by calibrating the GC/MS with standard mixtures of this compound.

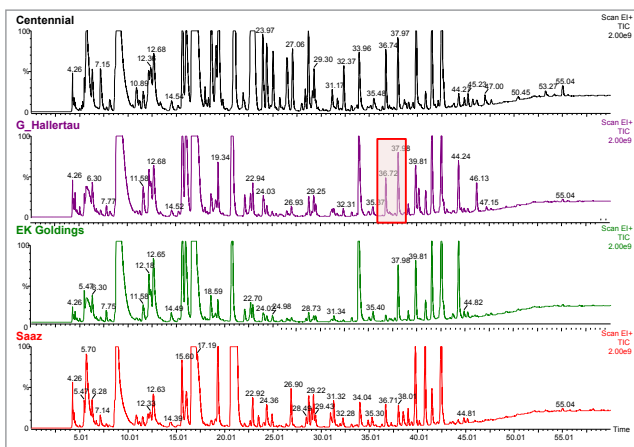


Figure 9. Typical TIC chromatograms of four hop samples.

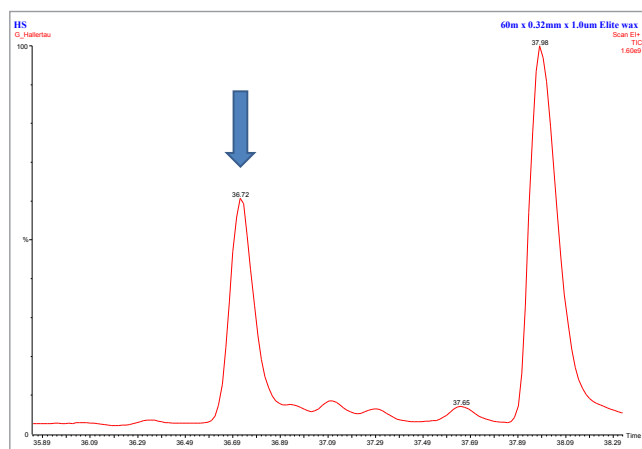


Figure 10. Highlighted detail from Figure 9.

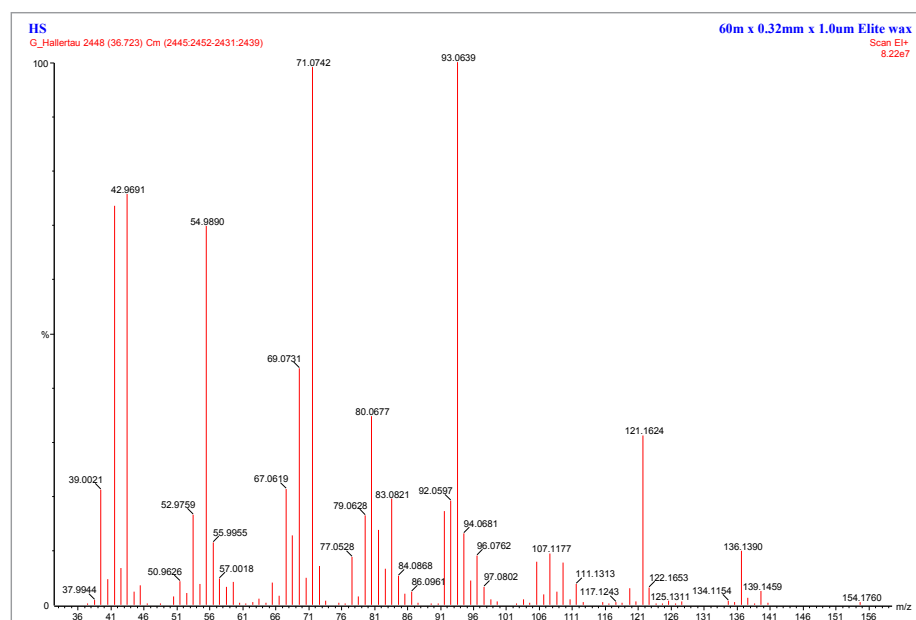


Figure 11. Mass spectrum from peak highlighted in Figure 10.

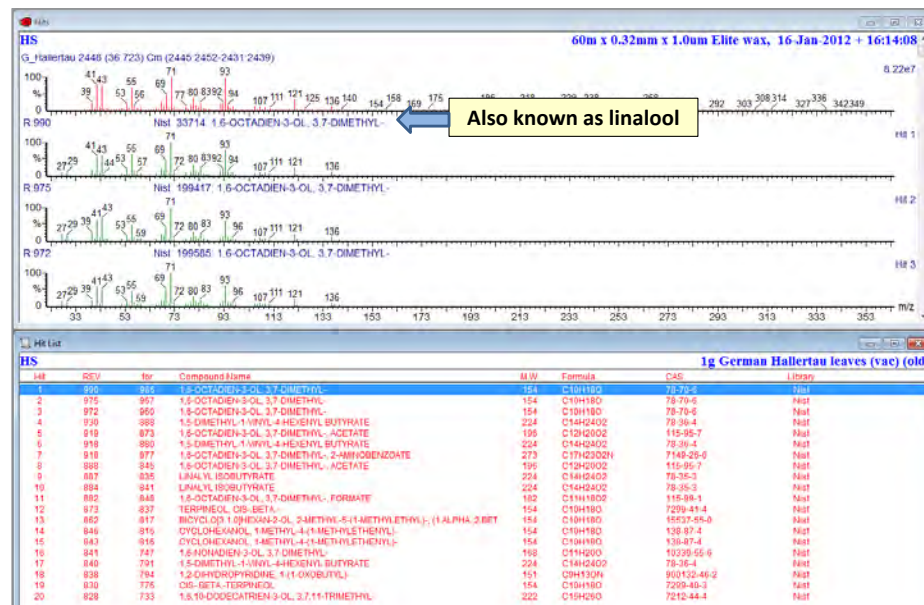


Figure 12. Results from library search on mass spectrum shown in Figure 11.

By performing further identifications of the chromatographic peaks, a profile of the hop character may be established. Figure 13 shows further peaks identified in the German Hallertau chromatogram previously shown in Figure 9. Annotated peaks are mainly aliphatic acids which indicate a degree of oxidation in the hops in this particular sample. The strongly flavored

myrcene peak is rather smaller than expected. These observations indicate that this particular sample is rather old (which was true – this was a really old sample that had been poorly stored).

Figure 14 shows chromatography of four additional hop samples.

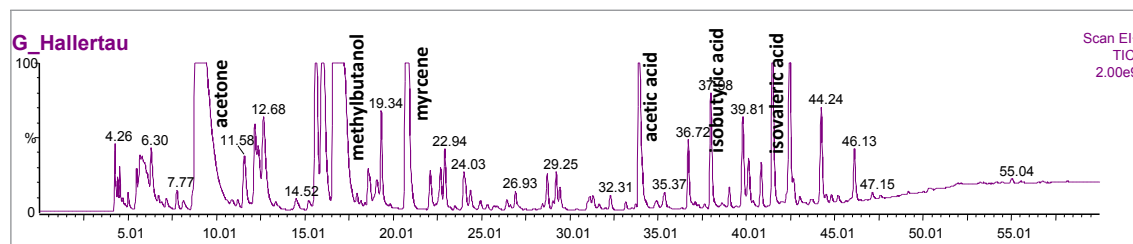


Figure 13. Typical TIC chromatograms of four hop samples.

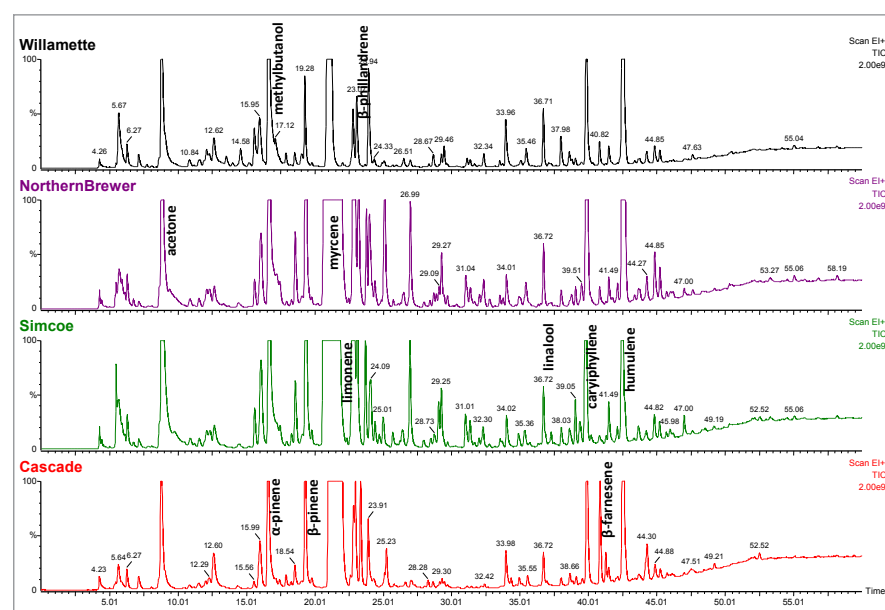


Figure 14. TIC chromatograms of a further four hop sample.

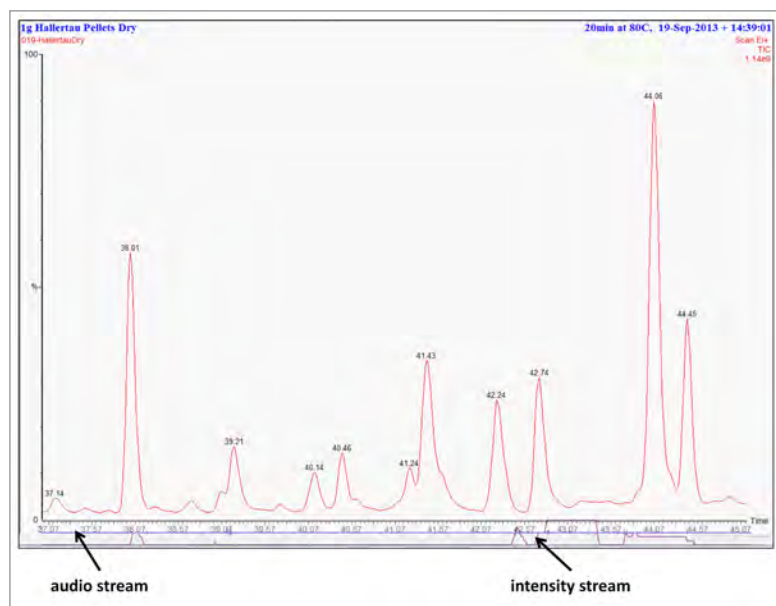


Figure 15. Example of a hop chromatogram being reviewed within the TurboMass™ software with the audio narration and aroma intensity graphically overlaid.

Olfactory Characterization

Figure 15 shows an example of a hop chromatogram with the audio narration and intensity recordings graphically overlaid. Audio narration is stored in a standard WAV file format that may be replayed from this screen to the operator from any point in the displayed chromatogram by means of a simple mouse-click. The narration WAV file may also be played back from most media applications including the Microsoft® Media Player, which is included with the Windows® operating systems. The audio data

may be transcribed into text at the time of the recording. The Nuance® Dragon® Naturally Speaking software performs this function. It is included in the SNFR product. Table 9 shows a typical report from a hop analysis showing the user's transcribed narration and the recorded aroma intensity from the joystick. This report is formatted as a comma-separated value (CSV) file suitable for direct importation into Microsoft® Excel® or other application software.

Table 9. Typical output report showing text transcribed from the audio narration and the corresponding aroma intensity data.

Project Name	OKTOBERFEST.PRO	
Sample Name	019-HallertauDry	
Start Time	9/19/2013 2:39:02 PM	
Duration	60.00	
Time Stamp	Spoken text	Intensity
1.05	coming up on a minute	0
2.13	two minutes	0
5.15	a sweet smell	0
5.20	very faint	0
6.07	nothing there	0
6.65	very very faint smell	2
6.88	off order	3
7.12	like sour milk	2
7.25	sour milk	4
7.30	was a very good banana smell	5
7.35	fruity smell	4
8.18	like a sour milk	4
8.23	sour milk	4
9.17	fruit there	2
10.02	nothing there	0
10.10	large peak and I smell nothing	0
11.52	burning smell	2
11.58	almost woody	0
12.00	little sweet	1
12.45	almost a hint of coffee	0
13.22	that's an off smell	3
13.25	a rancid smell	3
13.82	something	3
13.88	almost	0
13.90	medical	0
15.43	medical smell	2
15.47	is almost toffee like	2
15.57	very pleasing	4
16.43	off order	0
17.92	slight sweet	0
18.58	bubblegum	0
19.88	hint of something sweet	0
21.00	off order of skunk	3
21.08	definite skunk	5
22.90	something	3
23.02	almost like a match	1
23.07	a sulfur smell	0
25.18	subtle	2
25.22	subtle	0
25.33	not quite sure what that was	0
25.70	nothing there	0
30.70	little off odor	1
33.67	foul smell	2
36.23	smell of cardboard must	0
36.35	bananas	2
36.82	almost mint	2
38.08	that was a nice fruit	3
38.20	very citrus	0
42.47	hot	4
42.50	pepper	2
42.70	again	3
42.82	it's an off odor	6
42.85	are very bad off order	6
43.08	a sweaty socks smell	6
43.72	that's a fruity smell	2
43.73	very pleasing	2
45.78	floral	2
46.30	a burning smell	2
46.37	burning match almost	2
47.02	pepper smell	1
47.95	pepper	1
48.93	sweet	1
49.13	a sweet smell	3
49.88	interesting smell	1
49.92	can't describe it	0
50.32	ah	3
50.35	medical smell again	4
50.40	medicinal	4
54.08	solvent	1

Conclusions

The addition of an olfactory port to a HS GC/MS system extends its application for aroma characterization of samples such as hops. The ability to directly correlate organoleptic perception against hard analytical data provides insights difficult to obtain otherwise.

This system should be of interest to brewers and researchers involved in the following:

- Quality control of raw hops
- Product development
- Trouble shooting of off-flavors
- Storage/aging studies
- Comparison studies
- Aroma analysis of finished beer
- Reverse engineering of competitive products

Gas Chromatography

Author:

David Scott

PerkinElmer, Inc.
Shelton, CT

Aroma Study of Potable Spirits

Introduction

The production of whisky requires maturation in wooden casks for the full development of the finished product's character. Subtle differences in the casks' conditioning can produce quite different flavors and aromas that require skillful blending to achieve a consistent product. The PerkinElmer TurboMatrix™ headspace trap system coupled with a Clarus® SQ 8 GC/MS and SNFR™ olfactory port is an effective means of identifying low concentration volatile organic compounds (VOCs) in potable spirits.

Manufacturing whisky is a lengthy process due to Scottish law, which mandates that the distilled spirit be matured in oak casks for a minimum of three years and one day before it is bottled. During the maturation process the spirit takes on a distinct character in each cask, which must then be blended to give the recognized finished product. Much of the blending is performed by the master blender, a craft that can take 12 years in apprenticeship. One of the key characteristics of whisky enjoyment is the aroma from the spirit with a recently designed copita (a tulip-shaped sherry glass), having been developed to maximize this experience. Functional groups that give character to whisky include alcohols, esters, acids and carbonyls, and the odor thresholds of these analytes of interest vary greatly by each group.

Work by Salo¹ et al. explained that the majority of whisky's odor contribution comes from carbonyl compounds. Yet it is interesting to note that, while carbonyl compounds are the most prevalent odor components, of the compounds present they have the smallest combined mass with alcohol being a major component as whisky is legally required to be a minimum of 40% alcohol by volume.

There is usually some discussion among consumers as to the correct way to enjoy whisky. The range of opinions include; neat from the bottle with no change, in a chilled glass, over ice to chill the spirit or with the addition of some volume of room temperature water. The most common comment about ice is that the ice will melt adding water to the whisky. Not unsurprisingly the effect of temperature on the partitioning of flavor components into the headspace above the spirit is rarely discussed. When attempting to determine water's influence on the consumer experience, headspace sampling provides the capability to capture those headspace components and closely mimic the customer experience as they were enjoying a dram. After GC separation a mass spectrometer can identify those components that the consumer experiences at an olfactometry port enabling a detailed analysis of the direct customer experience

One of the unique challenges with headspace sampling versus the human interaction is determining the sample volume. Given the many compounds and the wide variation in their odor thresholds, to compare the headspace results with the direct sampling of the human nose from the glass a large injection of vapor is desirable. To achieve that goal the headspace vapor is collected on an adsorbent trap using the TurboMatrix HS trap system.

In this application note, the VOCs in single malt whisky were investigated. Sample preparation simply involved dispensing a fixed volume of whisky into a sample vial and sealing it. The headspace vial was then sampled for GC separation with MS and olfactometry detection Figure 1.

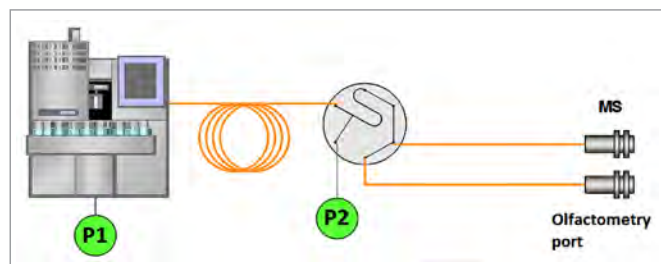


Figure 1. Instrumentation overview with headspace sampling, GC separation with MS and olfactometry detection.

Experimental Conditions

The PerkinElmer TurboMatrix HS trap increases the headspace volume that can be sampled by evacuating the entire sample vial onto an adsorbent chemical trap. A significant advantage of the HS trap is the capacity of the trapping material, which is greater than that yielded by other techniques such as SPME. The selected trap is an air monitoring trap, which has excellent

trapping properties for a wide variety of compounds from different functional groups. The trapping material is also hydrophobic, which assists with water management from the sample. This sample preparation consisted of 3 mL of sample pipetted into a vial and capped. The vials were thermostatted at 35 °C to mimic being held in a manner consistent with a consumer. Full experimental conditions are described in Table 1.

Table 1. TurboMatrix HS-110 Trap

Needle	100 °C
Oven	35 °C
Transfer line	120 °C

Trap Low	30
Trap Hi	300

Vial pressurization	1 minute
Vial desorb	3 minutes
Dry purge	10 minutes
Trap hold	5 minutes
Desorb	0.1 minutes
Thermostat	15 minutes
GC cycle time	72 minutes

Carrier pressure	52 psi
Desorb pressure	52 psi
Vial pressure	40 psi

Table 2. GC Conditions Injectors

GC conditions injectors	Both at 250 °C
Oven program	40 °C (no hold) ramp 4 °C/min to 240 °C (hold for 8 minutes).
Column	60 m x 0.32 id wax column

Table 3. MS Conditions

Transfer line temperature	200 °C
Source temperature	180 °C
Mass range	30 – 300 m/z
Scan time	0.2 sec
Interscan delay	0.1 sec
Ionization mode	El+
Run time	58 minutes

Swafer Micro-Channel Flow Technology

The S-Swafer™ employed here allows for the manipulation of the column flow rate and sample separation without impacting the active split between the mass spectrometer and olfactory port. Split ratios and flows are results of the selected transfer line geometries and carrier gas pressure(s). The addition of the second pressure source regulates the splitting and maintains the engineered configuration independent of the column head

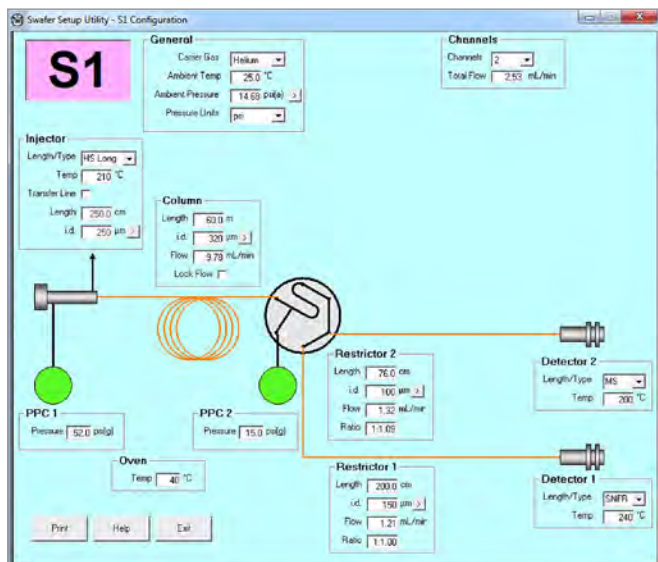


Figure 2. Swafer™ utility software describing dimensions and calculated flows.

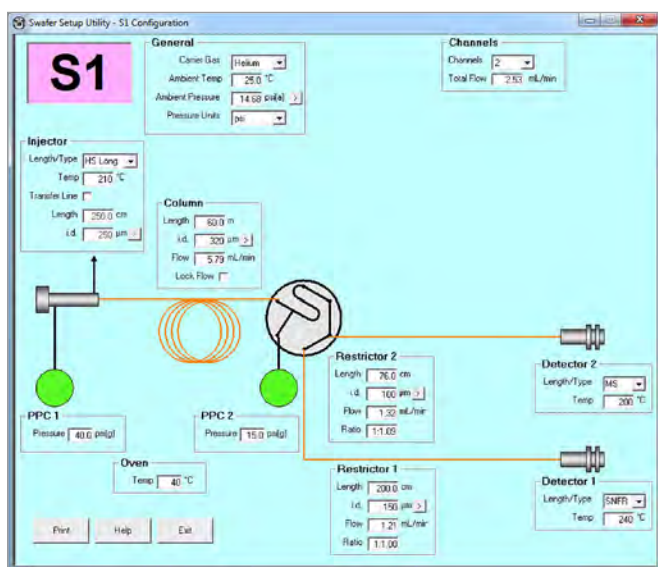


Figure 3. Swafer™ utility software describing dimensions and calculated flows. The adjusted column pressure, PPC1, has not changed the flow rates to either detector giving more freedom to adjust the separation conditions.

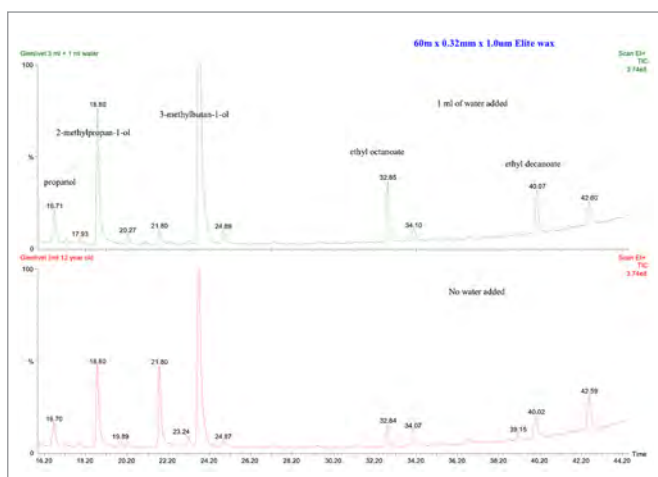


Figure 4. The effect of water to a sample of Glenlivet® is apparent with the increase of ester and alcohol compounds in the headspace.

pressure and maintains a stable flow into the MS detector and olfactometry port. Independence from the column head pressure increases the flow rate options available to a chemist in the separation. The separation is critical from both an identification and a human interaction standpoint. It can be desirable to have a greater separation than is typical for GC to give a human analyst the opportunity to identify what they are experiencing as certain components are persistent and can mask other more subtle scents of less intense compounds. Therefore, a 60 m x 0.32 id wax column was used with a GC oven program starting at 40 °C and ramping 4 °C/min to 240 °C (hold for 8 minutes).

Swafer™ utility software shown in Figure 2 details the dimensions and calculated flow rates that were employed in the study. The screen capture in Figure 3 demonstrates that changing the column head pressure from 50 psig to 40 psig adjusted the analytical column flow rate but had no impact on the flow rates to both detectors, and thus no impact on the split ratio between the detectors.

Results

The chromatogram in Figure 4 shows the comparison of a neat 12 year old single malt Glenlivet® scotch and the same scotch with water added. There are obvious differences in the alcohols and ester concentrations in the headspace.

The ethyl decanoate has a fruity fragrance, with a more subtle fruity odor and a somewhat waxy odor as well. Characteristic whisky odor is 3-methylbutan-1-ol with 2-methylpropan-1-ol, which has a malty odor. The addition of water to neat whisky has a significant increase in those compounds in the headspace.

The addition of increased volumes of water, in this case 2 mL Figure 5, further highlights the impact on the selected odor compounds. Ethyl octanoate, ethyl decanoate and 3-methylbutyl acetate show increased concentration in the headspace (all of which have fruity odors), whereas the alcohols are decreased in concentration as the partition changes to flavor the whisky with water. Such changes make the whisky smell fruitier. Another

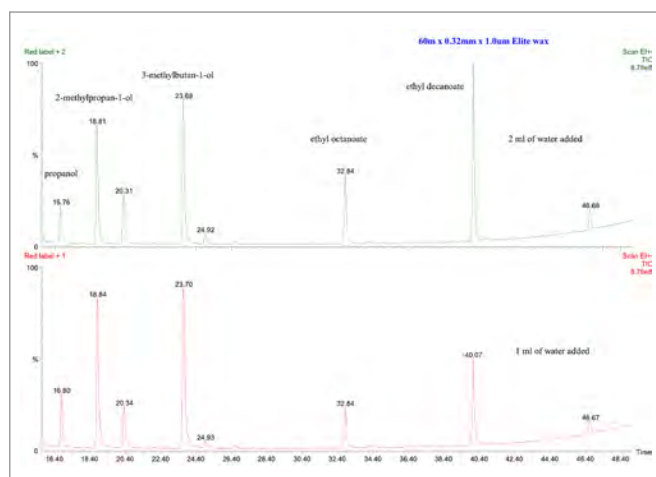


Figure 5. The effect of water to a sample of Glenlivet® is apparent with the increase of ester and alcohol compounds in the headspace.

interesting observation is that alcohol can desensitize the nose and can be recognized as a tingling sensation. Reducing the ethanol in the headspace then limits the desensitization further allowing enjoyment of the compounds present in the case of blended whisky there are also changes to the headspace due to the addition of water (see Figure 6). The changes are primarily the increase of analyte concentration in the headspace but the compounds at 33.98 and 34.94 minutes decrease in the headspace. The balance of flavors and odor compounds is changed by the addition of water.

A comparison of Glenlivet® with Dewar's® and Jim Beam brands (Figures 7 and 8, respectively) shows the distinct qualitative and quantitative differences between samples.

Conclusion

The addition of water to whisky changes the partitioning of the odor compound(s), which changes their concentration in the headspace and, by extension, in the liquid. Remaining compounds will impact the “mouth feel” and balance of the finished product and as such, the addition of water becomes very much a matter of taste.

Given the different starting materials and the fact that the “magic” of aging whisky differs from brand to brand, a consumer may add more water to some whiskies than to others.

References

1. P. Salo, L. Nykanen, and H. Suomalainen, J. Food Sci., 1972, 37, 394.

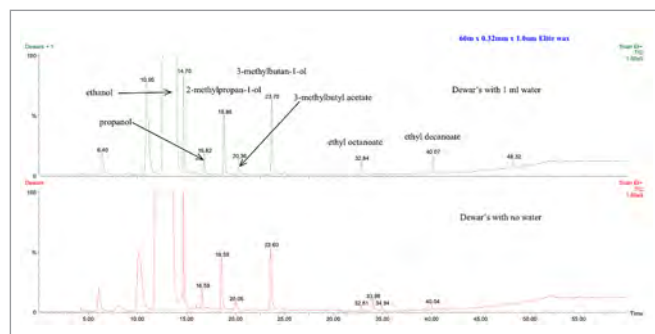


Figure 6. Blended Dewar's® whisky with and without water.

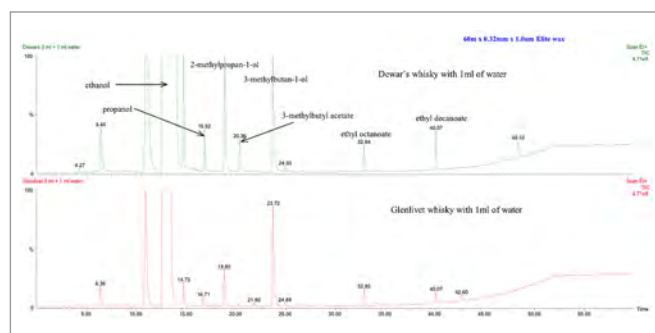


Figure 7. Comparison of Dewar's® and Glenlivet® with 1 ml of water added. Note that there are qualitative and quantitative differences between the headspace of two whiskies with the same amount of water added.

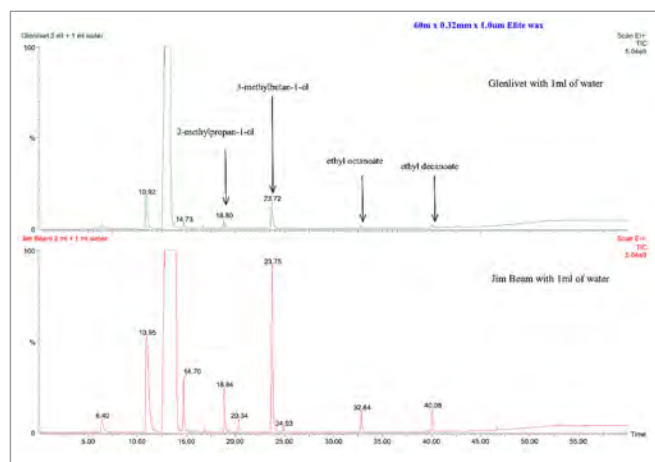


Figure 8. Comparison of single malt and bourbon whisky with water added.

UHPLC

Author

Padmaja Prabhu

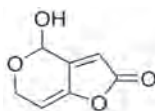
PerkinElmer, Inc.
Shelton, CT 06484 USA

Analysis of the Mycotoxin Patulin in Apple Juice Using the Flexar FX-15 UHPLC-UV

Introduction

Patulin is produced by various molds, which primarily infect the moldy part of apples. Removing the moldy and damaged parts of the fruit may not eliminate all the patulin because some of it may migrate into sound parts of the flesh.

Also, patulin can be produced within the fruit, even though it may not be visibly moldy. If moldy apples are used to produce apple juice, the patulin goes into the juice. It is not destroyed by heat treatments such as the pasteurization process. Patulin is a natural human toxin and therefore can have genetic affects within cells, including a developing fetus, the immune system and the nervous system. The recommended advisory level is 50 µg of patulin/kg in apple juice [50 parts per billion (ppb)].¹ Hydroxymethylfurfural (HMF), also 5-(Hydroxymethyl)furfural, is an organic compound derived from dehydration of sugars. HMF has been identified in a wide variety of heat-processed foods including milk, fruit juices, spirits, honey, etc.²



Synonyms: 2-Hydroxy-3,7-dioxabicyclo[4.3.0]nona-5,9-dien-8-one
Formula: C₇H₆O₄
MW: 154.12
MP: 110 °C

Figure 1. Structure and properties of patulin.

This application note will demonstrate a rapid method for the identification and quantification of patulin in apple juice using high performance liquid chromatography with UV detection. In addition to method optimization and standard analysis, a number of apple juice samples for patulin were analyzed. The samples were randomly collected from the local market in Mumbai.

Patulin is a colorless to white crystalline solid. It is soluble in water, methanol, ethanol, acetone, and ethyl or amyl acetate and less soluble in diethyl ether and benzene.

Experimental

The PerkinElmer® Flexar™ FX-15, Ultra High Performance Liquid Chromatograph (UHPLC), equipped with a programmable wavelength UV/Vis detector was used for this application. Table 1 presents the detailed operating parameters of the UHPLC and the extraction process of patulin from juice. The instrument interaction, data analysis and reporting was completed with the PerkinElmer Chromera® data system.

Table 1. Detailed instrument conditions used in the determination of patulin.

Instrument	Flexar FX-15 High Performance Liquid Chromatograph
Analytical Column	Brownlee™ analytical DB AQ C18 1.9 µm x 100 x 2.1 mm column
Column Temp.	35 °C
Flow Rate	0.5 mL/min
Mobile Phase A	Water pH 4.0 with acetic acid
Mobile Phase B	Water : Acetonitrile (50:50)
Injection volume	25 µL
Wavelength	275 nm
Extraction Procedure	10 mL of apple juice + three extracts with ethyl acetate, combine the three extracts and add 4 gm NaSO ₄ . 25 mL of this extract was evaporated to dryness under a stream of nitrogen. The residue was dissolved in 300 µL of mobile phase A and injected in to the chromatographic system.

Stock Solution of Patulin: 200 µg/mL of patulin was prepared in ethyl acetate.

Stock Solution of HMF: 200 µg/mL of HMF was prepared in ethyl acetate.

Resolution Standard Solution: 100 µL each of the stock patulin and HMF were evaporated to dryness in a 10 mL flask, and the residue was dissolved in mobile phase A. This gave a 2 µg/mL mixture of patulin and HMF.

Preparation of Spike Solution: 250 µL of stock solution of patulin was evaporated to dryness under a stream of nitrogen and the residue was dissolved in mobile phase A. This gave a 5 µg/mL solution of patulin.

Calibration Curve: Varying volumes of 5 µg/mL patulin were spiked into 10 mL of juice samples to produce the following calibration curve (Table 2).

Table 2. Scheme used for the creation of a six level calibration.

Cal Level	Volume of Juice (mL)	Std Sol Added (µL)	Final Conc. Patulin (ppb)
1	10	20	10
2	10	40	20
3	10	80	40
4	10	100	50
5	10	160	80
6	10	200	100

Calibration: The UV detector was calibrated across the range of 10 to 100 ng/mL; each calibration point was run in duplicate to demonstrate the precision of the system. The average coefficient of determination for a line of linear regression was 0.998 for patulin. The calibration curve for patulin is depicted in Figure 3. The precision of the system across the calibration range is excellent. The chromatograms from the analysis of standard material are shown in Figure 4.

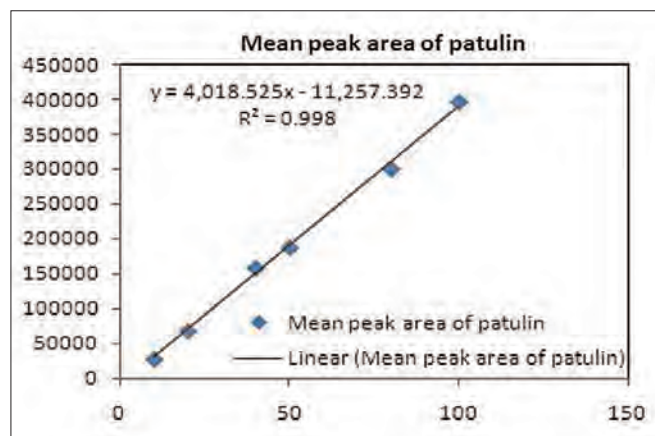


Figure 3. Calibration curve for patulin.

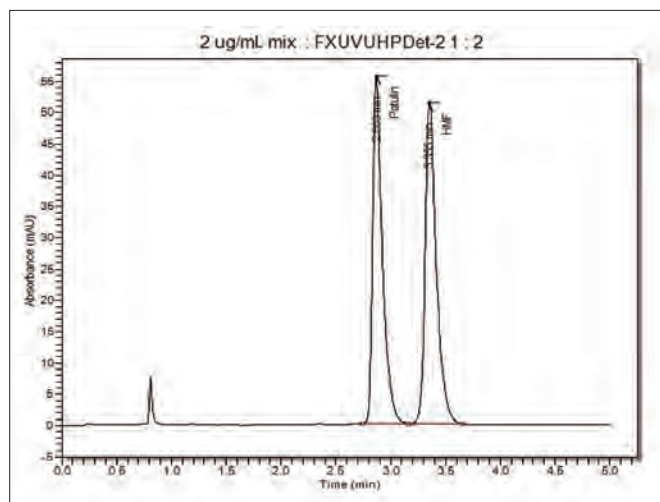


Figure 4. Example chromatogram for patulin.

The precision of the method was measured at both 5.0 and 10 ppb. The loss of precision below 10 ppb indicates the detection limit of this method to be approximately 5 ppb (Table 3).

Table 3. RSD values for detection limit and quantification level.				
Sr. No.	Conc. of Patulin in ppb	Area of Patulin	Conc. of Patulin in ppb	Area of Patulin
1	5	14894.7	10	41189.2
2	5	18836.3	10	44147.4
3	5	25627.5	10	45305.8
4	5	33795.2	10	44107.4
5	5	30614	10	39631.3
6	5	30640.4	10	43282.5
Mean		25734.6		42943.9
S.D.		7455.87		2123.57
%RSD		28.97		4.94

Summary of Method Validation Experiment	
Linearity:	10.0 ppb to 100 ppb of patulin
RSD for replicate analysis:	for 10.0 ppb 4.94%
Detection level:	5.0 ppb
Quantification level:	10.0 ppb
Recovery study:	at three levels for all the samples 80.52-109.48%

Sample Preparation: Samples were collected from the local Mumbai market. Samples included apple juice and apple squash. All the samples were refrigerated until analysis. Ten ml of juice sample was transferred into a 50 mL tube. The juice was extracted three times with 10 mL ethyl acetate. The three extracts were combined and 4 g of sodium sulphate was added to it, to remove moisture. 25 mL of the ethyl acetate layer was then evaporated (to dryness) under a stream of nitrogen. The residue was then reconstituted in 300 μ L of mobile phase A, filtered through 0.2 μ m nylon 66 syringe filter from Millipore® and 25 μ L was injected into the chromatographic system.

Method Validation

The recovery of the method was tested with the juice sample spiked at 3 different levels: 35, 50, 75 μ g/L. The measured amount was 32.53, 47.49, 63.15 μ g/L demonstrating that the technique is quantitative in its extraction of patulin from an aqueous matrix.

Results

Three samples of apple juice and one squash sample were analyzed using the method developed here.

Sample No.	Sample Details	Amount of Patulin Found in ppb
Sample 1	Juice T	N.D.
Sample 2	Juice S	N.D.
Sample 3	Juice R	N.D.
Sample 4	Apple squash	N.D.

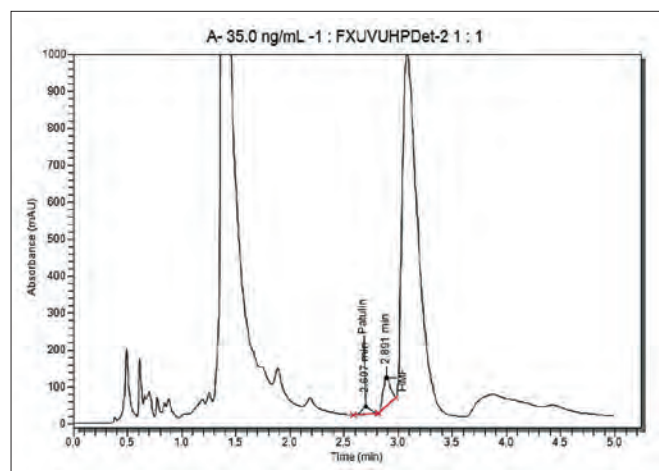


Figure 5. Chromatogram of patulin peak in sample.

Discussion and Conclusion

This application presents a method for the determination of patulin in apple juice. The method uses a Brownlee analytical DB AQ C18 1.9 μm x 100 x 2.1 mm column with a mobile phase of water of pH 4.0 with acetic acid. The flow rate is 0.5 mL/min. HMF elutes very close to patulin, therefore, it was necessary to demonstrate the separation between patulin and HMF. Ethyl acetate was used for the extraction of patulin and the extracts were treated with sodium sulphate to remove moisture. This was important because patulin may be destroyed when wet ethyl acetate is evaporated to dryness.³ Also, a lower temperature of 40 °C was used for evaporation of the ethyl acetate layer, since patulin is not stable at high temperatures in ethyl acetate.

Alternately, a Brownlee validated AQ C18 100 x 2.1 mm x 3.0 μm can be used at a flow rate of 0.7 mL per min to achieve the same resolution between patulin and HMF.

The samples collected from the market were analyzed by the above method and the level of patulin determined. All the samples contained less than 5 $\mu\text{g/L}$ of juice. The method was validated at several levels on juice matrix and the recovery values were between 80.52-109.48%.

References

1. Guidance on the control of patulin in directly pressed apple juice, <http://www.newark-sherwooddc.gov.uk/ppimageupload>.
2. Wikipedia.
3. AOAC Official Method 995.10, Patulin in Apple Juice, Liquid Chromatographic Method.
4. Journal of AOAC International, Vol. 90, No. 3, 879-883.



APPLICATION NOTE

HPLC/ICP-MS

Authors

Ken Neubauer

Pamela Perrone

Wilhad Reuter

PerkinElmer, Inc.
Shelton, CT USA

Determination of Arsenic Speciation in Apple Juice by HPLC/ ICP-MS Using the NexION 300/350

Introduction

Recent media coverage has brought the issue of arsenic (As) in apple juice into public awareness. Because arsenic can exist in several forms (some toxic, some non-toxic), it is important to identify the individual forms present in the juice. This is most easily accomplished through the use of liquid chromatography (HPLC), to separate the

species, and inductively coupled plasma mass spectrometry (ICP-MS), to detect them. A challenge with juice analysis is the high level of sugars which can affect both the chromatography and the ICP-MS.

This work demonstrates an HPLC/ICP-MS method for the separation and determination of arsenic species in a variety of apple juices.

Experimental

Samples and Sample Preparation

The apple juice samples were purchased from local grocery stores. Sample preparation involved a 2-fold dilution in the aqueous component of the mobile phase (i.e. without the methanol) with pH adjusted to 7.0 prior to analysis. All quantitative measurements were made against external calibration curves, with calibration standards prepared the same way as the samples.

Instrumental Parameters

Table 1 shows the ICP-MS conditions used for this analysis; the HPLC conditions were derived from previous work.¹ Because no arsenic interferences were found in the apple juice, Standard mode (i.e. no gas was used in the Universal Cell) was used for all analyses.

Table 1. ICP-MS Conditions.

Instrument	NexION® 300D ICP-MS
Nebulizer	Glass Concentric
Spray Chamber	Glass Cyclonic
RF Power	1600 W
Universal Cell Mode	Standard
Isotope	As75
Dwell Time	500 ms

Results and Discussion

From the analysis of several apple juice samples, the following arsenic species were found: trivalent arsenic (As₃), pentavalent arsenic (As₅), monomethyl arsenic (MMA), and dimethyl arsenic (DMA). These species were the focus of further investigation.

Figure 1 shows the chromatogram of a 0.5 µg/L mixed As standard, which demonstrates that the species of interest can be separated in under 4 minutes.

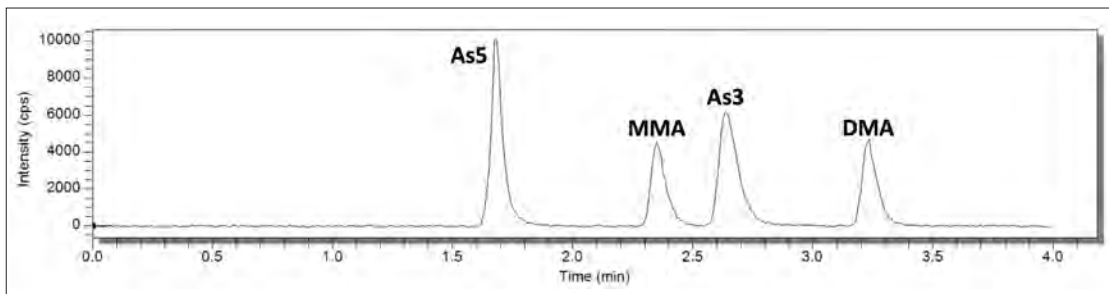


Figure 1. Separation of an arsenic standard containing 0.5 µg/L of each of As₅, As₃, MMA, and DMA.

To explore the effects of the apple juice matrix on the separation, a chromatogram of an arsenic standard was compared to the chromatogram of an apple juice sample. Figure 2 shows the chromatograms of a 0.5 µg/L mixed As standard and an apple juice sample. The juice matrix has a slight affect on the retention times of As₃ and DMA, but does not affect the peak shapes. These retention time shifts can be easily accounted for with appropriate retention time search windows.

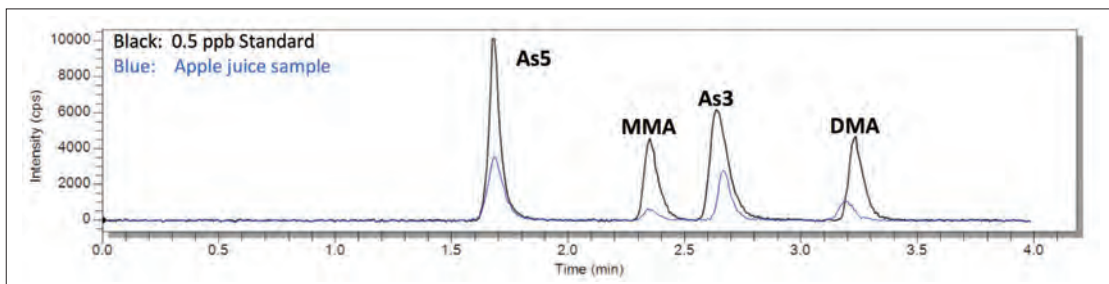


Figure 2. Chromatograms of a 0.5 µg/L mixed As standard (black) and an apple juice sample (blue).

The stability of the separation is demonstrated in Figure 3, which shows the chromatograms of 30 injections of the same apple juice sample over 2.25 hours, along with the concentration of each species.

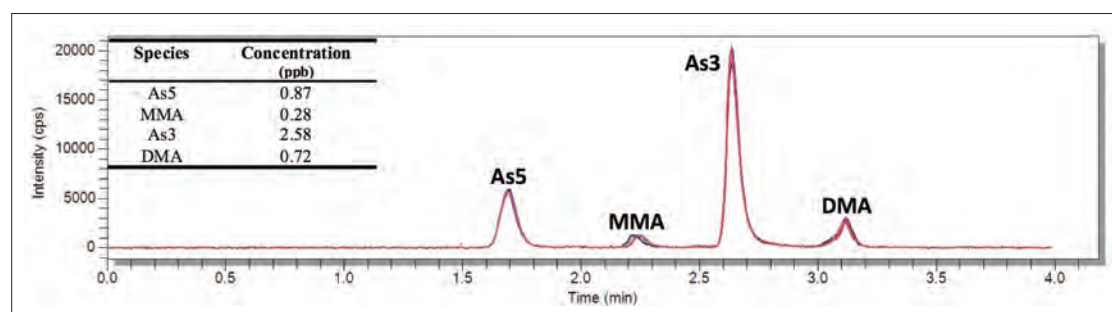


Figure 3. Chromatograms of 30 consecutive injections of the same apple juice sample, along with the concentration of each species.

Figure 4 shows the chromatograms for the calibration standards used in this work. Since the juice samples contain low levels of As, the calibration standards ranged from 0.1-1 $\mu\text{g/L}$ and gave regressions greater than 0.999.

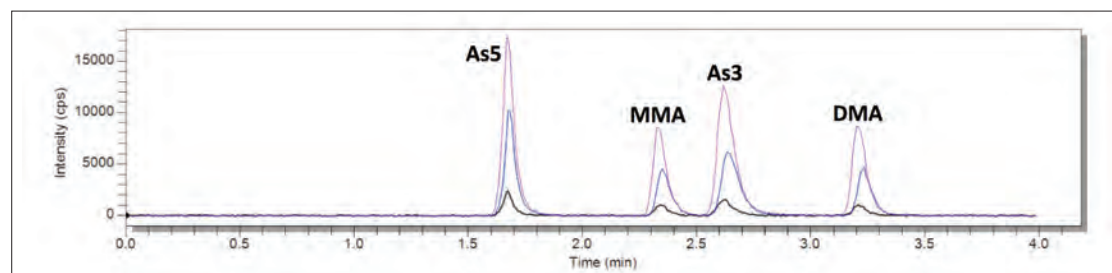


Figure 4. Chromatograms of As calibration standards between 0.1 and 1.0 $\mu\text{g/L}$.

To test the stability of the method, several samples were measured multiple times. Figure 5 shows the chromatograms and quantitative results from a typical sample over five consecutive injections. The consistency of the results demonstrates the short-term robustness of the method. Long-term robustness is demonstrated in Figure 6, which shows a stability plot over 8 hours, with all concentrations normalized to the first sample. For this test, a number of juice samples were analyzed, with a 0.5 $\mu\text{g/L}$ check standard being analyzed every 6 injections. All results are within 10% of the initial measurement, indicating both the reproducibility of the chromatography and robustness of the NexION ICP-MS.

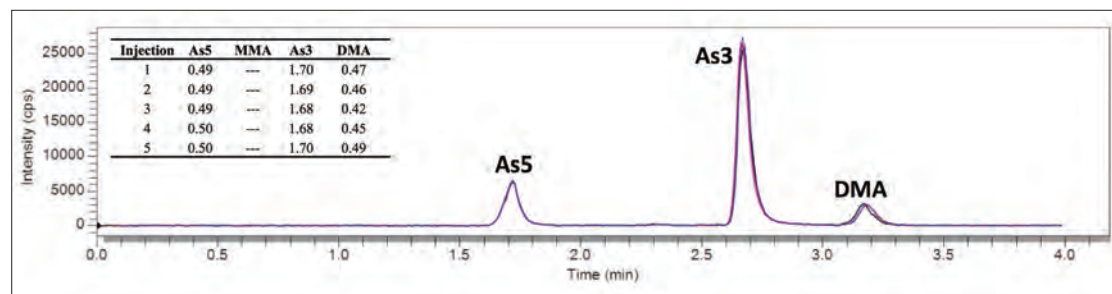


Figure 5. Chromatograms and concentration results from five consecutive injections of the same apple juice sample (units are $\mu\text{g/L}$).

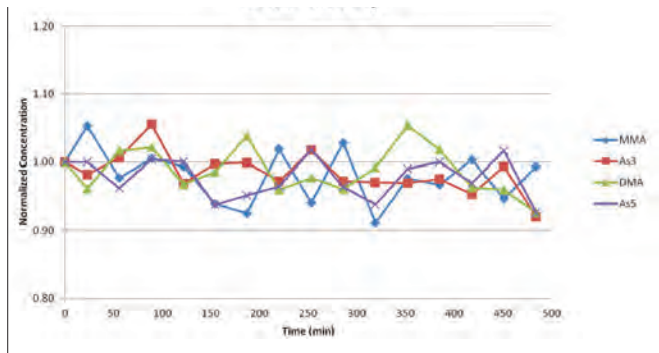


Figure 6. Eight-hour stability plot of a 0.5 µg/L check standard analyzed after every 6 injections of apple juice samples – all concentrations are normalized to the initial result.

Table 2 shows the results obtained from running a variety of different apple juice samples. Table 3 demonstrates the accuracy of the method by comparing the total arsenic values for eight samples obtained both by summing the speciation results (accounting for difference in concentrations between the arsenic species and arsenic as a component of the species) and ICP-MS measurement of total arsenic (i.e. ICP-MS analysis without the HPLC).

Table 2. Results from Various Apple Juice Samples (all values in µg/L).

Sample	As5	MMA	As3	DMA
1	1.69	–	2.07	0.85
2	0.95	–	0.21	0.62
3	2.17	1.21	1.17	0.50
4	2.02	–	1.88	0.69
5	0.79	0.36	2.37	0.67
6	0.56	0.19	0.40	0.31
7	0.47	0.44	0.82	0.45
8	0.79	–	3.23	0.92

(all values in µg/L).

Sample	Sum of Species	Total
1	4.24	4.22
2	1.55	1.49
3	4.14	4.26
4	4.18	4.27
5	3.95	3.67
6	1.46	1.23
7	1.88	1.77
8	4.52	4.73

Conclusions

This work has demonstrated a simple, rugged, fast method for arsenic (As) speciation in apple juice samples. To further validate the method, the analyses were repeated over multiple days on different instruments with columns from different lots. The similar results (not presented) verify the robustness of the method.

References

S. Miyashita, M. Shimoya, Y. Kamidate, et. al.
Chemosphere 75 (2009), 1065-1073.



APPLICATION NOTE

Mass Spectrometry

Author:

Avinash Dalmia

PerkinElmer, Inc.
Shelton, CT USA

Rapid Screening of Adulteration in Pomegranate Juice with Apple Juice Using DSA/TOF with Minimal Sample Preparation

Introduction

Pomegranate juice is in high demand due to its well documented health benefits. Studies based on a significant body of scientific research conducted on authentic pomegranate juice have established that pomegranate juice has superior antioxidant activity compared to other popular fruit juices such as grape, orange and apple^{1,2,3}. These superior health benefits have led to a meteoric rise in the popularity of pomegranate juice over the last 10 years. This has resulted in pomegranate juice having a significantly higher cost than other juices, especially in comparison to apple, orange and grape juice. This high cost has provided an economic incentive for the adulteration of pomegranate juice⁴. There are a number of other reasons for adulteration including: customers demanding their suppliers reduce costs; there comes a point when a supplier may adulterate the product to lower the cost and maintain a workable margin. Another reason for pomegranate juice adulteration is that it is in high demand and short supply, leading to incentives to extend limited supplies by the addition of other cheaper fruit juices.

The adulteration of pomegranate juice is accomplished by using cheap ingredients. One of the common adulterants of pomegranate juice is a cheaper so called filler fruit juice such as apple juice. The advantage of adulterating pomegranate juice with apple juice is that it is clear and provides no noticeable change to the sugar content. Organic acid analysis plays a fundamental role in testing the authenticity of pomegranate juice. One organic acid of interest is malic acid. Although it is present in both pomegranate and apple juice, the amount in apple juice is significantly higher than in pomegranate juice, 4.5 g/L and 0.57 g/L respectively^{5,6}. Therefore, the adulteration of pomegranate juice with apple juice can be detected by the elevated levels of malic acid present in the juice. Analytical methods used routinely for

for organic acid analysis in fruit juices are based on liquid chromatography (reverse phase or ion exchange) coupled to UV detection⁷ or mass spectrometry^{8,9}. These measurement techniques are either expensive or time consuming or both, and require extensive method development and sample preparation. In this work, we demonstrated that the AxION® Direct Sample Analysis™ (DSA™) system integrated with the AxION 2 time-of-Flight (TOF) mass spectrometer, with stable isotope dilution, can be used for rapid measurement of adulteration in pomegranate juice with apple juice with minimal sample preparation.

Experimental

Pomegranate and apple juices were purchased from a local supermarket. Both juices were diluted by a factor of 200 in water and spiked with an internal standard of deuterated malic acid (malic acid- d_3) at a concentration of 0.005 g/L. The juices were mixed in different proportions to simulate the adulteration of pomegranate juice with grape juice at levels of 5, 10, 20, 30 and 50 percent apple juice. In this analysis, the deuterated internal standard of malic acid was added to quantitate the amount of malic acid in both juices (pomegranate and apple) and their mixtures. 10 μ L of each sample was pipetted directly onto the stainless mesh of the AxION DSA system and the position of this was optimized, prior to ionization and analysis.

The DSA/TOF experimental parameters were as follows:

Corona current of 5 μ A, heater temperature of 300 °C, auxiliary gas (N_2) pressure of 80 psi, drying gas (N_2) flow of 3 l/min and drying gas (N_2) temperature of 25 °C. The AxION 2 TOF MS was run in negative ionization mode with a flight voltage of 8000 V. The capillary exit voltage was set to -80 V for the analysis. Mass spectra were acquired in a range of m/z 50-700 at an acquisition rate of 5 spectra/s. All samples were analyzed within 15 sec. To obtain higher mass accuracy, the AxION 2 TOF instrument was calibrated before each analysis by infusing a calibrant solution into the DSA source at 10 μ L/min.

Results

The diluted fruit juice samples of pomegranate and apple and their mixtures spiked with an internal standard (malic acid- d_3) were directly analyzed by DSA/TOF with no further sample preparation. Figure 1 and Figure 2 show the mass spectra for pomegranate and apple juice diluted by a factor of 200 respectively, and spiked with an internal standard (malic acid- d_3) at a level of 0.005 g/L in negative ion mode using DSA/TOF.

The data in Figure 1 and Figure 2 shows that the response ratio for malic acid with respect to malic acid- d_3 in pomegranate and apple juice was 0.575 and 3.453, respectively. In this analysis, we have used the stable isotope labeled analog of the analyte (malic acid) as an internal standard, which has identical chemical and structural properties to that of the analyte¹⁰. Therefore, it can be assumed that both the analyte and its internal standard (malic acid- d_3) will have similar ionization efficiencies. Based on

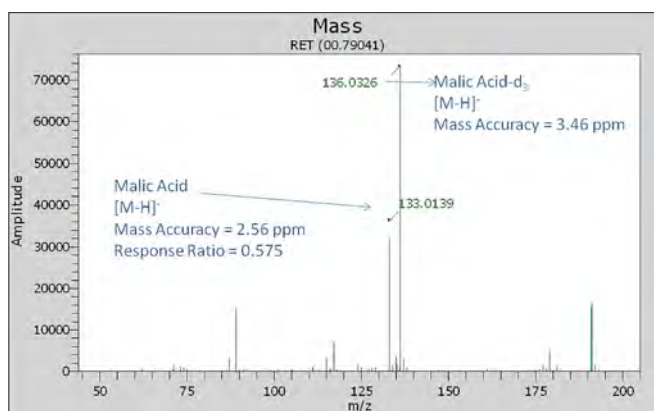


Figure 1. Mass spectra of pomegranate juice diluted by a factor of 200 and spiked with 0.005 g/L of internal standard.

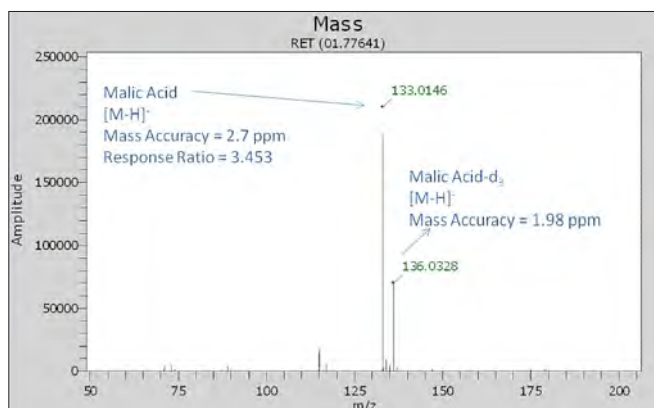


Figure 2. Mass spectra of apple juice diluted by a factor of 200 and spiked with 0.005 g/L of internal standard.

Type of Juice	Malic Acid Reported in Literature	Malic Acid Measured by DSA/TOF
Pomegranate	0.53 g/L ⁵	0.575 g/L
Apple Juice	4.5 g/L ⁶	3.453 g/L

Table 1. Measured versus literature values for amount of malic acid in pomegranate and apple juice.

this assumption and after accounting for the dilution, the amount of malic acid in pomegranate and apple juice was determined to be 0.575 and 3.453 g/L, respectively. The relative standard deviations of these measurements were 2% with and 20% without the internal standard. This demonstrates that the addition of an internal standard improves the accuracy of the measurement with DSA/TOF. Table 1 shows that there is a good agreement between the values for malic acid measured by DSA/TOF and those reported in the literature for pomegranate and apple juice. Figure 3 shows that the amount of malic acid in pomegranate juice increases linearly with the increase in apple juice adulteration with an excellent correlation coefficient value of R^2 equal to 0.9997. Using DSA/TOF, we can detect adulteration of pomegranate juice with 5% or higher of apple juice. Table 2 shows good correlation between the expected and measured values for malic acid in pomegranate juice adulterated with different levels of apple juice.

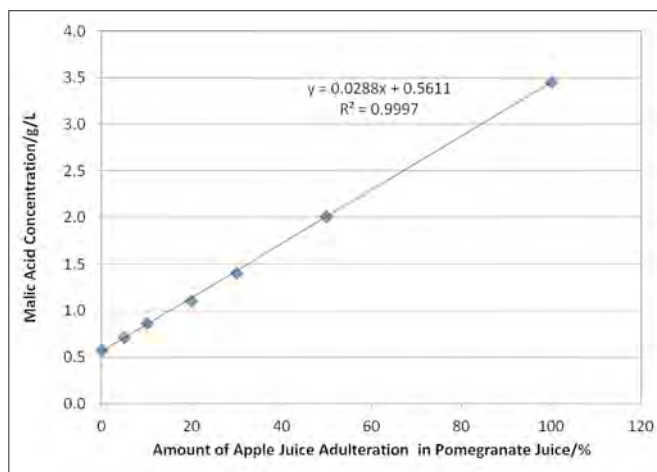


Figure 3. Malic acid concentration as a function of amount of adulteration of apple juice in pomegranate juice.

Apple Juice % in Pomegranate Juice	Expected Amount of Malic Acid	Measured Amount of Malic Acid	RSD
5	0.719 g/L	0.711 g/L	1.45%
10	0.863 g/L	0.865 g/L	2.12%
20	1.151 g/L	1.110 g/L	0.99%
30	1.438 g/L	1.408 g/L	1.80%
50	2.013 g/L	2.008 g/L	1.69%

Table 2. Expected versus measured amount of malic acid in pomegranate juice adulterated with different levels of apple juice.

Conclusion

This study shows the first work for the rapid measurement of adulteration of pomegranate juice with apple juice using DSA/TOF by quantitating the amount of malic acid present. The data showed that the level of malic acid in pomegranate juice increased linearly with the increase in apple juice adulteration.

The best internal standard is an isotopically labeled version of the molecule you want to quantify because an isotopically labeled internal standard will compensate for possible variations in sample preparation, sample injection and ionization efficiency in different matrices and improve accuracy of quantitation. This was demonstrated in this experiment, as the average relative standard deviation of the measurements without internal standard was 10 times higher in comparison to measurements done with internal standard. The average relative standard deviation of all measurements with DSA/TOF with stable isotope dilution was less than 2%. The mass accuracy of all measurements was less than 5 ppm with external calibration. All samples were screened, with minimal sample preparation, in 15 sec. per sample. In comparison to other established techniques such as LC/MS and LC/UV, DSA/TOF will improve laboratory productivity and decrease costs and analysis time.

References

- Seeram N.P., Aviram M., Zhang Y., Henning S. M., Feng L., Dreher M., Heber D., Comparison of antioxidant potency of commonly consumed polyphenol-rich beverages in the United States, *J. Agric. Food. Chem.*, 2008, 56, 1415-1422.
- Guo C., Wei J., Yang J., Xu J., Pang W., Jiang Y., Pomegranate juice is potentially better than apple juice in improving antioxidant function in elderly subjects, *Nutr. Res.*, 2008, 28, 72-77.
- Pantuck A. J., Leppert J. T., Zomorodian N., Aronson W., Hong J., Barnard R.J., Seeram N., Liker, H., Wang H., Elashoff R., Heber D., Aviram M., Ignarro L., Belldegrin A., Phase II study of pomegranate juice for men with rising prostate specific antigen following surgery or radiation for prostate cancer, *Clin. Cancer Res.*, 2006, 12, 4018-4026.
- Jimenez, D.M., Ramazanov A., Sikorski S., Ramazanov Z., Chkhikvishvili, I., A new method for standardization of health promoting pomegranate fruit (*punica granatum*) extract, *Georgian Med. News.*, 2006, 70-77.
- Krueger D.A., Composition of Pomegranate Juice, *J. AOAC Int.*, 2012, 95, 63-68.
- Organic Acid Analysis by Krueger Food Laboratories; available at <http://www.kfl.com/oa.html>.
- Association of official Analytical Chemists International Official Methods of Analysis, 18th Ed, Method 986.13, Gaithersburg, MD, 2008.
- Erk T., Bergmann H., Richling H., A novel method for quantitation of quinic acid in food using stable isotope dilution analysis, *J. AOAC Int.*, 2009, 57, 1119-1126.
- Ehling S., Cole S., Analysis of Organic Acids in Fruit Juices by Liquid Chromatography-Mass Spectrometry: An Enhanced Tool for Authenticity Testing, *J. AOAC Int.*, 2011, 59, 2229-2234.
- Jessome L. L., Volmer A. D., Ion Suppression: A Major Concern in Mass Spectrometry, *LCGC North America*, 2006, 24, 498-510.

PerkinElmer, Inc.
940 Winter Street
Waltham, MA 02451 USA
P: (800) 762-4000 or
(+1) 203-925-4602
www.perkinelmer.com



For a complete listing of our global offices, visit www.perkinelmer.com/ContactUs

Copyright ©2013, PerkinElmer, Inc. All rights reserved. PerkinElmer® is a registered trademark of PerkinElmer, Inc. All other trademarks are the property of their respective owners.

011009_01

Liquid Chromatography/ Mass Spectrometry

Author:

Avinash Dalmia

PerkinElmer, Inc.
Shelton, CT

Rapid Analysis of Apple Juice Adulteration with Pear Juice Using LC/TOF

Introduction

Adulteration of fruit juices is quite common in the market place and is often done through juice substitution.

Pear juice has a slightly lower market value than apple juice yet both have similarities in major chemical composition, making pear juice an ideal adulterant for apple juice. Both juices have similar carbohydrate, organic acid and amino acid levels, therefore the detection of apple juice adulteration with pear juice, based on these compounds, has limited applicability. According to various references¹⁻⁴, the phenolic profiles in pear and apple juice are slightly different. One of the phenolic compounds, arbutin, can be used as a marker compound to detect adulteration. The structure of arbutin is shown in Figure 1. In this application note, we present a rapid method for detecting apple juice adulteration with pear juice using LC/TOF, which requires minimal sample preparation.

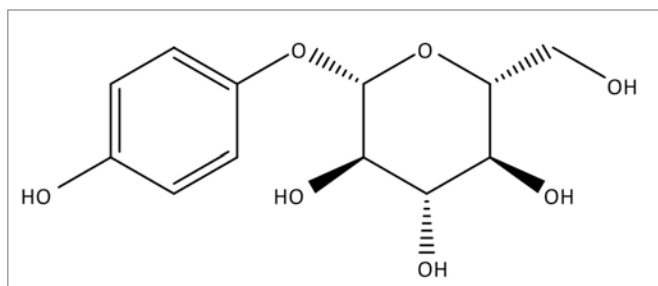


Figure 1. Chemical structure of arbutin.

Method

Pear and apple juices were purchased from a local supermarket. Both juices were diluted by a factor of 5 in water and filtered through a 0.2 μm PTFE syringe filter. The juices were mixed in different proportions to simulate the adulteration of apple juice with pear juice at levels of 10, 20, 30, 40 and 50 percent. The diluted and filtered juices and their mixtures were analyzed with LC/TOF without any further sample preparation.

Table 1. LC conditions.

Pump:	PerkinElmer Flexar™ FX-15 UHPLC pump
Flow:	0.3 mL/min
Mobile phase A:	100 % water with 0.1 % formic acid
Mobile phase B:	100 % acetonitrile with 0.1 % formic acid
Gradient conditions:	
Time (min)	%A %B Curve
0.5	95 5 1
7.0	60 40 1
7.5	60 40 1
Injection volume:	10 μL Full Loop Mode
Column:	PerkinElmer Brownlee™ SPP RP-Amide, 2.1x100 mm, 2.7 μm (part number N9308501)

Table 2. MC conditions.

Mass spectrometer:	PerkinElmer AxION® 2 TOF MS
Ionization source:	PerkinElmer Ultraspray™ 2 (Dual ESI source)
Ionization mode:	Negative
Capillary exit voltage:	-90 V
ESI source temperature:	350 °C
Drying gas flow rate:	10 L/min
Internal calibration:	Performed using m/z 112.9856 and 601.9790 as lock mass ions

Results and Discussion

A 7.5 minute gradient LC method coupled with TOF MS was developed to determine the presence of arbutin in apple and pear juices. Figures 2-4 show the extracted ion chromatograms (EICs) for the formate adduct of arbutin in a sample containing 10 $\mu\text{g/ml}$ arbutin, pear juice diluted by a factor of 5 and apple juice diluted by a factor of 5, respectively. The data in Figures 2-4 show that arbutin is present in pear juice, whereas, it is either absent or present below the TOF MS detection limit of arbutin in apple juice. Figure 5 shows that the presence of arbutin in pear juice was further confirmed by experimental accurate mass measurement of the deprotonated molecular ion and the formate adduct of arbutin in pear juice with TOF MS. The data demonstrates that arbutin can be used as a marker compound to determine the adulteration of apple juice with pear juice using LC/TOF. This is supported further by data in Figure 6, which shows that the response for arbutin increases linearly with the increase in adulteration of apple juice with pear juice from 10 to 50 %. It confirmed that the adulteration of apple juice with pear juice can be detected by the presence of arbutin. Figure 7 shows overlay of arbutin response in apple juice diluted by a factor of 5 in water and spiked with 10 $\mu\text{g/ml}$ arbutin and apple juice mixed with 10 % pear juice and diluted by a factor

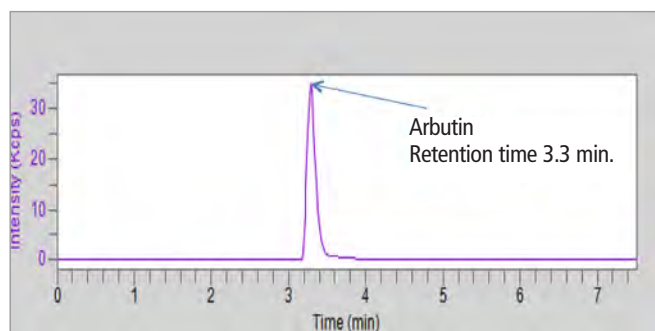


Figure 2. EIC for arbutin in a standard containing 10 $\mu\text{g/ml}$ arbutin with LC/TOF.

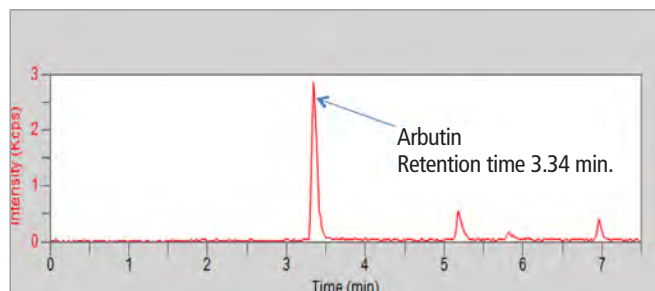


Figure 3. EIC for arbutin in pear juice, diluted in water by a factor of 5 with LC/TOF.

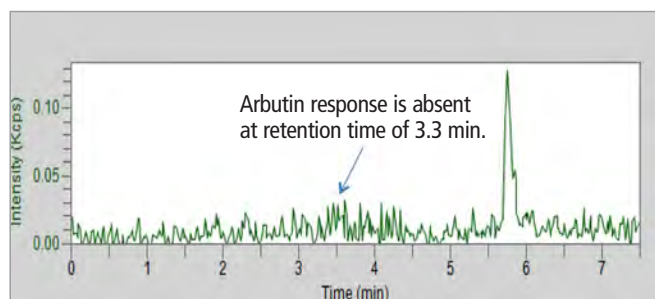


Figure 4. EIC for arbutin in apple juice, diluted in water by a factor of 5 with LC/TOF.

of 5. Based on the response for arbutin in diluted apple juice with 10 % pear juice relative to its response in diluted apple juice spiked with 10 µg/ml arbutin and after accounting for dilution factor, the amount of arbutin in pear juice was estimated to be about 66.3 µg/ml. In the references¹⁻⁴, it has been reported that the amount of arbutin in pear juice is in the range of 40.5-151.1 µg/ml with the mean value of 72.4 µg/ml. Therefore, the amount of arbutin measured in pear juice in this work with LC/TOF is consistent with the value for arbutin in pear juice as reported before in the literature.

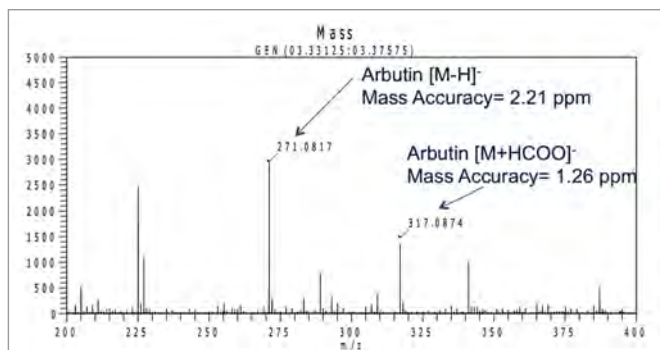


Figure 5. Mass spectrum of arbutin in pear juice, diluted by a factor of 5 in water with LC/TOF.

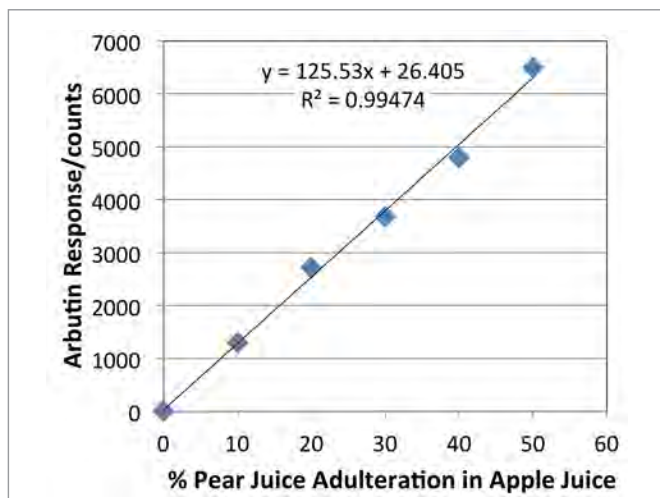


Figure 6. Arbutin response as a function of percentage of pear juice adulteration in apple juice.

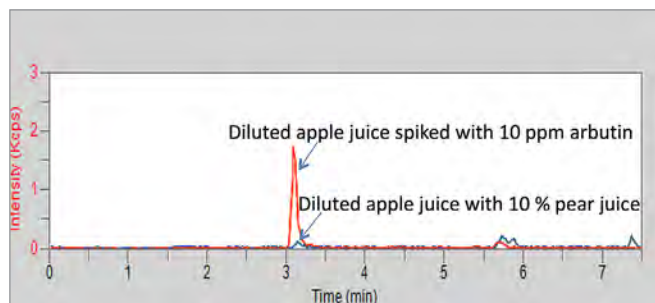


Figure 7. Overlay of EIC for arbutin in diluted apple juice spiked with 10 µg/ml arbutin and diluted apple juice with 10 % pear juice.

Conclusion

A dilute-and-shoot, rapid 7.5 minute LC/TOF method was developed for detecting 10 % or higher pear juice adulteration in apple juice. LC/TOF measurements showed the presence and absence of arbutin in pear and apple juice, respectively. The presence of arbutin in pear juice was confirmed unambiguously by retention time matching with arbutin standard and better than 3 ppm mass accuracy of arbutin's deprotonated and formate adduct ion. The arbutin response increased linearly as the amount of pear juice used to adulterate apple juice increased. This confirmed that arbutin can be used as a marker compound to detect the adulteration of apple juice in pear juice. The amount of arbutin determined in pear juice was 66.3 µg/ml.

References

1. L.Z. Lin, J.M. Harnly, Phenolic compounds and chromatographic profiles of pear skins, *J. Agric. Food Chem.*, 56, 9094-9101 (2008).
2. G.A. Spanos, R.E. Wrolstad, Influence of variety, maturity, processing, and storage on the phenolic composition of pear juice, *J. Agric. Food Chem.*, 38, 817-824 (1990).
3. G. A. Spanos, R. E. Wrolstad, Phenolics of apple, pear and white grape juices and their changes with processing and storage – a review, *J. Agric. Food Chem.*, 40, 1478-1487 (1992).
4. P. Thavarajah, N. H. Low, Adulteration of apple with pear juice: emphasis on major carbohydrates, proline and arbutin, *J. Agric. Food Chem.*, 54, 4861-4867 (2006).

Mass Spectrometry

Authors:

Avinash Dalmia
George L. Perkins

PerkinElmer, Inc.
Shelton, CT USA



Rapid Screening of Adulteration in Pomegranate Juice with Grape Juice Using DSA/TOF with No Sample Preparation

Introduction

Pomegranate juice is in high demand due to its well documented health benefits. Studies based on a significant body of scientific research conducted on authentic pomegranate juice have established that pomegranate juice has superior antioxidant activity compared to other popular fruit juices such as grape, orange and apple^{1,2}. These superior health benefits have led to a meteoric rise in the popularity of pomegranate juice over the last 10 years. This has resulted in pomegranate juice having a significantly higher cost than other juices, especially in comparison to apple, orange and grape juice. This high cost has provided an economic incentive for the adulteration of pomegranate juice³. There are a number of other reasons for adulteration including: customers demanding their suppliers reduce costs; there comes a point when a supplier may adulterate the product to lower the cost and maintain a workable margin. Another reason for pomegranate juice adulteration is that it is in high demand and short supply, leading to incentives to extend limited supplies by the addition of other cheaper fruit juices.

One of the common adulterants of pomegranate juice is grape juice. Grape juice is added as a sweetener and coloring agent substitute for natural pomegranate color. Organic acid analysis plays a fundamental role in testing authenticity of pomegranate juice. One of the organic acids, tartaric acid, is present in large amounts in grape juice (1 g/L) but it is absent in pomegranate juice^{4,5}. Therefore, the presence of tartaric acid in pomegranate juice can be used as an indicator of grape juice adulteration. Analytical methods used routinely for organic acid analysis in fruit juices are based on liquid chromatography (reverse phase or ion exchange) coupled to UV detection⁶ or mass spectrometry^{7,8}. These measurement techniques are either expensive or time consuming, or both and require extensive method development and sample



preparation. In this work, we demonstrated that the AxION® Direct Sample Analysis™ (DSA™) system integrated with the AxION 2 Time-of-Flight (TOF) mass spectrometer can be used for rapid screening of adulteration of pomegranate juice with grape juice with no sample preparation.

Experimental

Pomegranate and grape juices were purchased from a local supermarket. Both juices were mixed in different proportions to simulate the adulteration of pomegranate juice with grape juice at different levels of 1, 2, 5, 10 and 20 percent. All fruit juices and their mixtures were measured with an AxION 2 DSA/TOF system with no sample preparation. 10 µl of each sample was pipetted directly onto the stainless mesh of the AxION DSA system and the position of this was optimized, prior to ionization and analysis. The DSA/TOF experimental parameters were as follows: corona current of 5 µA, heater temperature of 300 °C, auxiliary gas (N₂) pressure of 80 psi, drying gas (N₂) flow of 3 l/min and drying gas (N₂) temperature of 25 °C. The AxION 2 TOF MS was run in negative ionization mode with flight voltage of 8000 V. The capillary exit voltage was set to -80 V for the analysis. Mass spectra were acquired in a range of m/z 50-700 at an acquisition rate of 5 spectra/s. All samples were analyzed within 15 sec. To obtain higher mass accuracy, the AxION 2 TOF instrument was calibrated before each analysis by infusing a calibrant solution into a DSA source at 10 µl/min. The data obtained with DSA/TOF was further analyzed with AxION Solo™ software.

Results

All fruit juice samples of pomegranate and grape were directly analyzed by DSA/TOF, with no sample preparation. Figure 1 and Figure 2 show the mass spectra for pomegranate and grape juice in negative ion mode using DSA/TOF, respectively. The mass spectra shows that the organic acids, citric and malic acid, are present in both juices, whereas, tartaric acid, is only present in grape juice. The data shows that tartaric acid can be used as a marker compound to determine the adulteration of pomegranate juice with grape juice using DSA/TOF. This is supported further by data in Figure. 3, which shows the presence of tartaric acid in a pomegranate fruit juice sample adulterated with 1% grape juice. Figure 4 shows that the response for tartaric acid increase with the increase in adulteration of pomegranate juice with grape juice from 1 to 20%. This confirmed that the adulteration of pomegranate juice with grape juice can be detected by the presence of tartaric acid. All mass measurements showed good mass accuracy with an error of less than 5 ppm.

DSA/TOF data obtained with authentic pomegranate and adulterated pomegranate samples with grape juice was centroided and further analyzed with AxION Solo™ software to demonstrate that data can be analyzed and visualized quickly. For this, adulterated pomegranate samples were

spotted on mesh spots number 1,6,9 and authentic pomegranate samples were spotted on rest of mesh spots. AxION Solo software provides fast visualization to determine if your target compound is present or not in sample analyzed. Therefore, the data was analyzed using tartaric acid as a target compound. Figure 5 shows analysis of data with AxION Solo software in plate format and provides a visual image that tartaric acid is present in adulterated pomegranate juice samples spotted on mesh spots 1,6,9 and it was absent in authentic pomegranate juice samples spotted on other mesh spots.

Conclusion

This study shows the first work for rapid screening of the adulteration of pomegranate juice with grape juice using DSA/TOF. The data showed that the presence of tartaric acid in pomegranate juice can be used to detect its adulteration

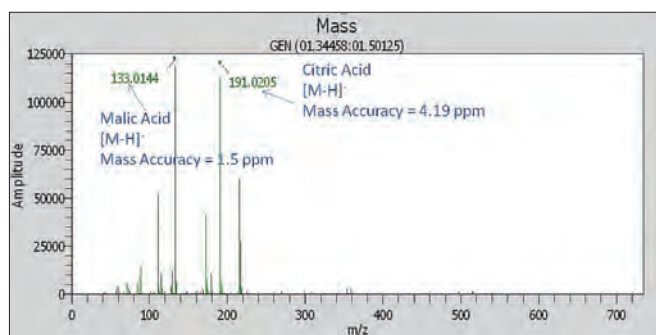


Figure 1. Mass spectra of pomegranate juice in negative ion mode using AxION DSA/TOF.

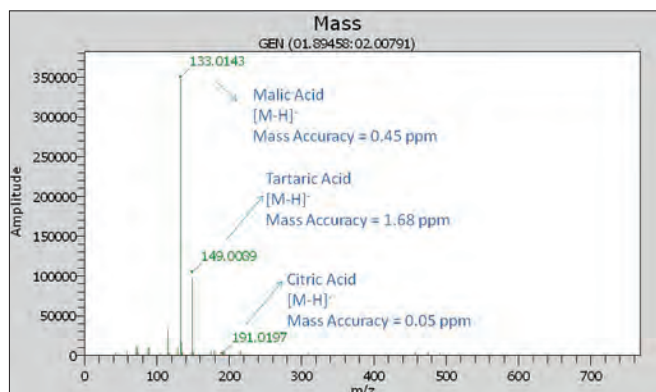


Figure 2. Mass spectra of grape juice in negative ion mode using AxION DSA/TOF.

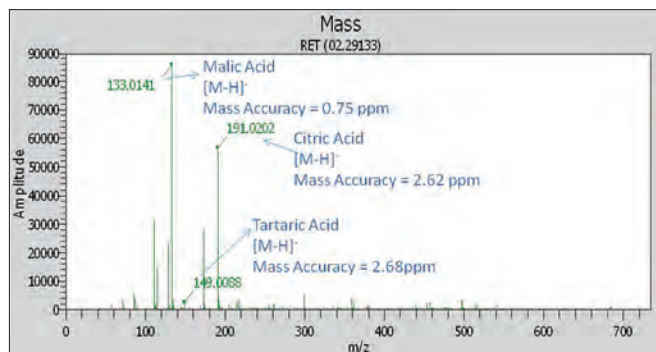


Figure 3. Mass Spectra of pomegranate juice adulterated with 1% grape juice in negative ion mode using AxION DSA/TOF.

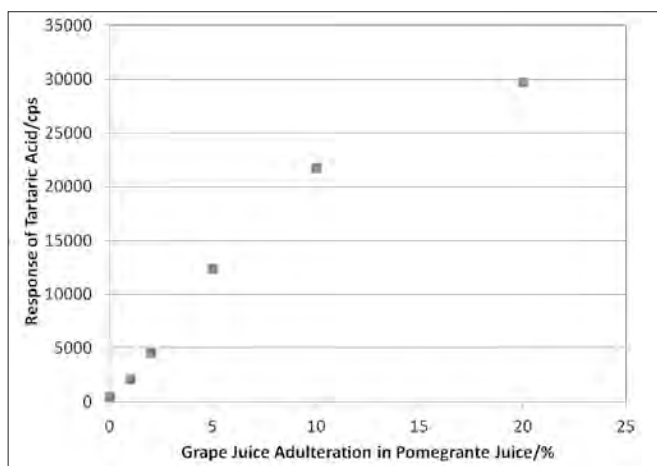


Figure 4. Tartaric acid response with increase in grape juice adulteration in pomegranate juice using AxION DSA/TOF.

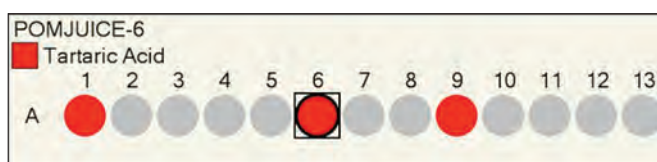


Figure 5. Analysis of authentic pomegranate juice and adulterated pomegranate juice samples with grape juice using AxION Solo software in plate format.

with grape juice. The mass accuracy of all measurements was less than 5 ppm with external calibration. All samples were screened, with no sample preparation, in 15 sec. per sample. We demonstrated that data obtained with DSA/TOF to detect pomegranate juice adulteration with grape juice can be analyzed and visualized quickly with AxION Solo™ software. In comparison to other established techniques such as LC/MS, DSA/TOF will improve laboratory productivity and decrease costs and analysis time.

References

1. Seeram N.P., Aviram M., Zhang Y., Henning S. M., Feng L., Dreher M., Heber D., Comparison of antioxidant potency of commonly consumed polyphenol-rich beverages in the United States, *J. Agric. Food. Chem.*, 2008, 56, 1415-1422.
2. Guo C., Wei J., Yang J., Xu J., Pang W., Jiang Y., Pomegranate juice is potentially better than apple juice in improving antioxidant function in elderly subjects, *Nutr. Res.*, 2008, 28, 72-77.
3. Pantuck A. J., Leppert J. T., Zomorodian N., Aronson W., Hong J., Barnard R.J., Seeram N., Liker, H., Wang H., Elashoff R., Heber D., Aviram M., Ignarro L., Belldgrun A., Phase II study of pomegranate juice for men with rising prostate specific antigen following surgery or radiation for prostate cancer, *Clin. Cancer Res.*, 2006, 12, 4018-4026.
4. Jimenez, D.M., Ramazanov A., Sikorski S., Ramazanov Z., Chkhikvishvili, I., A new method for standardization of health promoting pomegranate fruit (*punica granatum*) extract, *Georgian Med. News.*, 2006, 70-77.
5. Krueger D.A., Composition of Pomegranate Juice, *J. AOAC Int.*, 2012, 95, 63-68.
6. Association of official Analytical Chemists International Official Methods of Analysis, 18th ed., Method 986.13, Gaithersburg, MD, 2008.
7. Erk T., Bergmann H., Richling H., A novel method for quantitation of quinic acid in food using stable isotope dilution analysis, *J. AOAC Int.*, 2009, 57, 1119-1126.
8. Ehling S., Cole S., Analysis of Organic Acids in Fruit Juices by Liquid Chromatography-Mass Spectrometry: An Enhanced Tool for Authenticity Testing, *J. AOAC Int.*, 2011, 59, 2229-2234.



Pomegranate Juice Adulteration

Introduction

Pomegranate juice's popularity has skyrocketed in the last 10 years. This has been due to a combination of the perceived health benefits of consuming the juice's various antioxidant compounds (punicalagin, anthocyanins and ellagic acid) and its increased mainstream availability through Western pomegranate producers. This increase is highlighted by the rise in the consumption of 8-ounce servings of pomegranate juice in the U.S., which went from 75M servings in 2004 to 450M servings by 2008.¹ Interestingly, this data indicates that in 2004, there was 50:50 pure-to-blended pomegranate juice consumption, whereas in 2008, 100% pomegranate juice made up 75% of that consumed.¹ Popular juice blends, such as apple and grape, are less bitter and can make the overall juice taste more pleasant to those new to pomegranate. These blends have an additional advantage of being cheaper than pure pomegranate juice. Whereas a gallon of pomegranate juice concentrate costs \$30-60, a gallon of apple or grape juice is between \$5-7. This means if a pomegranate juice product is labeled as a blend with apple and grape juice, the consumer can expect to pay less than the cost of pure pomegranate juice.

Problems occur when lower cost juices are added and they are not mentioned on the label. This means that a producer can charge \$30-60 for a gallon that is only worth \$10-20. When asking how this happens, first consider where pomegranates have traditionally been grown. Iran is one of the world's largest producers, however other notable countries include Iraq, Syria, Afghanistan, Armenia, Georgia, Azerbaijan and many more. The countries have all had problems with suspicious food products in the past, with recent data suggesting a very high percentage of adulterated pomegranate juice is coming from the region. The question should then arise 'why not flag these countries imports into the West as suspicious?' This scheme should be effective but unfortunately the food supply chain is very complex. For example, these juices may be shipped to a distributor in India or China or Russia, before being shipped to the West for bottling and consumption with virtually no trace of the original grower. As such, some final products maybe adulterated without the final the bottler's knowledge.

How can we detect this?

While traceability is still an issue, detection of these fraudulent juices is important. Chromatography combined with mass spectrometry has been used to detect marker compounds for both pomegranate and the adulterant juices to good effect.² The issue with these techniques is that they require a certain amount of sample preparation before analysis and the chromatography process itself can take up to an hour. The AxION Direct Sample Analysis (DSA) system integrated to the AxION 2 Time of Flight Mass Spectrometer (TOF MS) allows for the direct ionization and detection of the juice in seconds without sample preparation or method development. This not only speeds up the analysis to less than 10 seconds, but it also means that non-scientists can test for adulteration without the need to understand the fundamental chemistry. Figure 1 shows the mass spectral profiles of 1a: pomegranate juice, 1b: grape juice and 1c: pomegranate juice with 1% grape juice adulteration carried out on a PerkinElmer AxION® DSA/TOF MS system with juice pipetted directly onto steel mesh for analysis, with gas temperature (25 °C), flow rate (3 L/min) and capillary exit voltage (-100V) previously adjusted to maximize signal, giving an average mass accuracy of less than 5 ppm. Figure 1a shows that there are significant contributions from citric and malic acid in pomegranate juice, Figure 1b shows that grape juice also has malic and citric acids but also a contribution from tartaric acid. As this is not present in pomegranate, this means tartaric acid can be used as a marker for grape juice addition to pomegranate juice. This is supported by Figure 1c where 1% grape juice has been added to pomegranate juice and the tartaric is still clearly viable. Hence, the juice is shown to be adulterated (with grape or another tartaric acid-containing fruit juice).

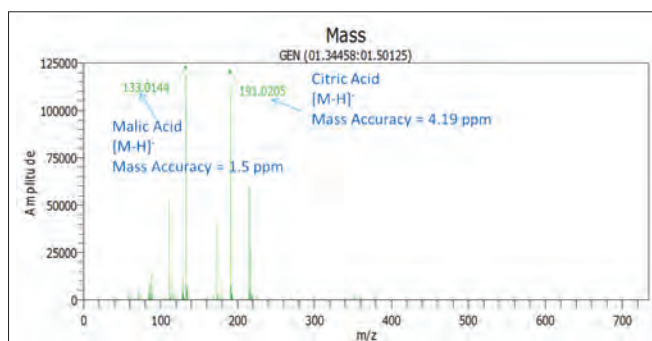


Figure 1a. Mass spectrum of pure pomegranate juice.

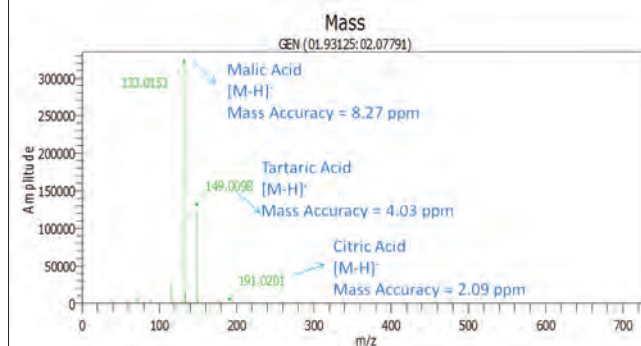


Figure 1b. Mass spectrum of pure grape juice.

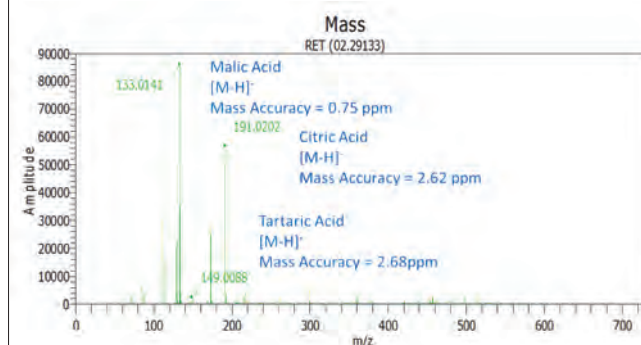


Figure 1c. Mass spectrum of pomegranate juice adulterated with 1% grape juice.

Is there an alternative technique?

DSA/TOF MS is a relatively simple, quick technique to carry out an accurate analysis of pomegranate juice adulteration but most cases of adulteration are in larger percentages. Given this, can we use a screening technique so that all samples can be scanned in an effective, yet efficient way? One possible technology that has been investigated is UV/Vis spectroscopy.³ For this work, 27 pomegranate, apple and grape mixtures were measured undiluted in 1 mm reduced-path length cuvettes (as the samples absorb strongly, a 10-mm cuvette would be unsuitable) and measured using a PerkinElmer LAMBDA™ 25 UV/Vis spectrometer with a fixed 1-nm bandpass and a 0.1-nm data interval (in order to produce as many data points as possible for the

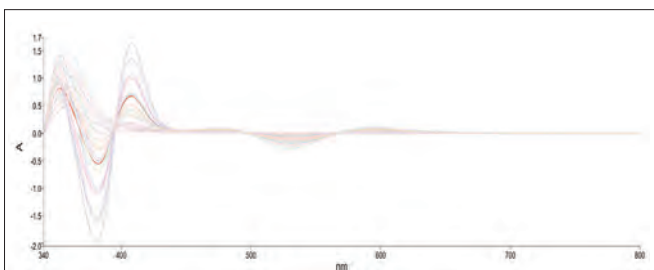


Figure 2a. Combined UV/Vis spectra for a range of pomegranate, apple and grape mixtures.

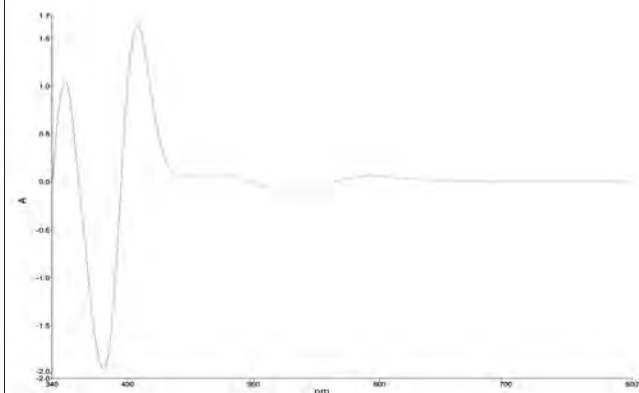


Figure 2b. UV/Vis spectrum of pure pomegranate juice.

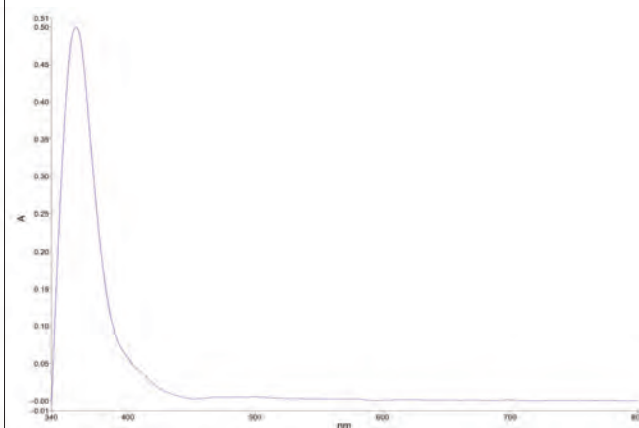


Figure 2c. UV/Vis spectrum of pure apple juice.

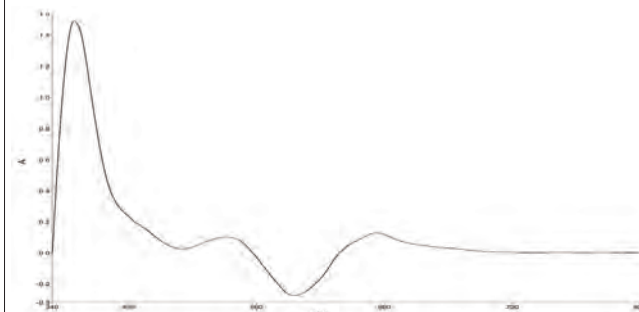


Figure 2d. UV/Vis spectrum of pure grape juice.

chemometric analysis) with the resulting second derivative spectra shown in Figure 2a, pure pomegranate shown in Figure 2b, pure apple in 2c and grape in 2d. Second derivative spectroscopy is a useful tool when measuring natural products as it tends to be less susceptible to non-specific background absorbance effects while, in this particular case, enhancing peaks of analytical interest. Most mixtures, Figure 2a, show two significant features – a feature at 530 nm which is seen in pomegranate, 2b, and grape, 2d. This is due to the red color of both pomegranate and grape juice and it is not surprising that apple juice has no observed feature. The spectra in Figure 2b also reveal features in the UV region for pomegranate juice that were present in all pomegranate-containing mixtures. These features are primarily due to the contributions from antioxidant compounds such as ellagic acid and give us a positive marker for pomegranate.

This means that UV/Vis spectroscopy can be used, by measuring the loss of absorbance in this region, as an indication of the extent to which the pomegranate juice has been adulterated. Alternatively, it could be used as a check for juice blends that the correct pomegranate, apple and grape ratios are present, as shown in Figure 3a, which is a quantitative fit to the data which shows excellent straight-line correlation. From this fit, it is shown in Figure 3b that for unknown mixtures of the juices, the ratios can be calculated.

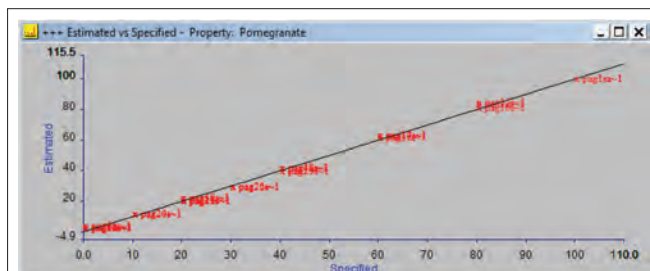


Figure 3a. Quantitative plot of the various juice mixtures.



Figure 3b. Prediction of unknown pomegranate, apple and grape blend using the generated calibration curve.

Conclusion

This work has shown that monitoring of incoming juices does not need to be difficult, time consuming or expensive with testing technologies such as DSA/TOF MS and screening technologies such as UV/Vis spectroscopy. Detection technologies such as these will be essential in ensuring that the food and beverage products that are being imported are both safe and authentic. However it will ultimately be when these technologies are linked to traceability software, allowing electronic tracking from the source, that the criminals will be dissuaded from adulterating products and detection evolves into prevention.

References

1. History of Pomegranate Juice Adulteration. Michael T. Roberts (2011) Intentional and Unintentional Adulteration of Food Ingredients and Dietary Supplements. USP workshop, Baltimore, USA.
2. Composition of pomegranate juice. D.A. Krueger (2012) J. AOAC Int., 95(1): 163-168.
3. A rapid method to assess authenticity of "100% pure" pomegranate juices by UV/Visible spectroscopy and multivariate analysis, R. Boggia *et. al.* (2012) J. Food and Agric. *Awaiting publication.*
4. Antioxidant Activity of Pomegranate Juice and Its Relationship with Phenolic Composition and Processing, M. Gil *et. al.* (2000) J. Agric. Food Chem. 48, 4581-4589.



APPLICATION NOTE

Gas Chromatography/ Mass Spectrometry

Author

A. Tipler, Senior Scientist

PerkinElmer, Inc.
Shelton, CT 06484 USA

The Qualitative Characterization of Fruit Juice Flavor using a TurboMatrix HS Trap and a Clarus SQ 8 GC/MS

Introduction

The PerkinElmer® TurboMatrix™ Headspace Trap system coupled with a Clarus® SQ 8 GC/MS is a very convenient means of identifying low concentration volatile organic compounds (VOCs) in foodstuffs. In this application note, the VOCs in various fruit juices were investigated. Sample preparation simply involved dispensing a fixed volume of fruit juice into a sample vial and sealing it. The analysis was fully automated.

Method

The experimental conditions for this analysis are given in Tables 1 to 4.

Table 1. GC Conditions.

Gas Chromatograph/ Mass Spectrometer	Clarus SQ 8
Column	60 m x 0.25 mm x 1.0 μ m Elite-SMS
Oven	35 °C for 5 min, then 6 °C/min to 245°
Injector	Programmable Split Splitless (PSS), 180 °C, Split OFF
Carrier Gas	Helium at 2.0 mL/min (28.6 psig initial pressure), HS Mode ON

Table 2. HS Trap Conditions.

Headspace System	TurboMatrix 110 HS Trap
Vial Equilibration	80 °C for 20 minutes
Needle	120 °C
Transfer Line	140 °C, long, 0.25 mm i.d. fused silica
Carrier Gas	Helium at 31 psig
Dry Purge	7 min
Trap	Air Toxics, 25 °C to 260 °C, hold for 7 min
Extraction Cycles	1 with 40 psig extraction pressure

Table 3. MS Conditions.

Scan Range	35 to 350 Daltons
Scan Time	0.1 s
Interscan Delay	0.06 s
Source Temp	180 °C
Inlet Line Temp	200 °C
Multiplier	1700V

Table 4. Sample Details.

Sample	1 mL of each of the following fruit juices:
	<ul style="list-style-type: none"> Orange juice Grapefruit juice Apple juice Lemon juice Lime juice Cranberry juice
Vial	Standard 22-mL vial with aluminum crimped cap with PTFE lined silicon septum

Results

The total ion chromatograms obtained from the six fruit juice samples are given in Figures 1 to 6. The component identities of the key peaks were established by performing mass spectral library searches. The results of these identifications are annotated in the following figures:

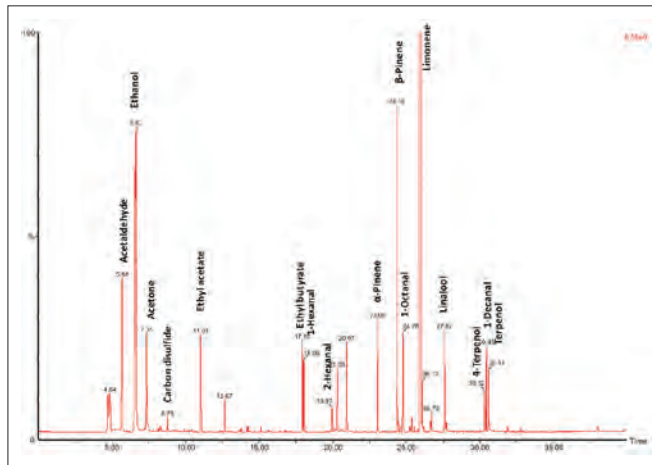


Figure 1. Full Total Ion Chromatogram obtained from orange juice.

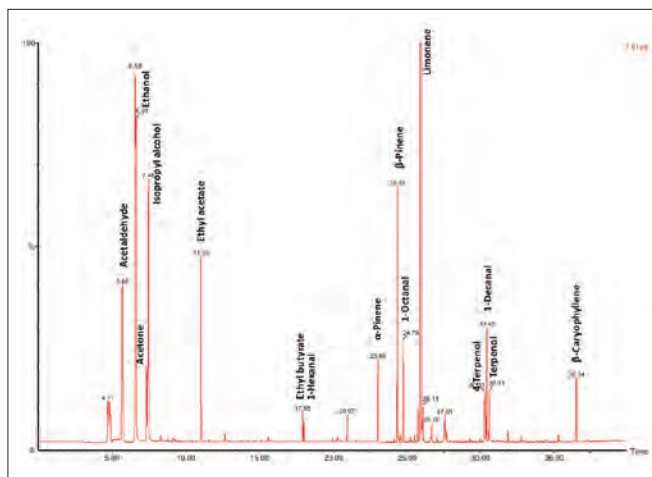


Figure 2. Full Total Ion Chromatogram obtained from grapefruit juice.

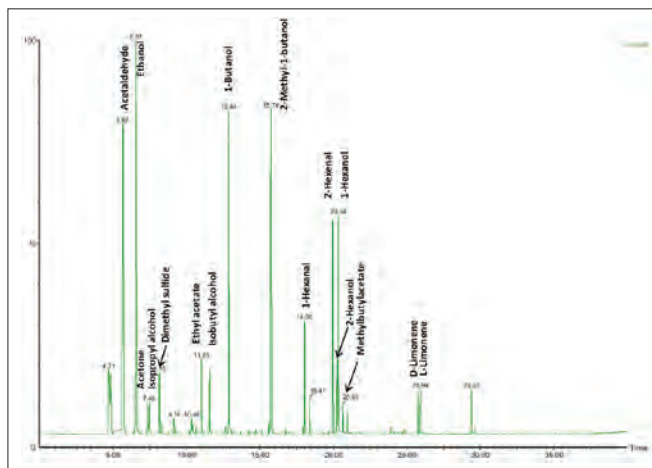


Figure 3. Full Total Ion Chromatogram obtained from apple juice.

Conclusions

This system provides a very simple and convenient way of characterizing the odor and flavor of natural products such as fruit juices. The use of GC/MS enables a very detailed aromatic profile of these fruit juices to be established. The use of a HS Trap system to perform the sample extraction enables low-level components to be visualized without compromising the system with injection of heavier, less volatile, unwanted sample material such as sugars and proteins.

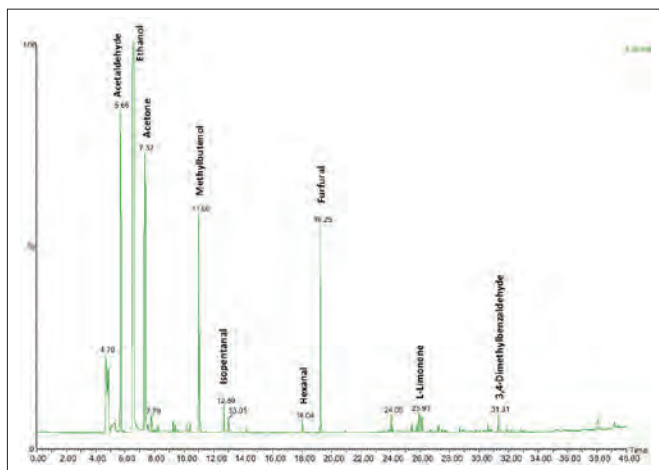


Figure 4. Full Total Ion Chromatogram obtained from lemon juice.

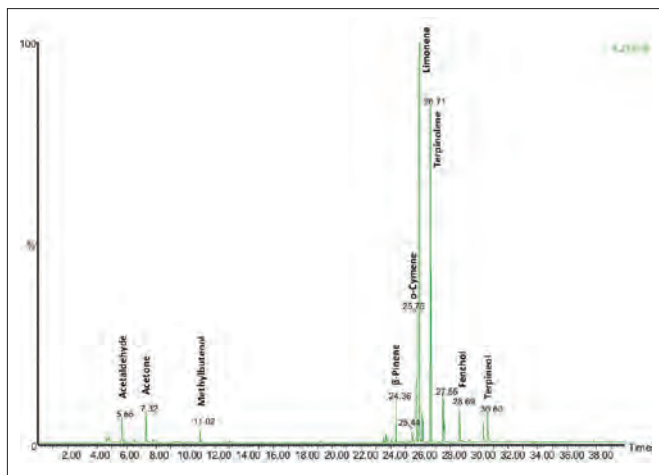


Figure 5. Full Total Ion Chromatogram obtained from lime juice.

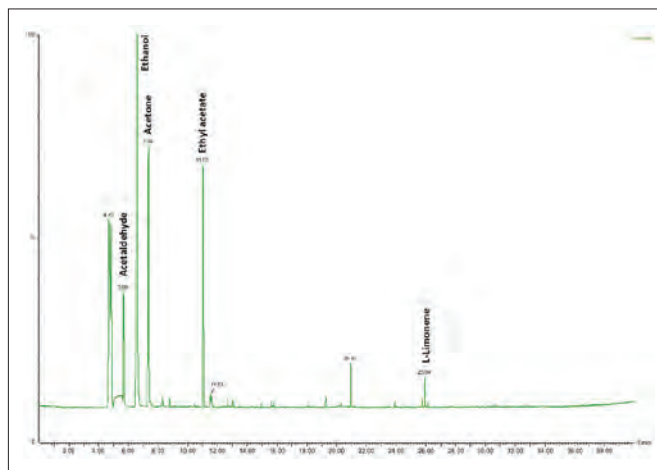


Figure 6. Full Total Ion Chromatogram obtained from raw cranberry juice.

Gas Chromatography

Authors:

Nathan Kuffel

Timothy Ruppel

PerkinElmer, Inc.
Shelton, CT

A Method for the Quantification of Ethanol Content in Consumable Fruit Juices by Headspace Injection

Introduction

The definition of an alcoholic beverage in the United States of America is a beverage that contains in excess of 0.5% ethanol by volume that is intended for consumption

alone or when diluted. Production of alcohol has been long established in society with many styles that take advantage of the metabolism of sugars into ethanol. While the production of ethanol is desirable for alcoholic beverages, it is undesirable for other beverages which contain sugars that do not wish to be sold as an alcoholic beverage. Such sugar metabolism is naturally occurring and is well understood to happen in raw fruit as well as processed juice and can vary by type, variety and maturation in the growing season.

A new application has been developed in the accurate determination of ethanol content in samples of these products utilizing the PerkinElmer® TurboMatrix™ headspace (HS) autosampler for better reproducible results. Additionally, since ethanol is the only desired peak, this method allows for a quick run time giving users the opportunity to analyze high volume throughput samples multiple times. The main focus of this method is intended toward fruit juices and it is confirmed to give accurate results amongst a wide range of store bought juices. This application note outlines the principles and technology of this method in the analysis and quantification of ethanol in consumable juices.

Experimental

System

Gas Chromatograph	PerkinElmer Clarus® 580
Injector	Programmable Split Splitless (PSS)
Detector	FID
Electronic Pneumatics	PPC Carrier for PSS (Hydrogen), PPC FID Gases (Air & Hydrogen)
Column	30 m x 0.32 mmID x 1.8 µm Elite BAC-1 Advantage #N9315071
Headspace Apparatus	TurboMatrix
Data Analysis	Data processed on Waters® Empower® 3 software

Headspace Conditions

Temperature	Oven 60 °C, Needle 110 °C, Transfer Line 120 °C
Timing	Thermostat - 12 min, Pressurize – 1 min, Injection – 0.02 min, Withdraw – 0.3 min
Pressure	16 psig of Hydrogen Gas
Transfer Line Column	Split connection 2 m of 0.32 mmID fused silica, terminated in injector
Options	Operative Mode: Constant Inject Mode: Time

GC Conditions

GC Oven	45 °C Isothermal, Run Time: 2.50 min Equilibration Time: 0 min
Carrier Pressure	12 psig for 2.50 minutes, Split Flow 5.0 mL/min
FID	Range: x1 Attn: x-1 Temp: 250 °C Air: 450 mL/min H ₂ : 45 mL/min

Reagents

Off the shelf juices and deionized water are used for sample preparation. The internal standard solution used is t-butanol in deionized water.

Calibration

Ethanol standards with known amounts over the quantification range of 50 to 500 mg/dl ethanol v/v with an ISTD at a constant concentration. Vial and capped securely with headspace vial crimper.

Sample Preparation

A 50 µL volume of t-butanol is diluted in 250 mL of deionized water attached to the automatic dilutor. Precisely 75 µL of a juice sample and 750 µL deionized water/internal standard mixture are combined with an automatic dilutor into a standard autosampler vial. The vial is then securely sealed with a headspace vial crimper.

Table 1. Retention times of BAC compounds.

Compound	Retention Time (min)
Methanol	0.663
Acetaldehyde	0.697
Ethanol	0.806
Isopropanol	0.957
Acetone	1.033
t-Butanol	1.112
n-Propanol	1.268
Ethyl Acetate	1.924

Note: These compounds will not all be present in all fruit juices but are used to show the proper separation from ethanol in the case that an addition peak is present. It was also used to determine a reliable internal standard that would not co-elute with the ethanol. In this method t-butanol was used as the internal standard.

Results

It is necessary to have a good calibration curve and an internal standard for reference. Since ethanol has a very distinct and repeatable retention time, it allows for reliable integration of the area of the peak. The internal standard used is t-butanol, which elutes well after ethanol. The isothermal GC method allows for a minimum time between injections of 3.0 minutes, also referred to as PII (period from injection to injection). As expected the calibration produces an excellent quantitative linearity (0.997) and a high precision (1 % RSD) was seen at 500 ppm of ethanol.

Several commercial juices were analyzed for ethanol content with the results in Table 2.

Table 2. Ethanol content of selected store purchased juices.

Fruit Juice	Concentration of ethanol (mg/dl)
Orange juice A	56.5
Orange juice B	3.7
Mixed berry juice	57.0
Grape juice	236.2
Lemonade	13.2
Apple juice	86.4
Pomegranate juice	39.7

The results would indicate that the ethanol content in all cases is safely below the required limit at which a beverage is considered to be alcoholic. Also, the data suggests that the ethanol content is independent of the variety of fruit in the juice but further analysis at the point of manufacturer would be required to definitively make such a claim. It has been shown that the ethanol content that occurs naturally in different varieties of orange, for example, could be the cause of the different results between the two orange juices examined.

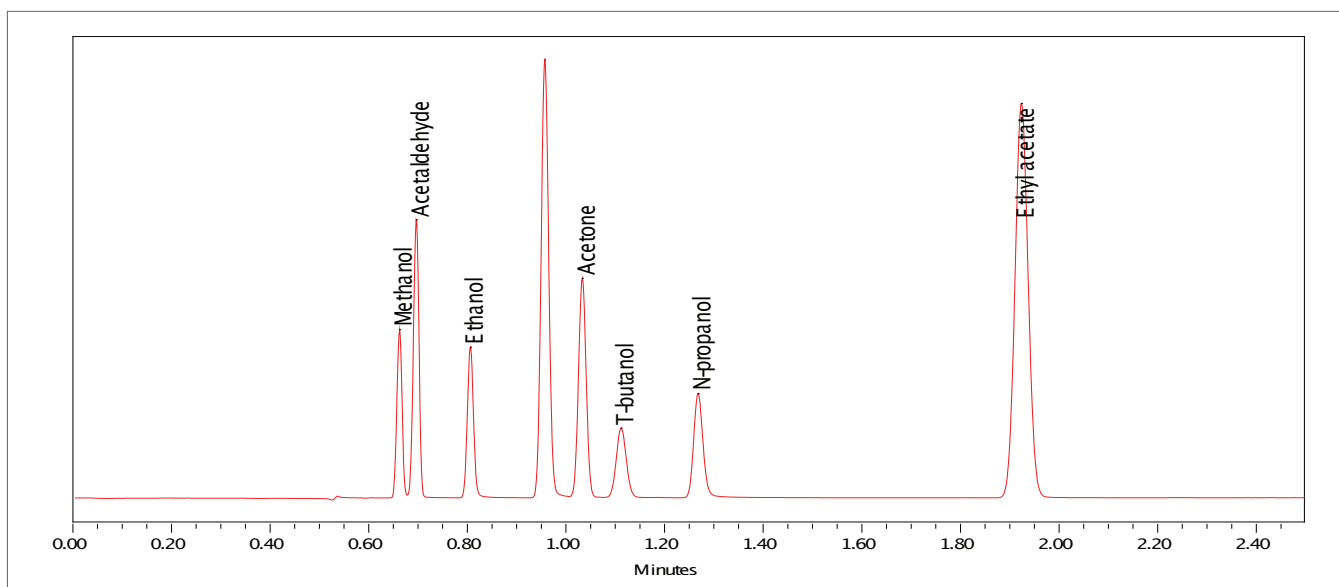


Figure 1. Chromatogram showing the elution order of the BAC mix that identified t-butanol as a suitable internal standard for the ethanol analysis.

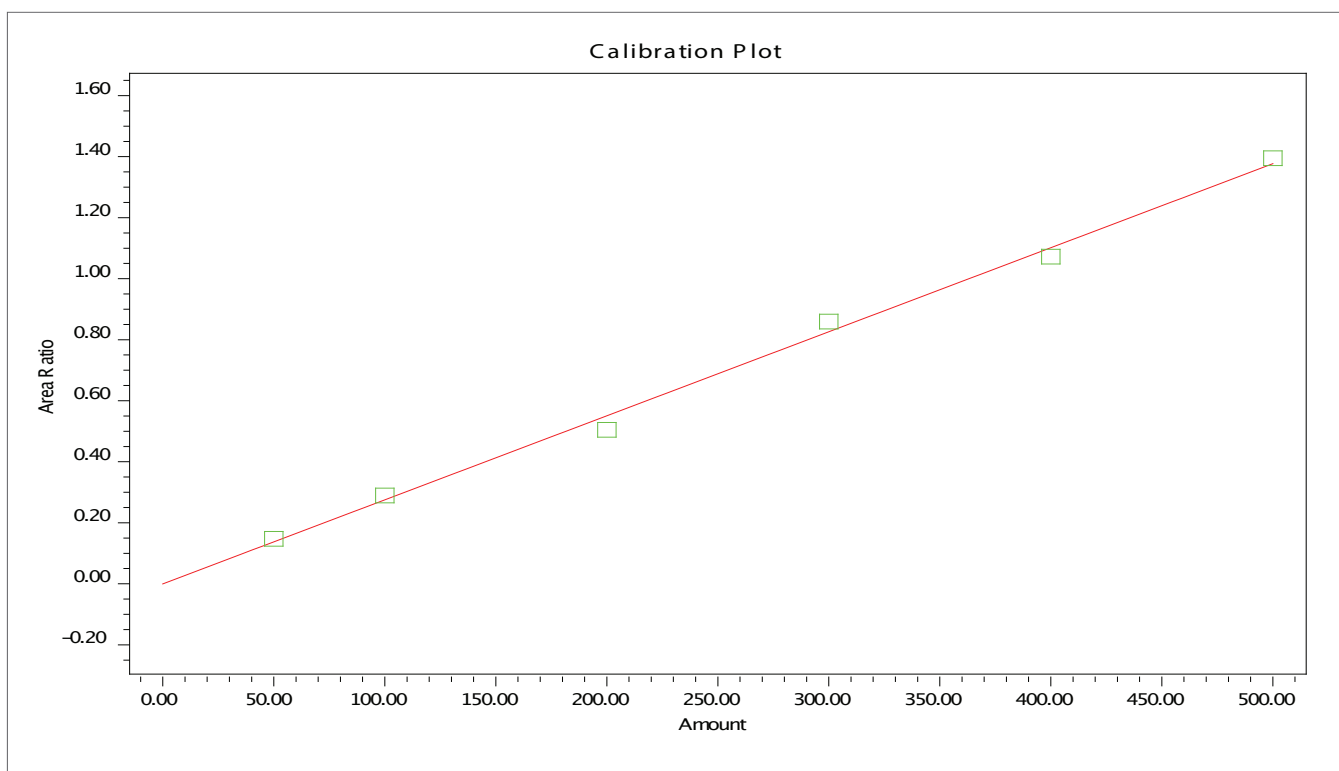


Figure 2. Calibration curve of ethanol used for the analysis of fruit juice.

Conclusion

This simplified method allows for favorable results in the quantification of ethanol content in consumable fruit juices. Additionally, the headspace introduction of the sample to the GC ensures that the amount of sample that gets on to the column is consistent. By decreasing the chance of errors in the preparation leads to concrete results that can be used as valid proof. These results are obtained from a TurboMatrix HS autosampler and the necessary time taken in sample preparation of each individual run due to the sensitivity of the headspace.

For Further Reading:

1. Timothy D. Ruppel; PerkinElmer Field Application Report, "Blood Alcohol Analysis Utilizing Headspace Autosampling and Dual-column GC Confirmation"
2. Timothy D. Ruppel; PerkinElmer Field Application Report, "Simultaneous and Rapid Separation of Blood-Alcohol Compounds and Commonly Abused Inhalants by Headspace-Gas Chromatography"
3. Paul L. Davis; Florida State horticultural Society, 1971, Pg 217- 222

Liquid Chromatography/
Mass Spectrometry**Authors**

Courtney Phillips

Avinash Dalmia

PerkinElmer, Inc.
Shelton, CT USA

Rapid Quantitative Analysis of Carbendazim in Orange Juice using UHPLC Coupled to the AxION 2 TOF Mass Spectrometer

Introduction

Fungicides in imported orange juice have been on the national stage in recent months, creating a need for simple and rapid detection methods.

When a private company alerted the FDA to the presence of the fungicide, carbendazim, in orange juice imported from Brazil, the agency expanded its testing of imports for this residue, which

is illegal in the United States. In response to the increased concern, we have developed a quick and straightforward method of analysis and quantitation of carbendazim at concentrations below 10 parts per billion.

We present a method for detecting both targeted analytes, such as carbendazim, as well as non-targeted components, by taking advantage of the full-spectrum, high mass accuracy data provided by the AxION® 2 time-of-flight (TOF) mass spectrometer (MS) using an Ultraspray™ 2 ionization source with lock mass for on-the-fly calibration. Unlike a triple quadrupole instrument, which requires predefined targets, a TOF instrument collects accurate mass and high resolution data across a full spectrum without a loss in sensitivity allowing analysis and identification of an unlimited number of compounds. Any emerging analytes of concern can be detected in pre-existing data simply by searching for the exact mass of the analyte of interest, and can quickly be confirmed by retention-time matching.

By using a superficially-porous particle (SPP) column, a dilute-and-shoot sample preparation was made possible while retaining the resolution and fast run times of a traditional UHPLC column.

Experimental

Instrumental parameters are described in Table 1.

Table 1. Experimental Conditions.			
Target Analyte:	Carbendazim		
Liquid Chromatography Conditions:			
Pump Type:	Flexar™ FX-15		
Column:	PerkinElmer Brownlee™ SPP C18 column (2.1 mm x 100 mm, 2.7 μm)		
Mobile Phase:	A: water containing 5 mM formic acid and 5 mM ammonium formate		
	B: methanol containing 5 mM formic acid and 5 mM ammonium formate		
Flow Rate:	0.3 mL/min		
Injection Volume:	10 μL		
Gradient:	Time (min)	%A	%B
	1.0	67.5	32.5
	2.0	45	55
	2.0	0	100
Mass Spectrometer Conditions:			
Mass Spectrometer:	PerkinElmer AxION 2 TOF MS		
Ionization:	Ultraspray™ 2 Dual ESI source		
Scan Range and TrapPulse Mode:	100 – 400 m/z (D7:66, D8:80)		
Capillary Exit Voltage:	+90 V		
Drying Gas Temperature and Flow Rate:	350 °C and 12 L/min		
LockMass Calibrant Flow Rate and Ions:	35 μL/min using m/z 322.04812 and 622.02896		

Sample Preparation

The high resolution and mass accuracy of the AxION 2 TOF MS and the large particle size and rugged nature of the SPP column allow for a simplified sample preparation. Juice samples were diluted 10-fold in water and centrifuged. The supernatant was collected and filtered directly into sample vials through a 0.2 µm PTFE syringe filter.

Results

Using the rapid RP-LC conditions described, carbendazim was found to have a retention time of just 2.2 minutes, with a limit of quantitation (LOQ) in orange juice calculated at 0.75 ppb. Figure 1 shows an extracted ion chromatogram of 100 ppb carbendazim in orange juice.

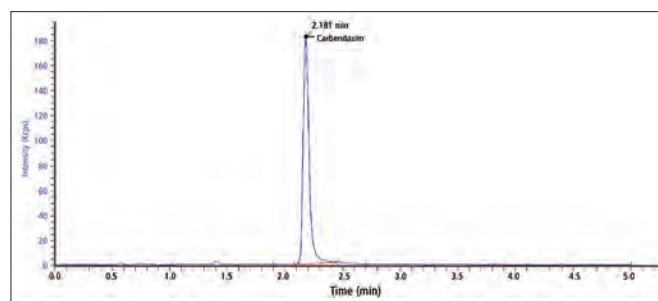


Figure 1. Extracted ion chromatogram (EIC) of 100 ppb carbendazim in orange juice.

The identification was confirmed by highly accurate mass and retention time matching, as well as by isotopic profile. By calculating the natural abundances of carbendazim isotopes, expected ratios could be compared to measured ratios as seen in Figure 2.

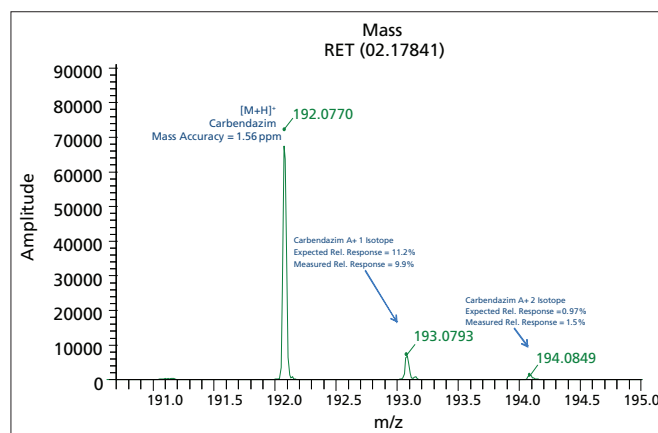


Figure 2. Isotopic profile afforded by the high resolution of the AxION 2 TOF MS allows an additional confirmation of identity without the need for fragmentation.

A calibration curve was created by spiking carbendazim standard into orange juice before dilution and analysis. The response is linear over a range of 1 ppb to 300 ppb with a correlation coefficient greater than 0.996 (shown in Figure 3).

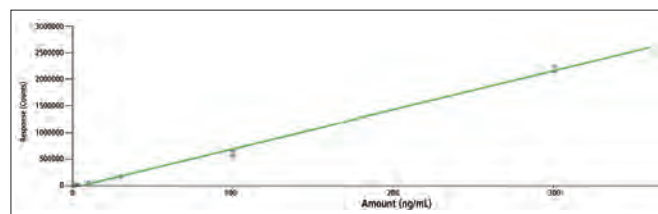


Figure 3. Linearity of carbendazim in orange juice from 1 ppb to 300 ppb.

It's important to note that the mass accuracy and resolution of the AxION 2 TOF MS allows a great deal of information to be collected in each run. Figure 4 demonstrates how much data is collected, and how easily high quality analytical results can be achieved even in less-than-ideal chromatographic conditions. The run time is able to be kept short because of very specific extracted ion chromatograms using narrow m/z ranges such as 5 mDa.

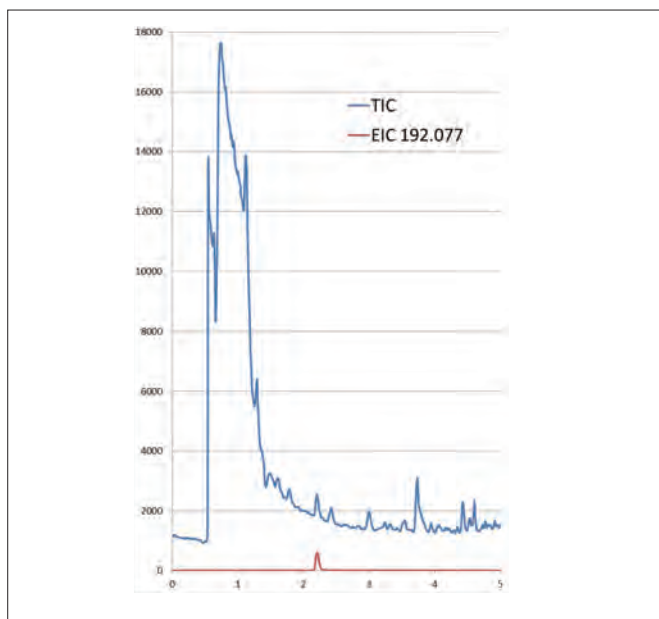


Figure 4. Total ion chromatogram and extracted ion chromatogram of carbendazim.

Identification of Non-Target Analytes

After the quantitation of carbendazim was considered, the orange juice data was further analyzed for non-target analytes, namely other pesticides common to oranges in the U.S. The following pesticides are the most frequently used on oranges and reported in orange juice:

- Aldicarb Sulfoxide
- Bromacil
- Carbaryl
- Chlorpyrifos
- Dimethoate
- Imazalil
- O-Phenyl Phenol
- Thiabendazole

By simply reanalyzing the data, a chromatographic peak with a retention time of 4.76 minutes was identified. The EIC of this peak provided a mass spectrum with the isotopic ratios described in Figure 5 and thus the peak was identified as carbaryl.

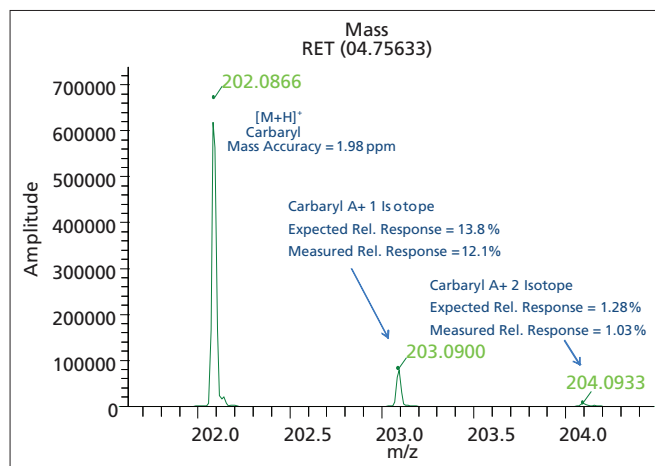


Figure 5. Isotopic profile of peak identified as carbaryl as compared to theoretical calculations.

High mass accuracy and isotopic profile can be used to check the peak identification. Running a standard allowed confirmation by retention time (Figure 6).

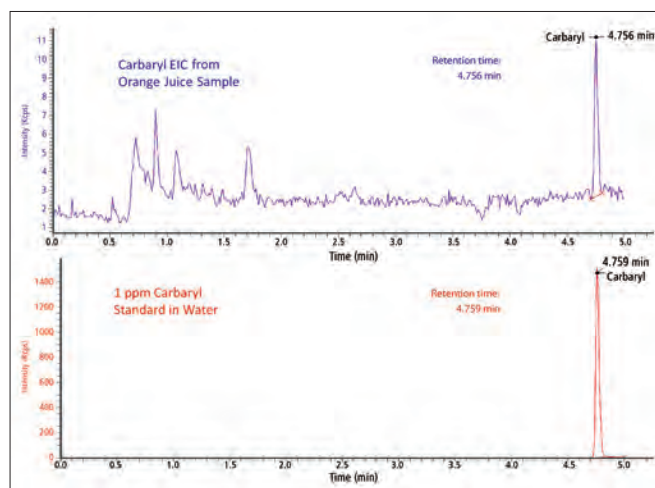


Figure 6. Retention time matching using ion EIC for carbaryl as extracted from existing data and the EIC of a standard prepared in water.

Conclusions

A less than 5 minute dilute-and-shoot LC-TOF method was developed for quantifying carbendazim in orange juice. The resultant analysis method was found to be rapid and efficient, rivaling or surpassing sample throughput of other published methods. The collected data was then screened for 8 additional pesticides most likely to be present in orange juice. Carbaryl was found to be present in the juice samples, with identification by exact mass, and confirmation by retention time matching with a standard, demonstrating the advantage of a full-spectrum mass analyzer over a scanning instrument.

PerkinElmer, Inc.
940 Winter Street
Waltham, MA 02451 USA
P: (800) 762-4000 or
(+1) 203-925-4602
www.perkinelmer.com



For a complete listing of our global offices, visit www.perkinelmer.com/ContactUs

Copyright ©2013, PerkinElmer, Inc. All rights reserved. PerkinElmer® is a registered trademark of PerkinElmer, Inc. All other trademarks are the property of their respective owners.

010244A_01

Near-Infrared Spectroscopy

Author:

Justin Lang, PhD

Lauren McNitt

Cory Schomburg, PhD

PerkinElmer, Inc.
Shelton, CT

Verification of Coffee Roast Using Fourier Transform Near-Infrared Spectroscopy

Introduction

With approximately 100 million people drinking coffee daily, it is no surprise that \$18 billion are spent on coffee, frappes, and cappuccino annually in

the United States. Grown around the world, coffees from different nations each have a distinct flavor. In most regions, beans are grown on small local farms then brought to market to sell. At the market, a buyer carefully inspects the beans before purchase and sends them off to be processed.

Processing coffee includes roasting the beans, as specific beans are roasted at different levels. The roast can be a dark, medium, or light with different levels within each. To determine what level of roast the coffee is while roasting, the master roaster has to listen for cracking noises or remove sample beans to distinguish the roast by color. When master roasters use the cracking method, there are two distinct noises they listen for. The first crack is caused by water and carbon dioxide bursting out of the bean; it also signifies the beginning of the bean becoming a light roast. The second crack is created by the cellulose matrices in the bean beginning to fracture. This also represents the beginning of the dark roast level. Near-Infrared (NIR) spectroscopy is shown here to be a fast and simple technique for measuring the roast levels of coffee beans and ground coffee.

Method

A coffee shop named Cool Beans™, which roasts its own coffee, donated eight samples of Columbian Coffee™ at multiple stages of roast. The stages included: the green beans, pale beans, early tan, late tan, into first crack, first crack plus, into second crack, and second crack plus. A PerkinElmer Frontier Fourier Transform Near-Infrared (FT-NIR) Spectrometer equipped with a Near-Infrared Reflectance Accessory (NIRA II) using a petri dish spinner were used to scan the coffee as whole beans. The beans were then ground to similar particle size by visual inspection in a coffee

grinder and scanned again with the FT-NIR. Spectra were collected from 10,000 to 4,000 cm^{-1} using 32 scans at 8 cm^{-1} resolution.

Results

Two methods were created to see if the spectra of each level of roast were different in both the whole beans and grounds. The methods for each were created with a Soft Independent Model by Class Analogy (SIMCA) algorithm using an offset baseline correction and a noise weighting filter.

Table 1. Table of the inter-material distances in whole beans.

Inter Material Distances								
Material	Roast Level 1	Roast Level 2	Roast Level 3	Roast Level 4	Roast Level 5	Roast Level 6	Roast Level 7	Roast Level 8
Roast Level 1	-	3.94	11.4	15.5	23.7	57.5	123	99.4
Roast Level 2	-	-	5.36	8.66	16.9	40.3	81.4	67.3
Roast Level 3	-	-	-	7.57	16.9	46.9	129	106
Roast Level 4	-	-	-	-	12	32.3	74.4	72.9
Roast Level 5	-	-	-	-	-	10	27.8	33.3
Roast Level 6	-	-	-	-	-	-	10.1	20.6
Roast Level 7	-	-	-	-	-	-	-	18.4

Table one is a display of the inter-material distance between each whole bean coffee type and from each other.

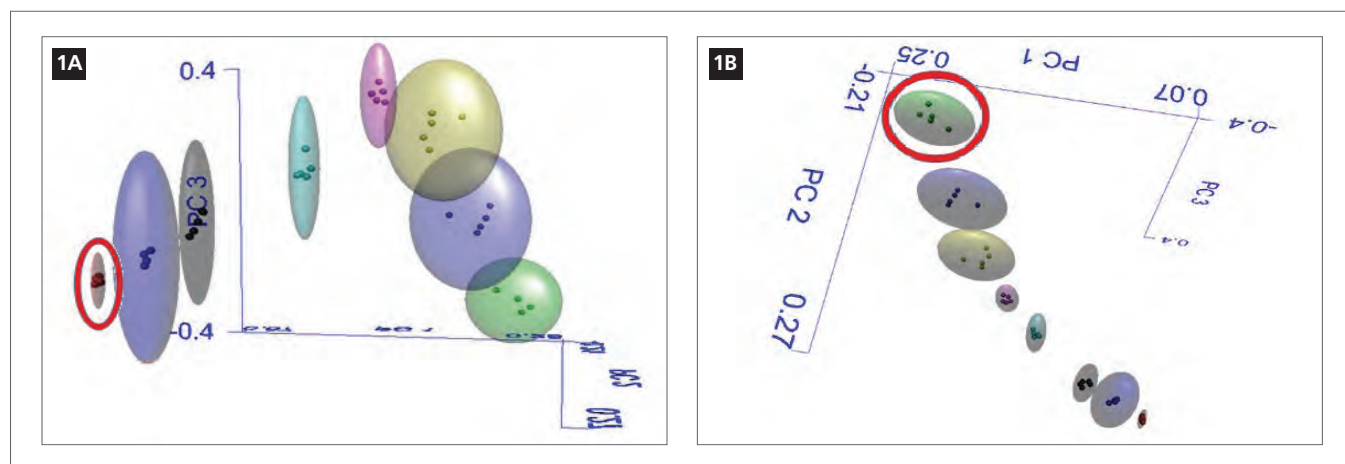


Figure 1A (left) and Figure 1B (right). Three dimensional representation of the SIMCA model for whole bean samples from different viewing angles.

Notice how the separation grows greater between each level of roast and from the initial green beans. The three bubbles in Figure 1A are the dark, medium, and light roasts (in that order from the right). Each is distinct with no overlap. The complete separation of each bubble is also present in Figure 1B. Dark roasted beans are highlighted in Figure 1A and the green beans highlighted in Figure 1B.

Table 2. Table showing the inter-material distances between ground coffee samples.

Inter Material Distances								
Material	Roast Level 1	Roast Level 2	Roast Level 3	Roast Level 4	Roast Level 5	Roast Level 6	Roast Level 7	Roast Level 8
Roast Level 1	-	6.5	15.7	25	46.5	89.5	90.9	134
Roast Level 2	-	-	18.8	36.2	86.3	178	161	259
Roast Level 3	-	-	-	14.1	59.8	140	138	209
Roast Level 4	-	-	-	-	47.4	128	133	201
Roast Level 5	-	-	-	-	-	97.1	116	190
Roast Level 6	-	-	-	-	-	-	38	112
Roast Level 7	-	-	-	-	-	-	-	56.4

Notice how the separation grows greater between each level of roast and from the initial green beans, as compared to the whole beans (Table 1).

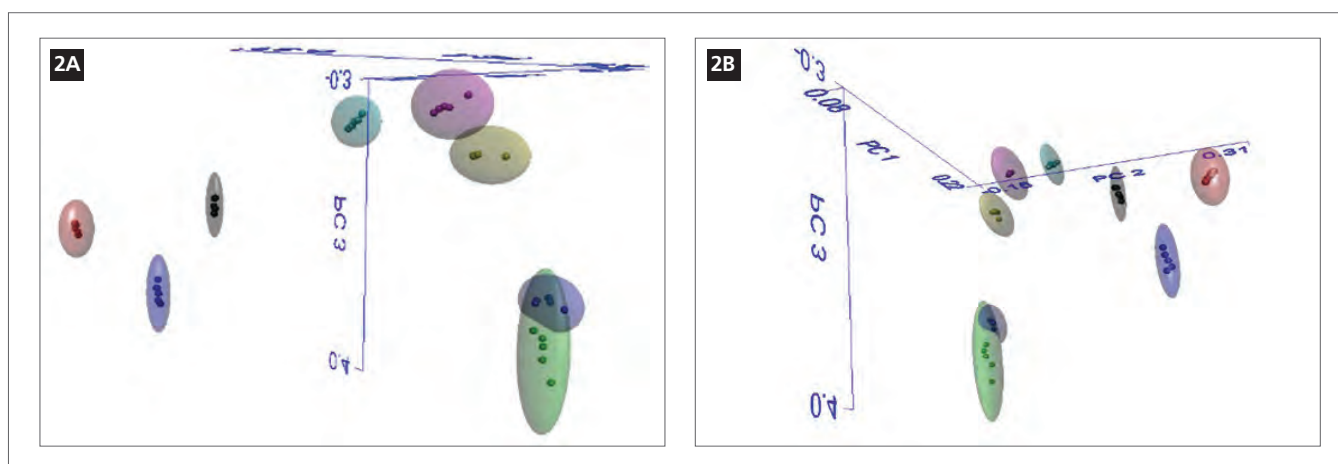


Figure 2A (left) and Figure 2B (right). Three dimensional representation of the SIMCA model from different viewing angles.

Figures 2A and 2B are Principal Component Analysis plots of where each coffee spectrum lies. All of the above figures demonstrate the separation seen in Table 2 between levels of roast. Note that the farthest right green and purple bubbles in figure 2A (green beans and pale beans) do overlap where they did not in Figures 1A and 1B. Conversely, the farther left bubbles in figure 2B (dark, medium, and light roasts) have a greater separation than they do in Figures 1A and 1B. This would suggest that although the whole beans data is suitable for the analysis, ground beans allow for greater separation between the levels of roast. This can be visualized by looking at Figure 3, the level of separation for the ground coffee samples appears to be much greater than for the whole beans.

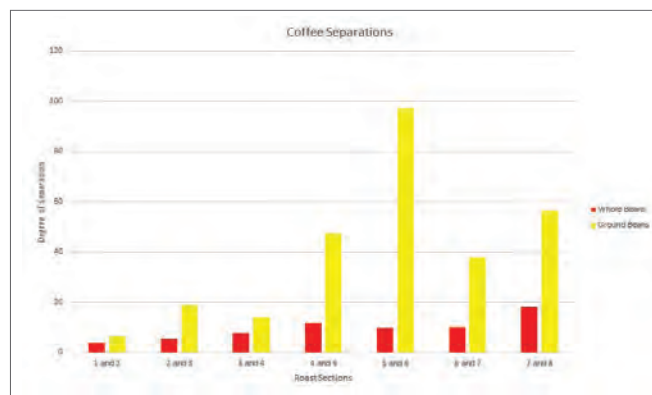


Figure 3. Bar graph plotting the inter-material differences between whole beans and ground beans.

An example execution of the method through Spectrum Touch™ is demonstrated in Figure 4. In this example, a sample of medium roast coffee, which was not included in the SIMCA model, was tested. The sample was set to identify the material, as opposed to verifying it. The model was able to correctly assign the sample as a medium roast.



Figure 4. Results table verifying a medium coffee roast using SIMCA analysis.

Conclusion

Due to the variety of large and small companies roasting their coffee beans with different techniques as well as the numerous types of coffee, it is hard to come up with an industry standard for each roast level. NIR provides a quick and easy way to distinguish between different roast levels, making it possible for coffee roasts to be compared. Regardless of whether the beans are whole or ground, there is a distinction among the dark, medium, and light roasted coffees. Using the Workflow application, companies will be able to rapidly test their samples (less than 30 seconds) and see if their product matches the required roast level.

References

- <http://www.statisticbrain.com/coffee-drinking-statistics/>
- <http://www.ncausa.org/i4a/pages/index.cfm?pageid=74>
- Coolbeanscoffeeroasters.com

Special Thanks:

To Cool Beans™, for providing PerkinElmer with specialty coffee. The experiment could not have been completed without their generous assistance.

Thermal Analysis



Dynamic Mechanical Analysis of Coffee



Summary

This application note demonstrates the ability of DMA to investigate a complex powder formulation. Both granulated instant coffee and granulated filter coffee were analyzed by DMA. A multi-frequency experiment clearly shows complex relaxation processes and other phase transitions. When run over a large temperature range, relaxations were observed as well as reproducible events below -150 °C. As the coffee is in powdered form, the Material Pockets were used to hold the sample in the PerkinElmer® DMA 8000.

Introduction

Dynamic Mechanical Analysis (DMA) is one of the most appropriate methods to study amorphous materials. The glass transition (T_g) is a key process in any material, and can be observed with ease by DMA. This technique provides very revealing information about these relaxations through the $\tan \delta$ vs. temperature data. Coffee, when in the final marketed state, is often in a powdered or granular form. This applies to both instant and filter coffee. Powders can be easily investigated in the DMA 8000 by using Material Pockets which sandwich the powder in a stainless steel prior to measurement.

DMA works by applying an oscillating force to the material and the resultant displacement of the sample is measured. From this, the stiffness can be determined and the modulus and $\tan \delta$ can be calculated. $\tan \delta$ is the ratio of the loss modulus to the storage modulus. By measuring the phase lag in the displacement compared to the applied force it is possible to determine the damping properties of the material. $\tan \delta$ is plotted against temperature and glass transitions are normally observed as a peak.

Coffee is a very complex formulation of various components. Even the simple coffee bean has multiple molecules, some of which are polymeric in nature, that make up the structure. In addition, the oils and other materials also affect the flavor.

Experimental

1. Multi-frequency scan of instant coffee. five frequencies from -80 °C to 250 °C at 5 °C/min.
2. Dual-frequency scan of instant and filter coffee. 1 Hz and 10 Hz from -190 °C to 220 °C at 3 °C/min.

About 10 mg of each sample was weighed into a Material Pocket before being mounted into the DMA 8000 in Single Cantilever Bending geometry.

Equipment	Experimental Conditions
DMA 8000	
1L Dewar	Sample: Tesco® medium blend filter coffee Nescafe® instant coffee granules
	Geometry: Single Cantilever Bending
	Support: Material Pocket
	Frequency: Multi-frequency and, 1 and 10 Hz

Results and conclusion

Figure 1 shows tan δ data from the multi-frequency scan of instant coffee. A very large and broad relaxation is seen which is almost certainly made up from several glass transitions. The peak position is frequency dependant proving this event, or series of events, is a relaxation.

The storage modulus data from the multi-frequency scan of instant coffee is shown in Figure 2. The conclusions from the tan δ plot are confirmed as this data also shows frequency dependence at the same temperature range. In addition, the material is seen to get less stiff as the temperature increases indicating a softening over the glass transition area.

Figure 3 shows data starting at a lower temperature for both filter and instant coffee. Both tan δ and modulus are superimposed on the same plot. This data was run at a lower scan rate than the previous examples and it shows a good separation of two glass transition peaks for the instant coffee. Again, a phase separation is observed. There are also clear transitions in the filter coffee sample. Although nothing is seen in the tan δ data, both filter and instant coffee show a small drop in modulus at about -165 °C

which is as yet unexplained. This very low transition temperature can only be seen using the DMA 8000 as most DMA cannot reach this low a temperature. Since the DMA 8000 can reach -190 °C it is ideal for low temperature work.

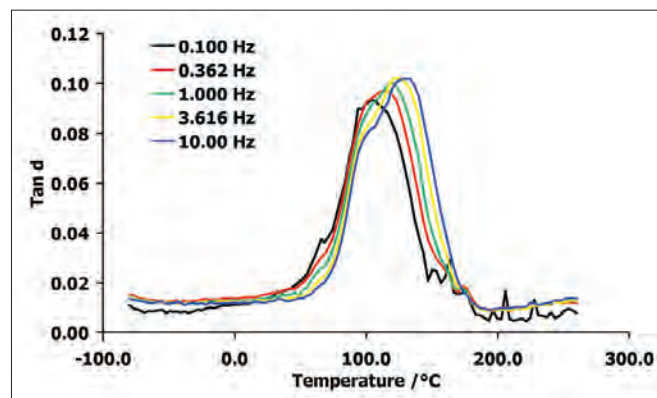


Figure 1. Tan δ data from scan of instant coffee.

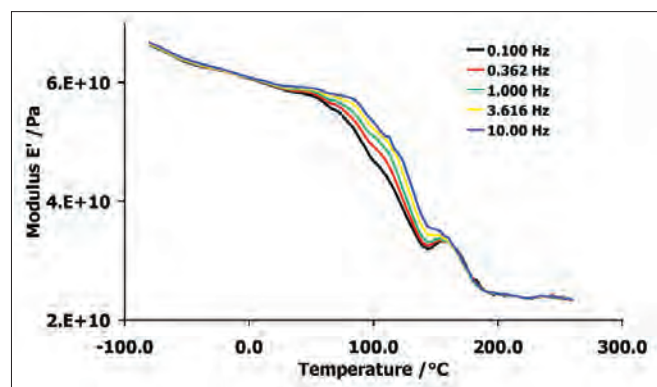


Figure 2. Storage modulus data from scan of instant coffee.

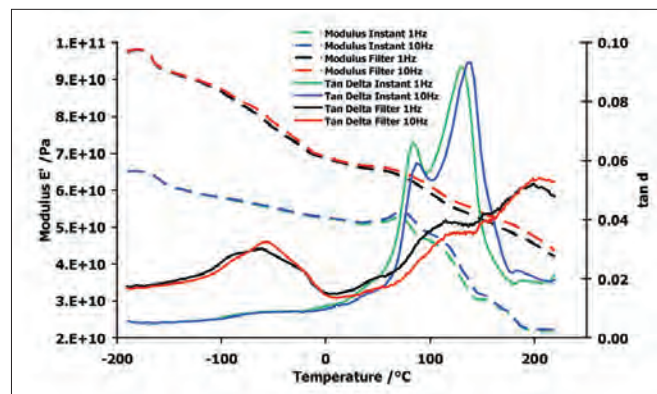


Figure 3. Scan data of both filtered and instant coffee.



APPLICATION NOTE

Gas Chromatography/ Mass Spectrometry

Author:

Andrew Tipler

PerkinElmer, Inc.
Shelton, CT

Coffee Characterization Using Clarus SQ 8 GC/MS, TurboMatrix HS Trap and GC SNFR Olfactory Port

Introduction

Coffee is a very popular drink in most parts of the world and is one of the most traded agricultural commodities on the planet. The drinking of coffee, however, is a

fairly recent activity. Although its origin may be attributed to Ethiopia a thousand years ago, its popularity as a beverage really started in the Middle East around the start of the 17th century.

Part of its popularity is due to the stimulating effect of its caffeine content (a cup of coffee may contain as much as 150 mg) and part is due to its rich complex taste. The taste of a cup of coffee depends on many factors – the coffee bean variety and horticulture and the way the beans are stored, roasted, ground and brewed. Even the water used to make the coffee can have an effect on its flavor.

For such a commercially significant product, it is important that there should be some means to characterize and control its taste at the various stages of production. This may be achieved organoleptically (i.e. by smelling and tasting) or by using powerful analytical tools like gas chromatography mass spectrometry (GC/MS) to determine chemical composition.

Aroma plays a very important part in the taste of coffee. This application note presents a system for characterizing finished coffee aroma while simultaneously performing a chemical analysis on a mass spectrometer. Further data may be acquired using a flame ionization detector (FID) for chemometric processing to provide further insight into the individual character of each coffee sample. The results provide a powerful insight into both the chemical composition and the sensory perception of coffee aroma. Such a system can be used for quality control purposes, process and product development, storage studies, trouble-shooting and evaluating competitive products.

Instrumentation

In this analysis, a headspace trap system may be utilized for sample introduction to characterize the flavor of roasted coffee beans. This technique ensures that non-volatile material in the beans does not enter the analytical system, which can cause interference in the chromatography and potential system contamination. The headspace trap extracts the volatile

components from a large sample and focuses them onto an inline adsorbent trap. It also facilitates very easy sample preparation – a weight of ground beans is dispensed into a vial and sealed. The subsequent analysis is then fully automated.

A PerkinElmer TurboMatrix™ Headspace Trap connected to a PerkinElmer Clarus® SQ 8 GC/MS with a flame ionization detector is used for these experiments. The MS provides the ability to identify each separated component and the FID is used to provide the quantitative data used in the chemometrics analysis. A schematic diagram of the GC system is given in Figure 1.

Using a headspace trap instead of the classical headspace technique enables up to 100 times improved detection limits over classical static headspace methods.

A polar 60 m x 0.25 mm x 1.0 µm Elite Wax column is used. This thick-film column provides sufficient chromatographic retention to separate the early-eluting most volatile component and provides the dynamic range necessary to chromatograph both high level and low level components in the coffee.

The column effluent is split between a PerkinElmer SNFR™ GC olfactory port, the MS detector and the FID. This splitting is performed using an S-Swafer™ in a standard active splitting configuration.

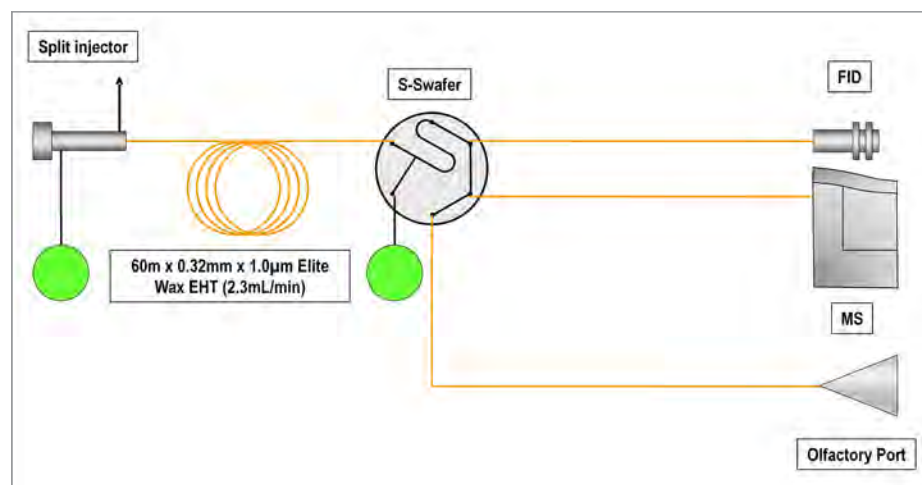


Figure 1. Schematic diagram of the GC system.

Experimental

Overview

Twenty seven varieties of pre-roasted and freshly roasted coffee beans from throughout the world were procured and examined in this work. These are listed in Table 1.

Table 1. Coffee samples examined.

1	Kona Cloud® Hawaiian coffee beans
2	Green Mountain® ground coffee (15 g packets)
3	Green Mountain® ground decaffeinated coffee (15 g packets)
4	Harar Longberry® Ethiopian coffee beans
5	Moka Harar® CP Select Ethiopian coffee beans
6	Kona Cloud® Hawaiian coffee beans medium roast
7	Kona Cloud® Hawaiian coffee beans dark roast
8	Other Kona coffee beans from Hawaii
9	Coffee beans from El Salvador
10	Coffee beans from Yemen
11	Coffee beans from Sidamo
12	Ground coffee from Trinidad
13	Ethiopian decaffeinated coffee beans
14	Guji Sueq'to Ethiopian coffee beans roasted before first crack
15	Guji Sueq'to Ethiopian coffee beans roasted just after first crack
16	Guji Sueq'to Ethiopian coffee beans roasted just before second crack
17	Guji Sueq'to Ethiopian coffee beans roasted just after second crack
18	Guji Sueq'to Ethiopian coffee beans roasted long after second crack
19	Guji Sueq'to Ethiopian coffee beans carbonized
20	Folgers® 5 g ground coffee bag
21	Folgers® 5 g ground decaffeinated coffee bag
22	Kona Cloud® freshly roasted beans
23	Trader Joe's® Cafe Pajoro beans (old)
24	Costa Rican El Trapiche beans bought at plantation
25	Costa Rican Britt® medium roasted beans
26	Costa Rican Britt® dark roasted beans
27	Barista® French roast ground coffee machine cartridge

Analytical Method

The experimental conditions for this analysis are given in Tables 2 to 8.

Table 2. HS trap conditions.

Headspace System	TurboMatrix 110 HS Trap
Vial Equilibration	80 °C for 20 minutes
Needle	120 °C
Transfer Line	140 °C, long, 0.25 mm i.d. deactivated fused silica
Carrier Gas	Helium at 25 psig
Dry Purge	7 min
Trap	Air Toxics, 25 °C to 260 °C, hold for 7 min
Extraction Cycles	1 with 40 psig extraction pressure

Table 3. GC conditions.

Gas Chromatograph/ Mass Spectrometer	Clarus 580 SQ 8
Column	60 m x 0.32 mm x 1.0 µm Elite-5MS connected directly to the HS Trap
Oven	40 °C for 1 min, then 5 °C/min to 200 °C for 5 min
Carrier Gas	Helium at 25 psig at injector and 13 psig at Swafer
Flame Ionization Detector	275 °C, range x1, attenuation x8

Table 4. MS conditions.

Scan Range	m/z 35 to 350
Scan Time	0.1 s
Interscan Delay	0.06 s
Source Temp	250 °C
Inlet Line temp	250 °C
Multiplier	1700V

Table 5. Olfactory port conditions.

Olfactory Port	PerkinElmer SNFR
Transfer Line	225 cm x 0.250 mm at 240 °C
Humidified Air	500 mL/min with jar set to 37 °C

Table 6. Chemometric.

Software	InfoMetrix Pirouette Version 4.0
Data	Collected using the flame ionization detector

Table 7. Swafer conditions.

Swafer	PerkinElmer S-Swafer in the S1 configuration
Settings	Developed using the Swafer Utility Software – see Figure 2.

Table 8. Sample details.

Sample Preparation	Beans were freshly ground and 1 g was weighed into a sample vial and sealed
Vial	Standard 22 mL vial with aluminum crimped cap with PTFE lined silicone septum

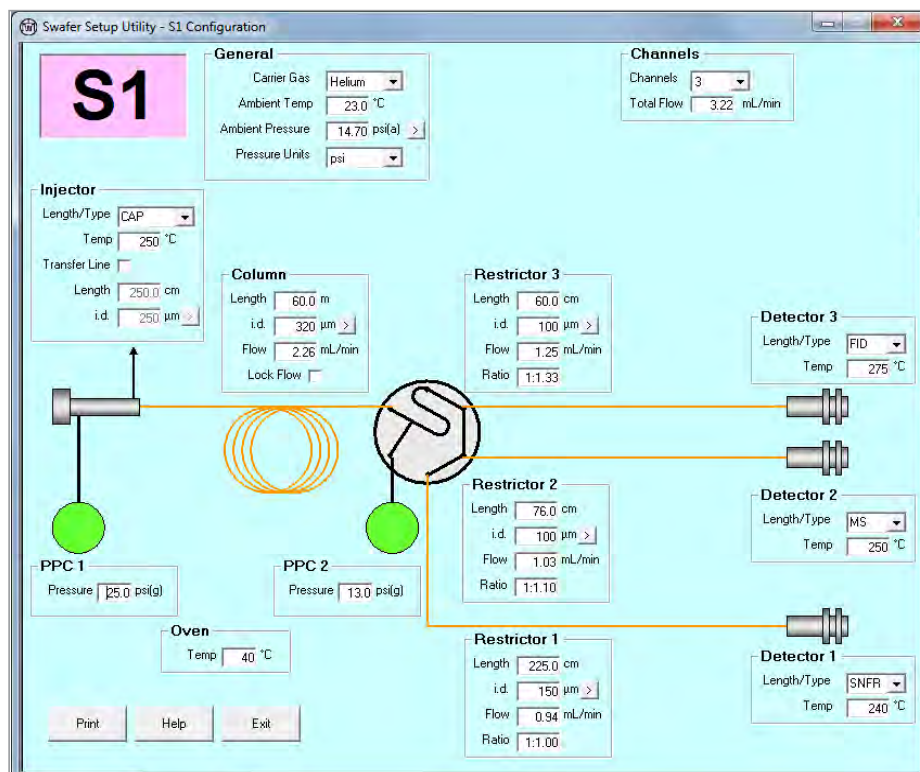


Figure 2. The S-Swafer in the S1 configuration for MS, FID and olfactory work.

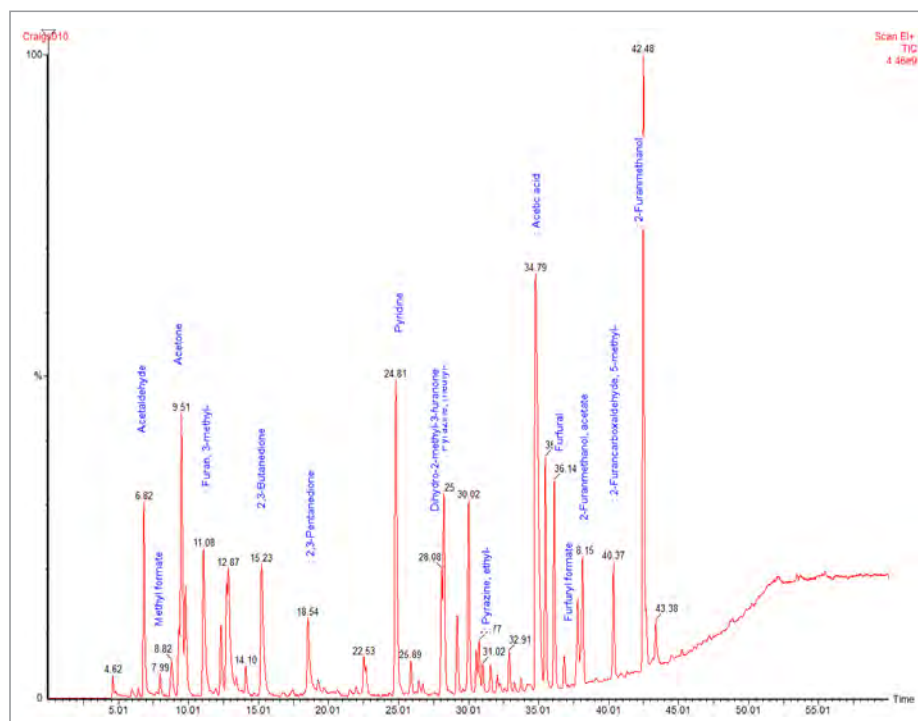


Figure 3. Typical chromatogram from 1 g coffee grains.

Results

Chromatography on the MS

Slow chromatographic times are preferred to enable the analyst to fully elucidate his or her sensory experience as the peaks elute. Faster chromatography is possible but then there is a risk that odors from adjacent peaks may start to overlap. Slower chromatography also gives the user more time to fully narrate and record their sensory perceptions.

Figure 3 shows a section from a chromatogram of coffee sample #3. The key components were identified using the library search capabilities of the TurboMass™ software supplied with the Clarus SQ 8 GC/MS.

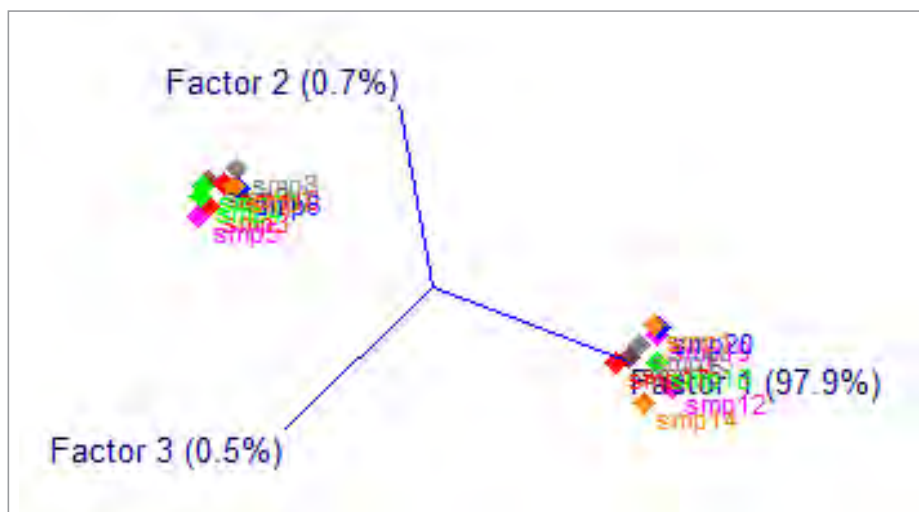


Figure 6. Detail from PCA map of two coffee sample chromatograms.

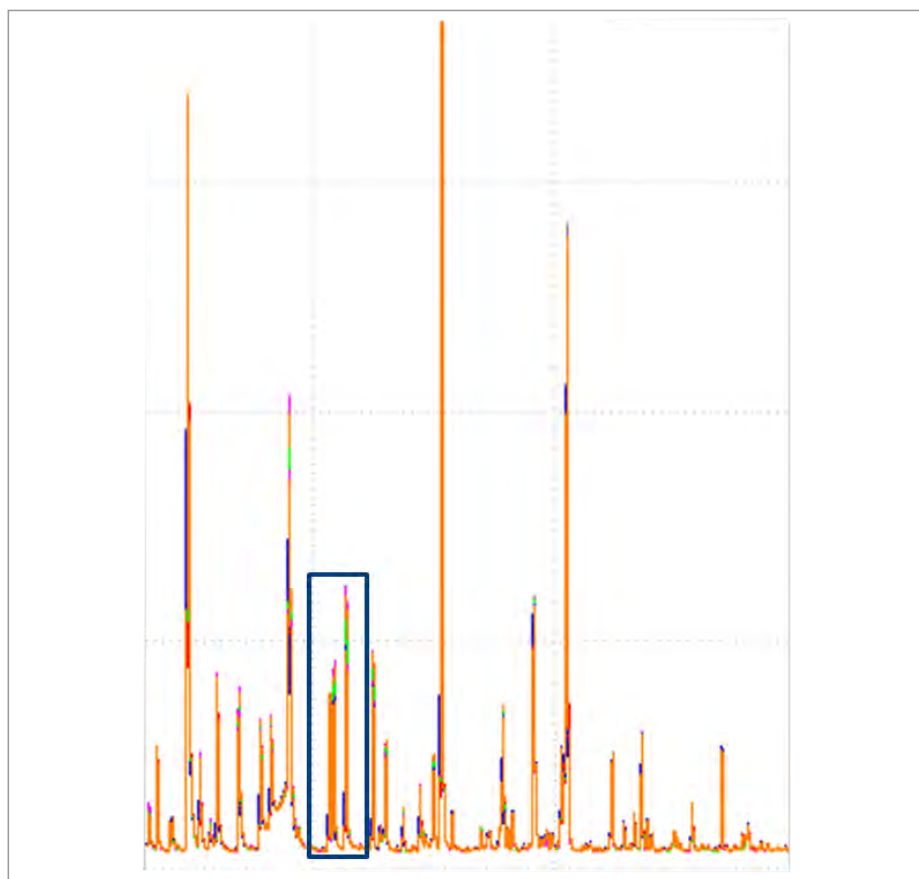


Figure 7. Chromatography of samples #2 and #22 overlaid.

For example, Figure 6 shows the PCA loadings for just two of the coffee samples. The replicate PCA results are tightly clustered for each sample type but well separated from the other sample type. Clearly there are differences in the chromatography between these two samples. Inspection of the PCA factors highlights an area in the chromatography where significant

differentiation is apparent. This area is shown in Figures 6 and 7. In this instance, the difference is clear but there may be areas in the chromatography where the difference may be more subtle or may be because of a combination of peaks (patterns). This is where PCA would be a powerful tool to highlight such areas.

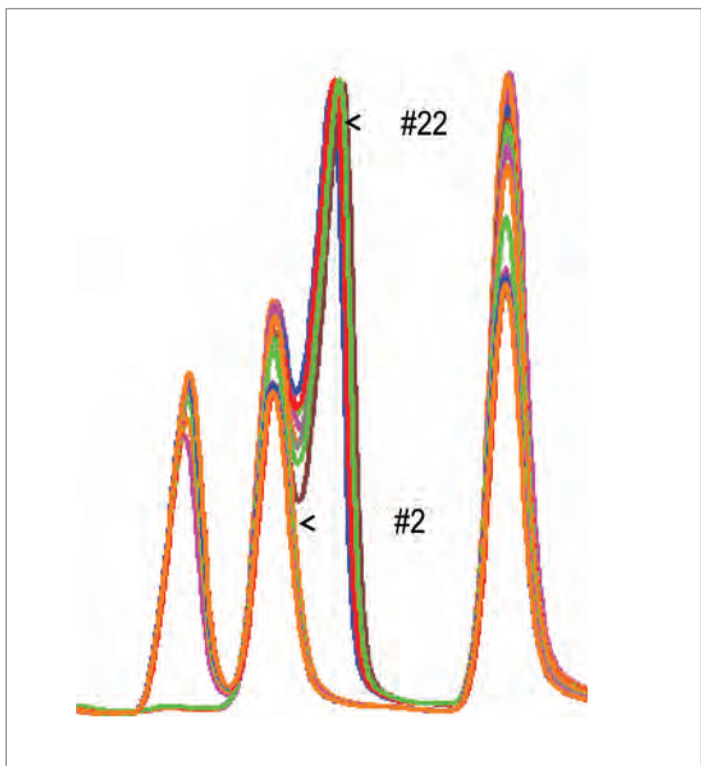


Figure 8. Detail from figure 7.

Olfactory Monitoring

Figure 9 shows an image of the SNFR system used for the olfactory monitoring. Figure 10 shows a photograph of Mr. Snow, a coffee expert, using the device to monitor the aroma of individual compounds. While the coffee aroma components are being monitored, the user is able to record

his or her sensory perceptions by voice into the supplied microphone and by positioning a joystick to indicate the intensity of the aroma. This information may be accessed and reviewed when displaying the chromatogram after the run is complete.



Figure 9. The GC SNFR system.



Figure 10. Photograph of coffee expert monitoring coffee aroma compounds.

Conclusion

The combination of chromatographic, mass spectral, chemometric and olfactory data from a single analysis provides a very powerful insight into the aroma and taste of complex samples such as coffee. Users can quickly identify which compounds are largely responsible for the aroma of a given coffee and what are the key differences and similarities between different coffees. The system that produces all this data would be at home in both a development laboratory or in a QC environment.

Acknowledgements

The author would like to thank the following for their support, help, advice and donations of free coffee samples during this work:

Craig Sellman, Village Coffee Roastery, Scottsdale, Arizona

Gerry Nicholls, Founder of Objective Coffee Tasters Group of America

James Ameika, Owner of Kona Cloud® Coffee Plantation, Hawaii

Brian Rohrback, President of InfoMetrix®

Scott Ramos, InfoMetrix®, Chemometrician and Coffee Drinker

Miles Snow, Coffee Expert and Principal Scientist at PerkinElmer

Thermogravimetric Analysis – GC Mass Spectrometry



TG-GC/MS Technology – Enabling the Analysis of Complex Matrices in Coffee Beans

Introduction

The combination of a thermogravimetric analyzer (TGA) with a mass spectrometer (MS) to analyze the gases evolved during a TGA analysis is a fairly well-known technique. In cases of complex samples, TG-MS often results in data in which it is nearly impossible to differentiate gases that evolve simultaneously.

Combining TGA with gas chromatography mass spectrometry (GC/MS) allows for a more complete characterization of the material under analysis and precisely determines the products from the TGA.

Experimental

This analysis was performed on a PerkinElmer® Pyris™ 1 TGA using alumina pans and the standard furnace. The instrument was calibrated with nickel and iron and all samples were run under helium purge. Heating rates varied from 5 to 40 °C/min, depending on the sample under test. The furnace was burned off between runs in air. Samples were approximately 10-15 mg. Data analysis was performed using Pyris 9.0 Software.

During the TG-GC/MS analysis, the PerkinElmer Clarus® 680 C GC/MS was used. A 0.32 mm I.D. deactivated fused-silica transfer line was connected to the GC injector port. The transfer line was heated to 210 °C and connected to the Elite™-1ms capillary GC column. In both cases, data analysis was performed using TurboMass™ GC/MS Software.

Results

In this TG-GC/MS application, coffee beans were analyzed. The TGA resulted in a complex thermogram with many different transitions (Figure 1).

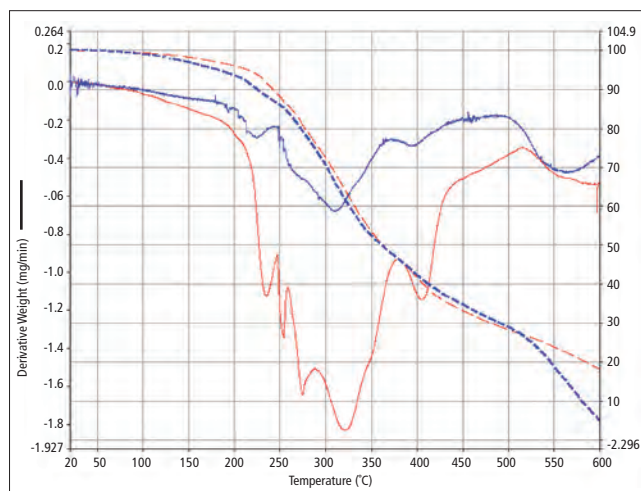


Figure 1. Resultant thermogram from the analysis of coffee beans. The blue curve is unroasted beans from Africa; the red curve is unroasted beans from Sumatra. The weight loss and the first derivative are shown.

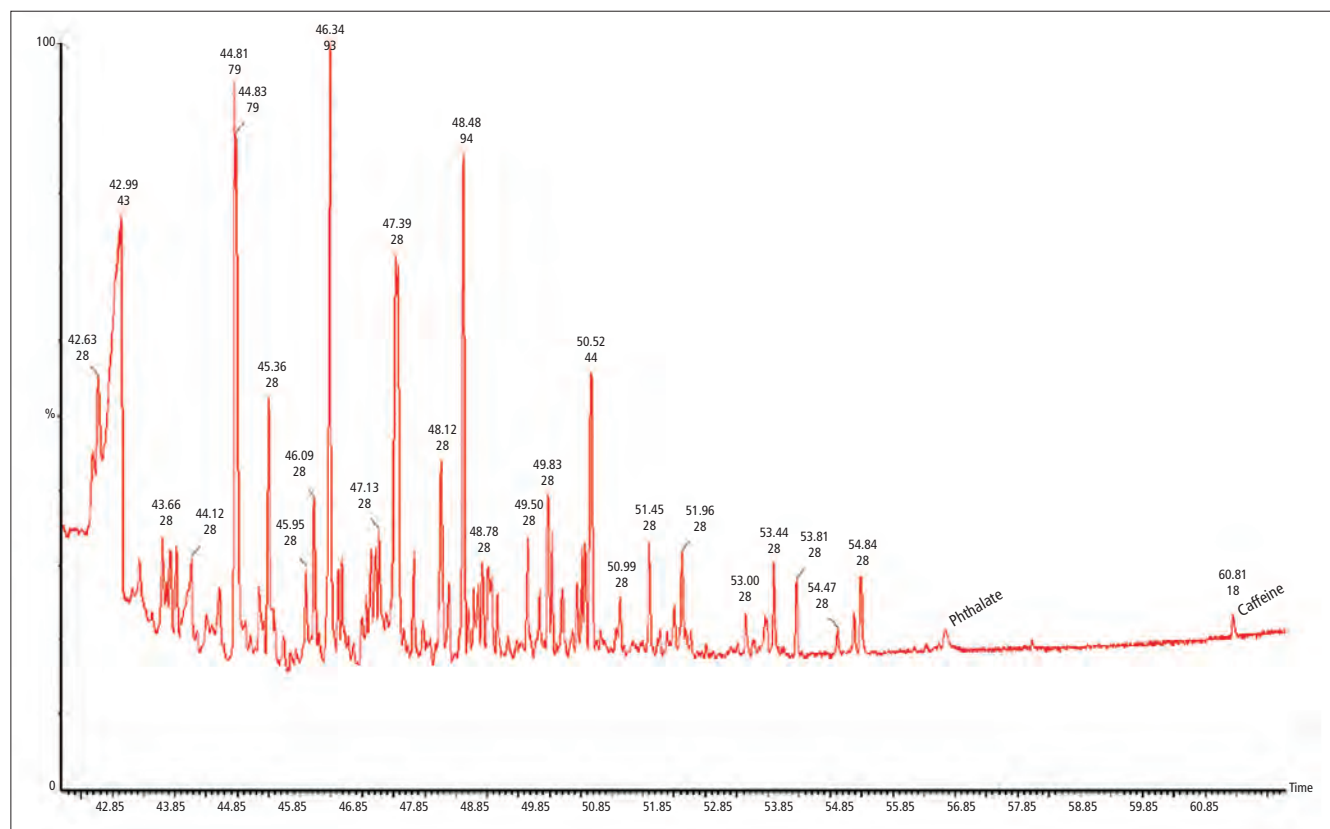


Figure 2. The GC/MS data resultant from the TGA of African coffee beans.

Complex data was expected as coffee beans are known to contain many different compounds. As a result, it was determined that the evolved gas would likely be too complex for TG-MS, thus TG-GC/MS was determined to be a better approach for this matrix.

The goal of the analysis was to search the complex data for two compounds that would be expected in a coffee sample, caffeine (m/z 194) and phthalates (m/z 149). The caffeine is obviously present in coffee, while the phthalates were a possibility as a result of storage in and contact with plastics. The resultant GC/MS data is shown in Figure 2 (Page 2), demonstrating a very complex chromatogram.

A search for significant peaks resulted in a spectral match for a phthalate (56 minutes), while a search for m/z 194 resulted in a spectral match for caffeine at 60 minutes. As expected, the TGA of coffee beans results in the simultaneous evolution of a large number of gases – TG-GC/MS is able to resolve many of these compounds enabling deeper investigation.

Conclusions

TGA analysis allows quantification of the weight loss of a material at specific temperatures. MS increases the power of the technique by providing the ability to identify the species evolved during thermal analysis. TG-GC/MS adds the additional capability of chromatographic separation of co-evolved gases. While not realtime, the improved separation by the GC/MS makes data interpretation easier than TG-MS. This allows the separation of fairly complex mixtures with minimal sample preparation by using the TGA to volatilize components.



Atomic Absorption

Author

Praveen Sarojam, Ph.D.

PerkinElmer, Inc.
Shelton, CT 06484 USA

Analysis of Pb, Cd and As in Tea Leaves Using Graphite Furnace Atomic Absorption Spectrophotometry

Introduction

Tea is drunk by about half of the world's population. It is widely cultivated and consumed in Southeast Asia. Tea is rich in many trace inorganic elements.^{1,2} In addition to many essential elements required for human health, some toxic elements may also be present in tea leaves. This could be due to polluted soil,

application of pesticides, fertilizers or industrial activities. There is often little information available about the safety of tea leaves and finished tea products with respect to heavy metal contamination. Due to the significant amount of tea consumed, it is important to know the toxic metal contents.

The toxicity and effect of trace heavy metals on human health and the environment has attracted considerable attention and concern in recent years. Among the heavy metals, lead (Pb), cadmium (Cd) and arsenic (As) are especially toxic and are harmful to humans even at low concentrations. They have an inherent toxicity with a tendency to accumulate in the food chain and a particularly low removal rate through excretion.³ Exposure to heavy metals above the permissible level can cause high blood pressure, fatigue, as well as kidney and neurological disorders. Heavy metals are also known to cause harmful reproductive effects.⁴

A major challenge in the analysis of tea leaves is the extremely low analyte levels and the very high matrix levels. For many years, graphite furnace atomic absorption spectrophotometry (GFAAS) has been a reliable technique and the preferred method for this analysis. The use of longitudinal Zeeman background correction and matrix modifiers help to achieve extremely low detection limits in high matrix samples such as tea leaves, making GFAAS an indispensable tool for carrying out such analyses.

Experimental Conditions

Instrumentation

The measurements were performed using a PerkinElmer® PinAAcle™ 900T atomic absorption (AA) spectrophotometer (Shelton, CT, USA) equipped with the intuitive WinLab32™ for AA software running under Microsoft® Windows™ 7, which features all the tools to analyze samples, report and archive data and ensure regulatory compliance. The high-efficiency optical system and solid-state detector used in the PinAAcle 900T spectrometer provide outstanding signal-to-noise ratios. The longitudinal Zeeman-effect background correction for graphite furnace analysis provides accurate background correction without the loss of light in other Zeeman systems. The use of a transversely heated graphite atomizer (THGA) provides uniform temperature distribution across the entire length of the graphite tube, eliminating memory effects and potential interferences that may occur with high-matrix sample analyses. Pyrolytically coated THGA tubes with end caps (Part No. B3000655) were used for all measurements. The instrumental conditions are given in Table 1, and the graphite furnace temperature programs are

listed in Appendix I (Page 5). Heated injection was used for lead; it can also be used for cadmium and arsenic. A high-performance microwave sample preparation system was used for the microwave-assisted digestion (Table 2). The samples were digested using ten 100 mL high-pressure vessels made of PTFE.



Figure 1. PerkinElmer PinAAcle 900T atomic absorption spectrophotometer.

Table 1. Optimized parameters for the analysis of tea leaves using the PinAAcle 900T in GFAAS mode.

Analyte	Pb	Cd	As
Wavelength (nm)	283.3	228.8	193.7
Slit (nm)	0.7	0.7	0.7
Mode	AA-BG	AA-BG	AA-BG
Calibration	Linear through zero	Linear through zero	Linear through zero
Lamp	EDL	HCL	EDL
Current (mA)	440	3	380
Standards (µg/L)	5, 10, 15, 20	0.5, 0.75, 1, 2	10, 20, 30, 40
Correlation Coefficient	0.9991	0.9996	0.9989
Read Time (sec)	3	5	3
Measurement	Peak Area	Peak Area	Peak Area
Injection Temp (°C)	90	20	20
Sample Volume (µL)	20	20	20
Matrix Modifier	0.05 mg NH ₄ H ₂ PO ₄ and 0.003 mg Mg(NO ₃) ₂	0.05 mg NH ₄ H ₂ PO ₄ and 0.003 mg Mg(NO ₃) ₂	0.005 mg Pd and 0.003 mg Mg(NO ₃) ₂
Modifier Volume (µL)	5	5	5

Table 2. Microwave digestion program.

Sequence	1	2
Power (watts)	1000	0
Ramp Time (min)	10	0
Hold Time (min)	10	20
Weight Taken (mg)	~500	
H ₂ O ₂ (mL)	1.0	
HNO ₃ (mL)	7.0	
Temp (°C)	180	

Standards, Chemicals and Certified Reference Materials

PerkinElmer Pure single-element calibration standards for Pb, Cd, and As were used as the stock standards for preparing the working standards (Part Nos. Pb: N9300128; Cd: N9300107; As: N9300102). Working standards were prepared by serial volume/volume dilution in polypropylene vials (Part Nos. B0193233 15 mL Conical; B0193234 50 mL Conical Freestanding) ASTM® Type I deionized water (Millipore® Corporation, Billerica, Massachusetts, U.S.) acidified with 0.2% nitric acid (HNO₃) (Tmapure®, TAMA Chemicals, Japan) was used as the calibration blank and for all dilutions. Thirty percent hydrogen peroxide (H₂O₂) (Kanto Chemicals, Tokyo, Japan) was used for digestion along with nitric acid.

Matrix modifiers were prepared from 10% NH₄H₂PO₄ (Part No. N9303445), 1% Mg as Mg(NO₃)₂ (Part No. B0190634) and 1% Pd (Part No. B0190635) stock solutions, by diluting with the 0.2% HNO₃ made above. Matrix modifiers were added automatically to each standard, blank and sample by the AS 900 autosampler, an integral part of the PinAAcle 900T spectrometer.

Sample and Certified Reference Material Preparation

Plastic bottles were cleaned by soaking with 10% volume/volume HNO₃ for at least 24 hours and rinsed abundantly in deionized water before use. The polypropylene autosampler cups (Part No. B3001566) were soaked in 20% nitric acid overnight to minimize sample contamination, and thoroughly rinsed with 0.5% HNO₃ acid before use. Five-point calibration curves (four standards and one blank) were constructed for each analyte. The calibration curve correlation coefficient was examined to ensure an $r^2 \geq 0.998$ before the start of the sample analysis.

NIST® 1568a Certified Reference Material (CRM) for Trace Metals in Rice Flour was used to validate the method. Three branded tea leaf samples available in Singapore markets (Tieguanyin tea leaves, Japanese green tea leaves and Loong Jin green tea leaves) were analyzed. Approximately 0.5 g of each sample or CRM, accurately weighed in duplicate, was transferred to the vessel of the microwave digestion system and the sample digestion method (Table 2) was performed in accordance with U.S. Environmental Protection Agency (EPA) Method 3052. The digested samples were diluted with 0.2% HNO₃ and brought up to 25 mL in polypropylene vials.

Results and Discussions

In GFAAS experiments, obtaining reproducible results is a challenging task, as one has to deal with analytes present at low levels in high matrix samples. The role of the sample introduction system is of paramount importance in optimizing the short-term stability of signals. The PinAAcle 900T spectrometer uses a unique built-in camera to monitor sample introduction into the graphite tube. With the furnace camera, it is easier and simpler to position the tip of the injector to the correct depth inside the tube so as to achieve highly reproducible pipetting. The capability to use full Stabilized Temperature Platform Furnace (STPF) conditions along with longitudinal Zeeman background correction and automatic matrix modification made the analysis of low-level analytes in tea leaves an almost effortless task with little to no influence by the concomitant elements in the sample matrix.

The developed method has been validated by incorporating Certified Reference Materials (CRMs) (Table 3). Method detection limits (MDLs) obtained under routine operating conditions were calculated based on the standard deviation of seven replicates of the reagent blank and took into account the 50x dilution factor for the samples (Student's t-value = 3.14, $p = 0.02$) (Table 4). The detection limits obtained show the capability of the PinAAcle 900T spectrometer in analyzing difficult matrices at the measured concentrations.

Table 3. Analysis of certified reference material by GFAAS.

Analyte	NIST® 1568a Rice Flour	
	Certified Value (µg/g)	Measured Value (µg/g)
Pb	<0.010	0.0093
Cd	0.022 ± 0.002	0.020 ± 0.004
As	0.29 ± 0.03	0.24 ± 0.02

Table 4. Estimated method detection limits (MDLs).

Analyte	MDL (µg/L)
Pb	9.5
Cd	2.35
As	9.5

Tea leaves contain a number of organic substances of different stability and impurities of sparingly soluble mineral components. Incomplete mineralization of samples during the microwave-digestion process may cause difficulty in transferring analytes into solution, which can disturb spectrochemical measurements.⁵ Application of concentrated HNO₃ along with H₂O₂ for mineralization of tea leaves leads to the complete digestion of samples, which is proven by determination of the values of the analytes in the CRM (Table 3). A post-digestion recovery study was done and the results are summarized in Table 5. The recoveries obtained for the post-digestion spikes indicate there was no interference from the matrix towards the analyte signals.

The results in Table 6 show that the level of lead, cadmium and arsenic in all the samples analyzed were well within the permissible limits of 10, 0.3 and 10 mg/kg respectively, as specified by the U.S. FDA for edible plant parts. The results confirmed that the determination of arsenic, cadmium and lead in tea leaves, after acid solubilization by microwave digestion, can be performed by GFAAS without any interference.

Table 5. Post-digestion spike recoveries (%).

Analyte	Pb	Cd	As
Tieguanyin tea leaves	102	96	98
Japanese green tea leaves	92	100	99

Conclusions

Toxicity of food materials is of much greater concern today than ever before. In recent years, greater emphasis has been given to toxic-element contents. A method for the accurate determination of arsenic, cadmium and lead in tea leaves using the PinAAcle 900T atomic absorption spectrophotometer in the GFAAS mode after utilizing microwave-assisted sample digestion was developed. Spike recoveries and the analysis of a CRM showed the method to be accurate, while the MDLs proved the method to be robust and precise. The PinAAcle 900Z (Longitudinal Zeeman Furnace only) spectrometer can also be used for this application.

References

1. F. Shen, & H. Chen. Bulletin of Environmental Contamination and Toxicology, 80, (2008) 300-304.
2. M. Ö. Mehmet, Ü. Ahmet, U. Tolga & A. Derya, Food Chemistry, 106, (2008) 1120–1127.
3. O. Sadeghi, N. Tavassoli, M.M. Amini, H. Ebrahimzadeh, N. Daei, Food Chemistry 127 (2011) 364–368.
4. H. Mubeen, I. Naeem, A. Taskeen and Z. Saddiqe, New York Science Journal, 2 (5) (2009) 1554-0200.
5. I. Baranowska, K. Srogi, A. Włochowicz, K. Szczepanik, Polish Journal of Environmental Studies, 11(5) (2002) 467-471.

Table 6. Results for the detection of toxic metals in tea leaf mixtures (mg/kg) – two replicates (n=2) were performed for each sample or sample duplicate.

Analyte	Pb		Cd		As	
	Sample	Duplicate	Sample	Duplicate	Sample	Duplicate
Tieguanyin tea leaves	0.68	0.88	0.032	0.026	0.038	0.047
Japanese green tea leaves	0.23	0.27	0.021	0.025	<MDL	<MDL
Loong Jin green tea leaves	0.88	0.95	0.058	0.064	<MDL	<MDL
U.S. FDA limit	10		0.3		10	

Appendix I – Graphite Furnace Temperature Program

Table 7. Furnace program for lead (Pb).

Analyte	Step	Temp °C	Ramp Time (sec)	Hold Time (sec)	Internal Gas Flow (mL/min)	Gas Type
Pb	1	110	1	30	250	Argon
	2	130	15	30	250	Argon
	3	850	10	20	250	Argon
	4	1600	0	5	0	–
	5	2450	1	3	250	Argon

Table 8. Furnace program for cadmium (Cd).

Analyte	Step	Temp °C	Ramp Time (sec)	Hold Time (sec)	Internal Gas Flow (mL/min)	Gas Type
Cd	1	110	10	30	250	Argon
	2	130	15	30	250	Argon
	3	500	15	35	250	Argon
	4	1500	0	3	0	–
	5	2450	1	3	250	Argon

Table 9. Furnace program for arsenic (As).

Analyte	Step	Temp °C	Ramp Time (sec)	Hold Time (sec)	Internal Gas Flow (mL/min)	Gas Type
As	1	110	5	30	250	Argon
	2	130	20	30	250	Argon
	3	800	15	40	250	Argon
	4	1200	15	30	250	Argon
	5	2200	0	5	0	–
	6	2450	1	3	250	Argon

Appendix II – Calibration Graphs for Different Analytes

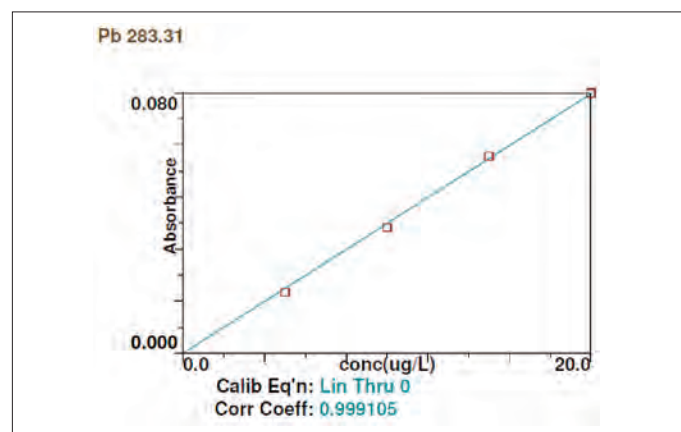


Figure 2. Calibration curve for lead (Pb).

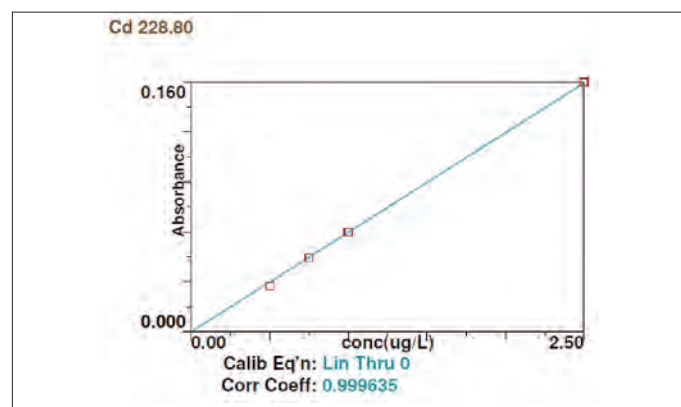


Figure 3. Calibration curve for cadmium (Cd).

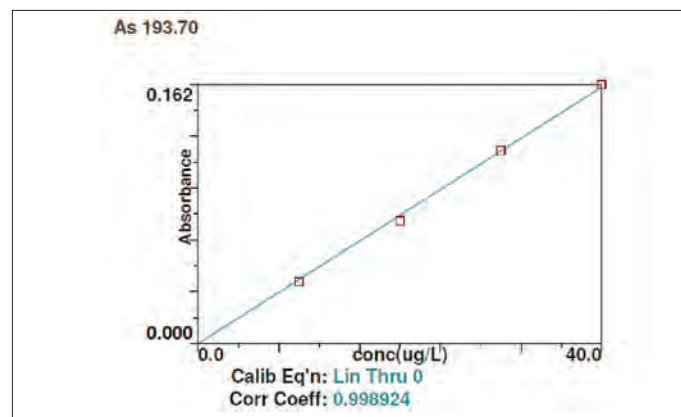


Figure 4. Calibration curve for arsenic (As).



ICP-Mass Spectrometry

Author:

Ewa Pruszkowski

PerkinElmer, Inc.
Shelton, CT

TotalQuant Analysis of Teas and Wines by ICP-MS

Introduction

TotalQuant is a software feature unique to the

ELAN® ICP-MS systems for quantifying 81 elements in a sample by interpretation of the complete mass spectrum. Measuring the full mass range takes only a minute, and the spectral interpretation itself takes a few seconds. During the TotalQuant analysis, each element is assigned a response value (cps/ppm) which is updated when a calibration is performed. Even though TotalQuant is an ideal tool for semiquantitative analysis during method development, it can also be used for a final material characterization.

When using TotalQuant, spectral interpretation is performed automatically by the software and intensities are assigned to elements after correction for interferences on individual isotopes. Intensities are compared with a stored response table to convert them into concentrations. TotalQuant, being a semiquantitative program, gives quantitative results typically within +/-25% of the real value in simple matrices.

A large number of articles can be found in the literature discussing the chemical characterization of wines, teas and other drinks. These studies usually concentrate on two aspects: heavy metal contamination during the growth of grapes or leaves and contamination during the manufacturing process. In the last 150 years, toxic metal emissions have increased ten-fold, leading to air, water, soil, and food contamination. TotalQuant can be a rapid, convenient, and valuable tool for the evaluation of the levels of contaminants and essential elements in environmental and food matrices.

Experimental

The standard instrumental conditions were used for analysis of tea and wine samples (Table 1). Wine samples were diluted 50 times. Tea samples were analyzed without dilution after tea bags were soaked in hot tap water for one minute.

Results

Three different teas were analyzed (ginseng, green and dark tea) along with tap water; and the results appear in Figure 1. Tap water was analyzed to provide a reference point for the tea results. The data in Figure 1 clearly shows the difference in mineral and metal content between the tea varieties.

Another application of TotalQuant is to use it to establish a product's origin by providing a fingerprint of nearly every element in the periodic table. Food species originating from different

Table 1. Instrumental Conditions

Instrument	ELAN 9000
RF Power	1400 W
Nebulizer Flow	0.95 L/min
Method	TotalQuant
Calibration Type	External (as defined in TotalQuant algorithm)
Calibration Standard	Blank, 40 µg/L mix of 25 elements in 1% HNO ₃
Sample	Tea – 1 min brew (no dilution) Wine – 50 x dilution in DI water
Measurement Time	67 seconds per sample

locations in the world can have characteristic metal concentrations based on the content of the water and soils in which they were grown. An example of this is shown in Figure 2, where elemental fingerprints of four different wines are displayed. Significant variation between wines is obvious from comparing elements, such as Be, Zr, Ru and Cd, as well as many others.

Conclusion

TotalQuant is a very useful tool for the rapid quantitation of elements within a sample. This algorithm functions by intelligently interpreting the complete mass spectrum and giving quantitative results for all elements. The analysis time is very fast, and the analysis requires only a single calibration standard. Even though TotalQuant is a perfect tool for the initial screening of “unknown” samples, its accuracy is often sufficient for final sample characterization, such as total metal content and fingerprinting.

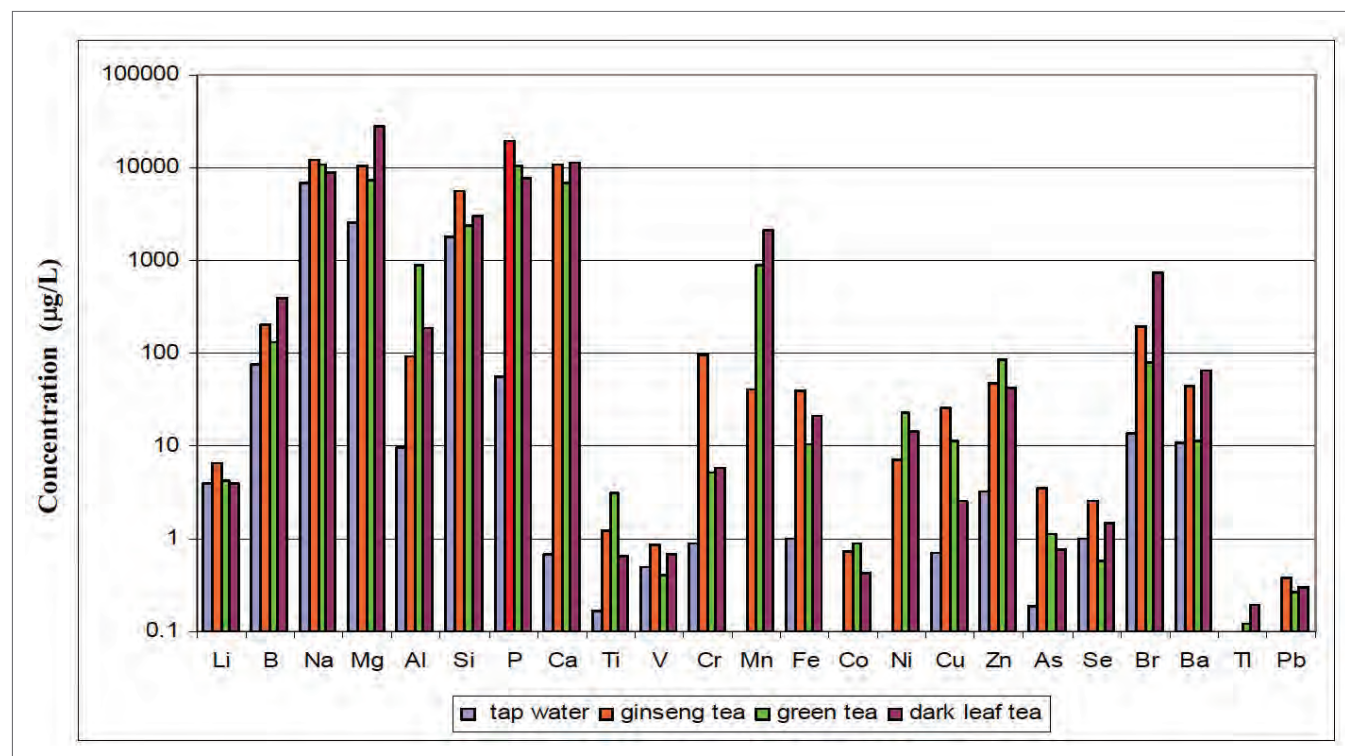


Figure 1. Results from TotalQuant analysis of tea. Tap water results are shown as a reference.

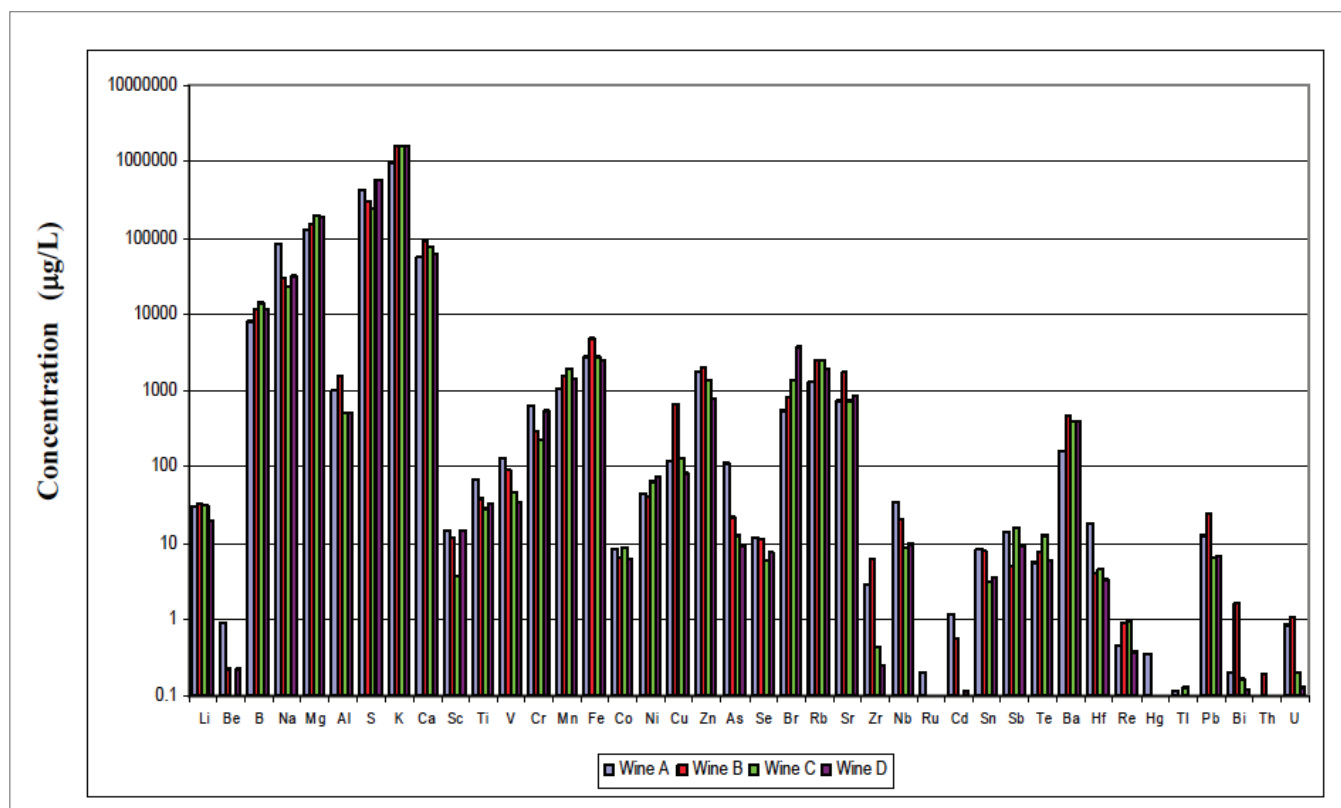


Figure 2. Results from TotalQuant analysis of wine samples .

PerkinElmer, Inc.
940 Winter Street
Waltham, MA 02451 USA
P: (800) 762-4000 or
(+1) 203-925-4602
www.perkinelmer.com



For a complete listing of our global offices, visit www.perkinelmer.com/ContactUs

Copyright ©2015, PerkinElmer, Inc. All rights reserved. PerkinElmer® is a registered trademark of PerkinElmer, Inc. All other trademarks are the property of their respective owners.

012283_01

PKI